Sede Amministrativa: Università degli Studi di Padova
Dipartimento di Biologia

SCUOLA DI DOTTORATO DI RICERCA IN BIOSCIENZE E BIOTECNOLOGIE
INDIRIZZO BIOLOGIA CELLULARE
CICLO XXVIII

The unique histidine of F-ATP synthase subunit OSCP mediates regulation of the permeability transition by matrix pH

Direttore della Scuola : Ch.mo Prof. Paolo Bernardi
Coordinatore d'indirizzo: Ch.mo Prof. Paolo Bernardi
Supervisore : Ch.mo Prof. Paolo Bernardi

Dottorando : Manuela Antoniel

I would like to express my sincere gratitude to my supervisors Prof. Paolo Bernardi and Prof. Giovanna Lippe for the continuous support of my Ph.D study and related research, for their patience, motivation, and immense knowledge. Their guidance helped me in all the time of research and writing of this thesis.

TABLE OF CONTENTS

SUMMARY

The “Permeability transition” (PT) is one of the most studied events that may trigger cell death and is due to a Ca2+- and ROS-dependent opening of a nonspecific pore, called PTP, whose molecular nature has been long debated. Recently, our research group has demonstrated that PTP forms from F_oF_1 ATP synthase dimers, demonstrating the ability of this complex to switch from the key enzyme for the aerobic synthesis of ATP into a potential cell death mediator.

The goal of this PhD thesis has been to define which structural changes of ATP synthase are responsible for the pH modulation of PTP. Indeed, it is well known from nineties that the optimum matrix pH for PT occurrence is about 7.3, and a decrease leads to decreased probability of PTP opening. The pH effect has been ascribed to reversible protonation of His residues located on the PTP that can be blocked by the histidine modifying reagent diethyl pyrocarbonate (DPC). Moreover, in mammalian cells, similarly to the drug Cyclosporin A (CsA), acidic pH also promotes release from the inner membrane of the matrix protein Cyclophilin D (CyPD), which is a well-known PTP activator.

As our group demonstrated that CyPD binds to the ATP Synthase OSCP subunit, mainly through electrostatic interactions and resulting in partial enzyme inhibition, the hypothesis has been advanced that the unique histidine located on OSCP, His112 according to bovine numbering, may be responsible for both the pH effects on CyPD (un)binding to ATP synthase and on PTP/ATP synthase opening. OSCPHis112 is exposed to the solvent and is located in the flexible linker region between the structured N- and C-terminal domains of OSCP.

The results obtained by ATP synthase immunoprecipitation from bovine heart mitochondria showed that acidic pH induces CyPD release that is prevented by DPC, perfectly matching the effect of DPC on CyPD-PTP interaction. DPC also prevented the binding at low pH of the inhibitor protein IF1 to ATP synthase, but this effect is probably not relevant to PTP modulation. ESI-MS and ESI-MS/MS analyses of the OSCP isolated from DPC-treated mitochondria revealed that the 95-113 peptide shows a mass shift of +72 Da, which is indicative of carbethoxylation of the unique His112. These data therefore strongly support the hypothesis that OSCP His112 is part of the binding site of CyPD on the protein, so that its protonation by lowering

pH favors CyPD release. Of note, this region contains several residues of glutamic acid conferring a low potential surface, which is complementary to the mainly high potential surface of CyPD. Consistently to this model, DPC inhibits the ATPase activity of ATP synthase only when CyPD is released from OSCP, i.e. in the presence of CsA and in mitochondria from CyPD-null mice. Replacement of OSCPHis112 with a Gln in HEK cells, by the CRISPR/Cas9 system, showed its involvement even in the effect of low pH on PTP opening. Indeed, the PTP open probability is not affected by acidic pH only in mutated cells, while DPC reverts the pH inhibition exclusively in wild type cells. Finally, evaluation of the structural stability of the ATP Synthase dimers at low pH by Blue-native PAGE excluded their destabilization, which could affect PTP formation.

In summary, these data provide a convincing model for the pH modulation of PTP, as well as a compelling evidence that ATP synthase and PTP are the same molecular entity.

RIASSUNTO

La transizione di permeabilità (PT) mitocondriale è uno degli eventi coinvolti nella morte cellulare tra i più studiati e implica l'apertura nella membrana mitocondriale interna di un poro aspecifico, definito PTP, indotta da ioni calcio in presenza di stress ossidativo, la cui natura molecolare è stata a lungo dibattuta. Recentemente, il gruppo di ricerca presso cui è stata svolta la presente tesi di dottorato ha dimostrato che il PTP si forma da complessi dimerici dell'enzima F_oF_1 ATP Sintetasi, trasformando l'enzima essenziale per la sintesi aerobica di ATP in mediatore di morte cellulare.

L'obiettivo della presente tesi è stato quello di definire le basi molecolari della modulazione del PTP da parte del pH di matrice rispetto alle proprietà strutturali di ATP Sintetasi. E' infatti noto dagli anni '90 che le probabilità di apertura del PTP sono massime a pH 7.3 e diminuiscono rapidamente al diminuire del pH. Tale effetto è stato imputato alla protonazione di residui di istidine del PTP, in quanto l'inibizione veniva bloccata dal reagente specifico per le istidine dietilpirocarbonato (DPC). Inoltre, era stato dimostrato che in cellule di mammifero un pH acido favorisce, similmente alla Ciclosporina A (CsA), il rilascio dal PTP della proteina di matrice Ciclofilina D (CyPD), che, quando legata al PTP, è un ben noto attivatore del poro.

Poiché studi recenti dello stesso gruppo avevano dimostrato che in mammifero la ciclofilina D interagisce, prevalentemente mediante interazioni elettrostatiche, con la subunità OSCP di ATP Sintetasi, inducendo un'inibizione parziale dell'attività catalitica dell'enzima, si è ipotizzato che l'unico residuo di istidina di OSCP, His112 in base alla numerazione in bovino, fosse coinvolto nella modulazione pH-dipendente sia del legame della CyPD che della probabilità di apertura del PTP/ATP Sintetasi. OSCPHis112 è esposto al solvente ed è localizzato nella parte non strutturata della proteina, legante i domini ad α-elica N- e C-terminali.

I risultati ottenuti mediante immunoprecipitazione di ATP Sintetasi da mitocondri di cuore bovino hanno dimostrato che pH acidi inducono il rilascio della CyP e che tale rilascio viene bloccato dalla presenza di DPC, in perfetto accordo con quanto precedentemente osservato rispetto al PTP. L'analisi ESI-MS e ESI-MS/MS

della subunità OSCP isolata da mitocondri trattati con DPC ha stabilito che il peptide 95-113 di OSCP subisce un aumento della sua massa molecolare corrispondente a 72 Da, indicativo della carbetossilazione dell'unica istidina. Questi dati suggeriscono quindi che OSCPHis112 sia coinvolta nel sito di legame della CyPD, in quanto l'interazione viene sfavorita dalla sua protonazione. His112 è infatti localizzato in una regione caratterizzata dalla presenza di numerosi residui di acido glutammico avente un potenziale di superficie negativo, che è complementare al potenziale di superficie della CyPD prevalentemente positivo. In accordo con questo modello, il DPC è risultato un inibitore dell'attività catalitica di ATP Sintetasi esclusivamente quando la CyPD non è legata ad OSCP, come in presenza di CsA o nei topi KO per la CyPD *(Ppif-/-)*. Inoltre, la sostituzione di OSCPHis112 con un residuo di Gln mediante il sistema di mutagenesi CRISPR/Cas9 in una linea cellulare umana (HEK293T) ha permesso di verificare che la stessa istidina è coinvolta nell'effetto del pH sull'apertura del PTP, in quanto solo nelle cellule mutate la probabilità di apertura del PTP non diminuisce a pH acido, e, in accordo, il DPC reverte l'inibizione a pH acido esclusivamente nelle cellule wild type. Infine, l'analisi della stabilità strutturale dei dimeri di ATP Sintetasi in funzione del pH mediante Blue-native PAGE ha consentito di escludere una loro destabilizzazione a pH acidi, che avrebbe potuto influire sulla formazione del PTP.

In conclusione, questi risultati, oltre a fornire un modello convincente per la modulazione pH-dipendente del PTP, costituiscono altresì una prova molecolare importante che ATP Sintetasi e il PTP sono la stessa entità molecolare.

ABBREVIATIONS

Å	Ångström (1Å = 0.1 nm)
ADP	Adenosine diphosphate
ANT	Adenine nucleotide translocator
ApoM	Apomyoglobin
ATP	Adenosine triphosphate
BHM	Bovine heart mitochondria
BSA	Bovine serum albumin
Ca^{2+}	Calcium ion
CsA	Cyclosporin A
CyPD	Cyclophilin D
CRC	Calcium retention capacity
Da	Dalton
DPC	Diethylpyrocarbonate
DDM	n-DODECIL-β-maltoside
E. coli	*Escherichia coli*
EDTA	Ethylene diamine tetraacetic acid
EGTA	Ethylene glyol-bis (β-aminoethyl ether) N,N,N'tetracetic acid
ESI-MS	Electrospray ionisation mass spectometry
ERK2	Extracellular signal regulated kinase
FCCP	Carbonyl cyanide 4-(trifluoromethoxy) phenylhydrazone
g	Gravitational force
Gln	Glutamine
GSK-3	Glycogen synthase kinase 3
H	Histidine
HBHM	Heavy bovine heart mitochondria
HEK293T	Human embryonic kidney 293T cell line
His	Histidine
Hsp90	Heat shock protein 90
IF1	Inhibitor factor 1
IMM	Inner mitochondrial membrane
IP	Immunoprecipitation
IR	Ischaemia-reperfusion
LC-MS/MS	Liquid chromatography-tandem mass spectometry
MOPS	3-(N-Morpholino)propanesulfonic acid
NADH	Nicotinamide adenine dinucleotide hydrate
NBD-Cl	4-Fluoro-7-nitrobenzofurazan
OCR	Oxygen consumption rate
OMM	Outer mitochondrial membrane
OSCP	Oligomycin sensitivity conferral protein
PC	Cardiac preconditioning
Pi	Inorganic phosphate
PiC	Phosphate carrier protein

PKC	Protein kinase C
PT	Permeability transition
PTP	Permeability transition pore
Q	Glutamine
RP-HPLC	Reversed phase liquid chromatography
ROS	Reactive oxygen species
SDS	Sodium dodecyl sulfate
SDS-PAGE	Sodium dodecyl sulfate -polyacrylamide gel electrophoresis
TEMED	N,N,N‘,N‘-tetramethylene diamine
Tris	2-amino-2-(hydroxymethyl)-1,3-propanediol
TSPO	Translocator protein
VDAC	Voltage-dependent anion channel

LIST OF FIGURES

LIST OF TABLES

1. Introduction

1.1 Structural organization of mitochondria

Mitochondria are cytoplasmic organelles of variable size, with a diameter between 0.5 and 5 µm, responsible of the aerobic production of ATP by the oxidative phosphorylation system (OXPHOS). They also participate in intermediary metabolism of lipids, nucleotides, heme and urea and are involved in the early stages of cell death (Wallace et al. 1999) These organelles, which are present only in the eukaryotic cells, may vary greatly in terms of number and size, depending on the cell type. Their number varies from a few hundred to several thousand in more metabolically active cells, such as heart, muscle and kidney cells, where they occupy 20-25% of the cell volume.

While the first electron microscopy (EM) images suggested that mitochondria were separate entities in the cytoplasm, the use of specifically addressing recombinant probes definitely demonstrated that within living cells they form a dynamic network (Rizzuto et al. 1998), which is subject to ongoing arrangements by the fusion and fission machinery (Westermann 2008). Moreover, mitochondria continuously move along cytoskeletal tracks and are in close association with membranes of the endoplasmic reticulum (Rutter & Rizzuto 2000; Mannella 2000).

Mitochondria are delimited by two membranes, the inner and outer membrane. The space between the two membranes is called intermembrane space (Figure 1.1).

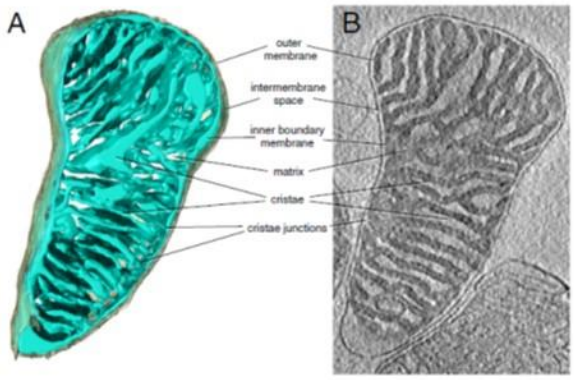

Figure 1.1: Tomography volume of mouse heart mitochondrion. A) Three-dimensional volume of a mouse heart mitochondrion determined by cryo-ET. The outer membrane (grey) envelops the inner membrane (light blue). The inner membrane is highly folded into lamellar cristae, which criss-cross the matrix. **B)** Tomographic slice through the map volume From (Kühlbrandt 2015).

The outer membrane (OMM), which forms a continuous envelope around the mitochondrion, has a smooth surface and is highly permeable to small molecules and ions through channels that cross the lipid bilayer. The inner membrane (IMM) instead, is impermeable to most molecules of small size and to ions, including protons and possesses numerous invaginations called cristae , which significantly enhance its surface (Figure 1.1). It is well established that the IMM is a dynamic structure able to quickly change its shape in response to metabolic alterations (Hackenbrock 1966) or osmotic stress, such as those induced by the opening of an aspecific pore, originally defined as permeability transition pore (PTP) (Hunter et al. 1976), whose nature has only recently been defined.

The IMM accomodates large copy numbers of the five complexes of the OXPHOS (complexes I-V). Complexes I to IV are oxidoreductases which, with the exception of complex II, couple electron transport with translocation of protons across the inner membrane. The generated proton motive force is used by ATP synthase (complex V) for the endergonic synthesis of ATP from ADP and phosphate. Complex I or NADH dehydrogenase is the first and major entrance point of electrons to the respiratory chain. It transfers electrons from NADH molecules to a lipophilic quinone, ubiquinone, which in man has a side chain of 10 isoprenoid units (Q10). Complex II or succinate dehydrogenase transfers electrons from succinate to ubiquinone. From reduced ubiquinone electrons are transferred to complex III, or cytochrome c reductase, which exists in the membrane as a functional dimer. The small protein cytochrome c mediates electron transfer from cytochrome c reductase to cytochrome c oxidase (complex IV). Finally, electrons are transferred to molecular oxygen which is reduced to water (Figure 1.2) ATP synthesized by complex V is exchanged with cytosolic ADP through a specific adenine nucleotide translocator (ANT) of the IMM (Pebay-Peyroula et al. 2003). The IMM also contains channels, and transporters that translocate inorganic ions and metabolites, including phosphate, thereby determining the compartmentalization of the metabolic functions of mitochondria (Kunji 2004; Robinson et al. 2008)

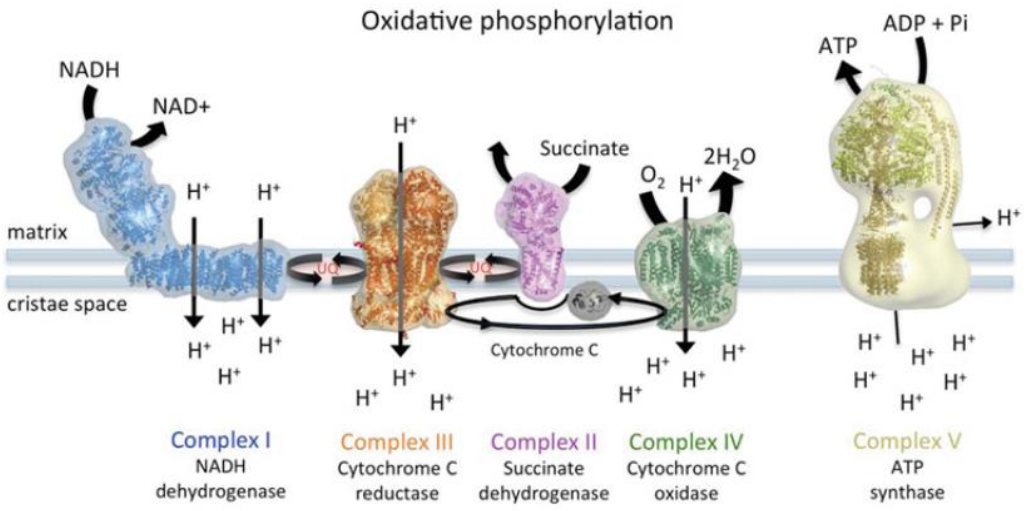

Figure 1.2: Schematic representation of the OXPHOS system. This figure shows individual components of the OXPHOS system. The position of the matrix and cristae or inner membrane is indicated .From (Davies & Daum 2013).

Globally, mitochondria contain ~800 (yeast) to 1500 (human) different proteins. Although the majority of mitochondrial proteins are encoded in the nucleus and post-translationally imported into the organelle by a complex protein-import machinery (Baker et al. 2007), some subunits of the OXPHOS (13 in human) are encoded by the mitochondrial genome (mtDNA). This is a circular double-stranded molecule of approximately 16.5 kb without introns and histone proteins and also encodes rRNA and tRNA. On average, mtDNA is present in two copies per organelle and is maternally inherited.

Defects in mtDNA are associated with mitochondrial diseases, which encompass a wide variety of degenerative diseases, but also with aging, and cancer (Wallace 1999). Deficiencies in OXPHOS appear to be the main pathogenic factors, although other mechanisms are involved, such as generation of reactive oxygen species (ROS) by the respiratory complexes and/or altered apoptotic signaling that are implicated in neurodegenerative diseases (McKenzie et al. 2004).

1.2 F_oF_1 ATP Synthase (Complex V)

The mitochondrial ATP synthase, also named F_oF_1 ATP synthase or complex V, is a 600 kDa multisubunits complex localized in the IMM that uses the energy of the transmembrane proton gradient to drive the synthesis of ATP from ADP and Pi. Its molecular structure and catalytic mechanism were mostly understood by the seminal work of the Nobel Laureates Mitchell (in 1979), Boyer and Walker (in 1997) that revealed its complexity and the functional steps driving the synthesis of ATP.

ATP synthase is also present in the thylakoid membrane of chloroplasts, and in the plasma membrane of bacteria., It is extremely conserved, in spite of its structural complexity and of the early divergence of bacteria, plants and animals (Nelson 1992). Proton translocation and ATP synthesis are coupled by a unique mechanism, subunit rotation. The electrochemical energy contained in the proton gradient is converted into mechanical energy in form of subunit rotation and back into chemical energy as ATP (Stock et al. 2000; Capaldi & Aggeler 2002; Weber & Senior 2003). The enzyme is also able to work in the direction of ATP hydrolysis, sustaining the formation of the proton gradient, when there is loss of membrane potential.

Traditionally, ATP synthase is divided into two subcomplexes, the membrane-embedded F0 subcomplex through which the protons flow, and the peripheral F1 subcomplex that carries the nucleotide binding sites. These sectors are linked by central and peripheral stalks (Stock et al. 2000; Rubinstein et al. 2003; Rubinstein et al. 2005) (Figure 1.3A). Approximately 85 % of the structure of the whole complex is known at high resolution from X-ray crystal structures of constituent domains, which have been assembled into a mosaic structure within the constraints of a cryo-EM map at 18 Å resolution (Baker et al. 2012). Interestingly, 3D classification of images revealed seven distinct states of the enzyme that show different modes of bending and twisting in the intact ATP synthase (Zhou et al. 2015).

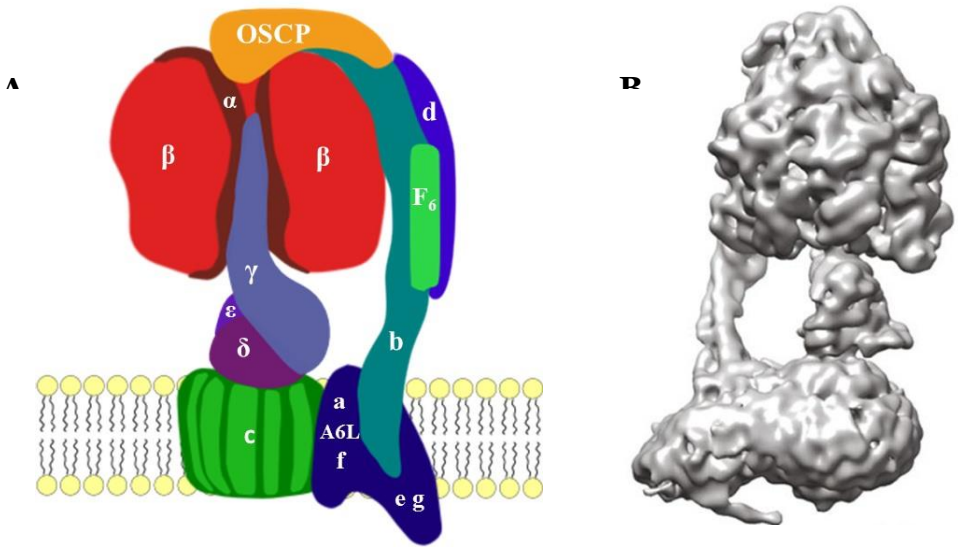

Figure 1.3: The mitochondrial FoF1 ATP synthase. A) subunit organization. Subunits are color-coded and labelled. F1 is the globular catalytic domain made of subunits α_3,β_3 and the three central stalk subunits, γ,δ and ε. The Fo domain is comprised of the c oligomer, subunit a, A6L, e, f, and g and the peripheral stalk subunits b, d, F6 and OSCP**.** From (Antoniel et al. 2014) **B) 3D structure of the whole complex** From (Zhou et al. 2015).

1.2.1 F_o domain

The membrane bound domain, named FO due to the interaction with the specific inhibitor oligomycin, is the site of the proton channel, and during evolution, it has undergone variations in its polypeptide composition. In the simplest form of the enzyme, typical of bacteria like *Escherichia coli*, Fo consists of three different subunits, named a, b and c (Fillingame et al. 2000), with molecular masses of 30.3, 17.2 and 8.3 kDa respectively and stoichiometry $ab_2c_{10\text{-}15}$ (Watt et al. 2010). The c subunits form a ring structure connected to F_1 by the central stalk. The a subunit associates with the c-ring peripherally forming at the interface two half transmembrane water channels through which protons are transported *via* the conserved carboxylic acid present on each c subunit (cAsp61 in *E.coli* and almost always a glutamate in other species). Subunit a also associates with the lateral stalk, which is formed by the homo-dimer of subunits b and by δ subunit located at the top of F_1. Chloroplast and cyanobacteria Fo are composed of four subunits because the two b subunits are not identical (Fromme et al. 1987). The animal mitochondrial enzyme has a more complicated structure. Ten subunits have been originally identified, named a, b, c, F6, d, e, A6L, f, g and oligomycin sensitivity conferring protein (OSCP) (Collinson et al. 1994). The a, b and c subunits share great similarity

with the bacterial subunits, except for subunit c stoichiometry which comprises 10 copies in yeast and only 8 copies in all vertebrates and all or most invertebrates (Watt et al. 2010). Electron cryomicroscopy of *Polytomella* (Allegretti et al. 2015) and bovine (Zhou et al. 2015) ATP synthase recently established that subunit a forms four long, horizontal membrane-intrinsic α-helices, arranged in two hairpins at an angle of approximately 70° relative to the c-ring helices. OSCP is analogous to *E.coli* δ-subunit, whereas the remaining subunits are unique of the mitochondrial complex (Table 1). The membrane-embedded part of F_O also comprises subunits e, f, g and is connected to F_1 by a complex peripheral stalk (or "stator stalk"), composed by one copy each of subunit b, d, F_6 and OSCP (Weber 2006; Rees et al. 2009) and possibly by subunit A6L (Lee et al. 2015). Besides these subunits, two hydrophobic proteins, namely MLQ/6.8-kDa proteolipid(Chen et al. 2007; Meyer et al. 2007), and AGP/DAPIT (Ohsakaya et al. 2011), are associated to the F0 part and interact with the e and g subunits (Lee et al. 2015). Subunit DAPIT is encoded only in the genomes of metazoans and subunit 6.8PL is restricted to vertebrates (Lee et al. 2015). Moreover, in animal mitochondria the e and g subunits interact with the matrix metalloprotein Factor B, named subunit s, which is also in contact with the ADP/ATP carrier (Lee et al. 2008). All together, the mitochondrial membrane domain is constituted by approximately 30 trans-membrane α-helices (Carroll et al. 2009).

1.2.2 F1 domain

The structure of the F1 complex is highly conserved. In all cases it is composed of five different subunits, α through ε, with stoichiometry $\alpha_3\beta_3\gamma\delta\varepsilon$ (Walker et al. 1984; Walker 1985). This protein complex has a total mass of 371kDa and has the shape of a flattened sphere having heigh of 80Å and width of 100Å.

In the F1 sector the α- and β-subunits, which carry the nucleotide binding sites, are arranged alternatively, forming a hexagonal cylinder around the coiled-coil structure of the γ subunit. The α, β and γ subunits from different sources are highly conserved sharing great homology. Conversely, the small δ and ε subunits are not analogous in enzymes of different origin; bacterial and chloroplast δ and ε correspond to OSCP and δ subunit respectively of the mitochondrial ATP synthase, while the ε subunit of the mitochondrial complex has no counterpart in the bacterial enzyme (Walker et al. 1991; Abrahams et al. 1994) (Table 1).

Despite differences among complexes of different origin, the mechanism of active proton transport and ATP synthesis/hydrolysis is highly conserved, as supported by the pioneering use of mitochondrial and chloroplast subunits as functional replacement in the bacterial complexes (Richter et al. 1986; Lill et al. 1993; Burkovski et al. 1994; Puri et al. 2005).

The steady state catalytic mechanism for ATP synthesis/hydrolysis requires all the catalytic sites, which are located in the β subunits at each β-α interface and interact each other in a highly cooperative manner. The ATP (and sometimes ADP) molecules bound to the α subunits at α-β interfaces are not-exchangeable and therefore these sites are considered as non-catalytic, whose role is still unknown.

Table 1 : Equivalence of subunits of ATP synthase from different sources[1].

Mitochondria		E.coli, P.modestum and A.woodii	Chloroplast, cyanobacteria[2] and rhodobacteria[3]
Bovine	**Yeast**		
α	α (ATP 1)	α	α
β	β (ATP 2)	β	β
γ	γ (ATP 3)	γ	γ
δ	δ (ATP 16)	ε	ε
ε	ε (ATP 15)	-	-
OSCP	OSCP (ATP 5)	δ	δ
b	4 or b (ATP 4)	b[4]	b and b' (I and II)
A6L	8 iATP8p (aap 1)	-	-
F6	h (ATP 14)	-	-
a	a (ATP 6) or 6	a	a (IV)
c	9 or c (ATP 9)	c	c (III)
	d (ATP 7)	-	-
e	e (Tim 11)	-	-
f	f (ATP 17)	-	-
g	g (ATP 20)	-	-
-	i/j (ATP 18)	-	-
-	k (ATP 19)	-	-
MLQ/6-8 kDa	-	-	-
AGP/DAPIT	-	-	-

[1]Subunit equivalence is based on sequence homology .[2]*Synechococcus*, [3]*Rhodospirillum rubrum* and *Rhodopsmonas blastica*. [4]ATP synthase from *E.coli* and *P.modestum* have two copies of the b subunit and ATP synthase from chloroplasts, cyanobacteria and rhodobacteria have one copy of each b and b'. The b and b' are homologous. (-) No subunit equivalence. From (Antoniel et al. 2014)

Numerous atomic structures have been resolved : i) of the isolated F1 part from bovine (Abrahams et al. 1996; van Raaij et al. 1996; Orriss et al. 1998; Braig et al. 2000; Menz et al. 2001; Kagawa et al. 2004; Bowler et al. 2007; Bason et al. 2011; Rees et al. 2012) and yeast mitochondria (Kabaleeswaran et al. 2006; Kabaleeswaran et al. 2009),; ii) of bovine F1 in complex with full-length or truncated subunits of the lateral stalk (Rees et al. 2009); and iii) of the bovine F1c8 (Watt et al. 2010) and yeast F1c10 subcomplexes (Stock et al. 1999; Dautant et al. 2010; Giraud et al. 2012). All these structures established that the three β-subunits adopt three different tertiary structures and are in three diverse nucleotide-bound states. According to the original paper published at the beginning of the Nineties (Abrahams et al. 1994) the first conformation, named β_{TP}, hosts the binding site for ATP; the second, called β_{DP}, binds with high affinity ADP and Pi; the third, β_E, does not efficiently bind any nucleotide. This asymmetry supported the binding change mechanism theorized by Boyer (Boyer 1993), according to which the sequential interconversion between these different conformations, driven by the central stalk rotation, enables the catalysis. This is constituted by the γ, δ and ε subunits in chloroplasts and mitochondria and by the γ and ε subunits in bacteria. More recent findings established that β_E is not likely to exist during catalysis and all the three catalytic sites bind nucleotides at any time (Menz et al. 2001; Rees et al. 2012) (Figure 1.4). Differently from β, the three α subunits adopt the same conformation, but are named according to their adjacent β.

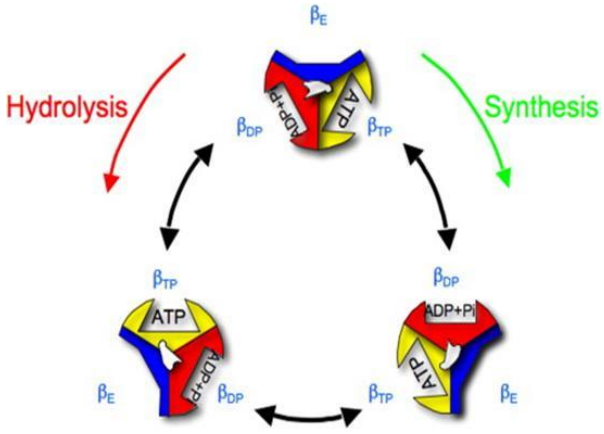

Figure 1.4: Change of the states of three β subunits during hydrolysis or synthesis of one ATP. The rotation occurs in opposite directions during ATP synthesis and hydrolysis, resulting in different sequences and specific interconversion of catalytic sites .From (Yoshida et al. 2001).

1.2.3 Oligomycin sensitivity conferring protein (OSCP)

Located on top of the catalytic F_1 sector in the mitochondrial complex, OSCP makes stable contacts with both F_1 and the peripheral stalk, ensuring the structural and functional coupling between F_O and F_1. Indeed, truncation mutants of N-terminal and C-terminal OSCP showed an impaired coupling or failed to survive (Prescott et al. 1994).

The physical location of OSCP has been defined in the crystal of a F_1-peripheral stalk subcomplex from bovine (Rees et al. 2009). Its N-terminal domain (residues 1-113) contains 6 α-helices, of which helix 1 and 5 provide the binding site (i) for residues 6-17 of subunit α_E (which contacts β_E in $\alpha_3\beta_3$ subcomplex), largely via hydrophobic interactions; (ii) for the N-terminal β-barrel domains of especially the β_{DP}-subunit. These interactions are capable of resisting the torque generated by the rotary motor of the enzyme. The structure of the C-terminal domain of OSCP consists of a β-hairpin, which precisely locates along the α/β interface (Baker et al. 2012), followed by two α-helices, helix 7 and 8, which make extensive helix-helix interactions with the C-terminal of subunit b and with the N-terminal α-helix of subunit F_6 of the lateral stalk. The linker region between the N- and C- domains appears to be flexible, enabling a bending of the peripheral stalk towards the top of F_1 in the intact ATP synthase (Zhou et al. 2015).

1.2.4 Rotational catalysis

The peculiar structural organization of ATP synthase is the base of the catalytic mechanism of the enzyme, which is the smallest rotary motor existing in nature. Boyer originally suggested that Fo is a rotary motor driven by the proton flow, and that F1 is another rotary motor driven by ATP hydrolysis. The two motors have a common stalk (central stalk), but the genuine rotary directions of the two sectors are different. When the free energy liberated by the downward flow of protons is greater than the free energy of ATP hydrolysis, the Fo motor rotates the central stalk in the Fo's genuine direction. The F1 motor is forcibly rotated in its reverse direction, resulting in ATP production in its catalytic sites. If the free energy of ATP hydrolysis is higher, the F1 motor gains control and rotates the stalk in its own direction. Protons are then pumped out by Fo against an uphill potential, resulting in membrane potential generation (Boyer 1993).

It is now widely recognized that during ATP synthesis, the clockwise (viewed from the membrane) c-ring rotation in F_O powered by the proton traslocation into

the mitochondrial matrix trough (half) channels located at the interface of a and c subunits drives the γ subunit rotation within the $\alpha_3\beta_3$ F_1 subcomplex (at about 100 times per second) that takes each of the three catalytic sites through at least three major functional states denoted as β_E, β_{DP} and β_{TP}, thereby synthesizing three ATP molecules from ADP and Pi during each 360° rotation. When the enzyme works in the direction of ATP hydrolysis passing through the β_E, β_{DP} and β_{TP} functional states, drives the counterclockwise rotation of the γ subunit and the c-ring, thereby causing proton traslocation into the intermembrane space.

To reveal the dynamic features of F1 rotation, several single molecule rotational assays (Oosawa & Hayashi 1986; Boyer 1993; Funatsu et al. 1995; Yasuda et al. 1998) have been developed since the method was first developed in 1997 (Boyer 1993). In most assays, the $\alpha_3\beta_3$ F_1 subcomplex is immobilized onto a cover slip, and a rotation marker tag is fixed to the protruding part of the γ subunit allowing the visualization of its ATP-driven rotation. While a fluorescently labeled actin filament was used as the rotation marker in the pioneering studies, micron-sized plastic beads or gold colloids of 40-60 nm are frequently used at present. In some experiments, a magnetic bead was attached to the subunit γ , which was controlled by an external magnetic field to first force the backward (clockwise) rotation of F_1, leading to ATP synthesis. When the magnetic field was switched off, the F1 molecule underwent anticlockwise rotation at a speed proportional to the amount of synthesized ATP (Rondelez et al. 2005; Nakanishi-Matsui et al. 2013). A further technical sophistication used a sub-millisecond resolution camera to detect the rotation of gold beads attached to the γ subunit of the $\alpha_3\beta_3\gamma$ subcomplex along with fluorescence changes of an ATP hydrolysable analog. This technique allowed to display in real time the binding and release of nucleotides at the three catalytic sites simultaneously with the γ rotation (Adachi et al. 2007). Single molecule technology studies have been applied also to the whole F_oF_1 complexes from *Propionigenium modestum* and *Escherichia coli*. Rotation was probed with probes attached to the c-ring in the immobilized F_oF_1 and, as expected, occurred in the opposite direction when c-ring rotation was driven by ATP or by proton-flow (Ueno et al. 2005).

In accordance with its pseudo three fold symmetrical structure, F1 hydrolyzes threes ATP molecules per rotation. The γ subunit rotation is not continuous, but rather proceeds in 120° steps, each driven by hydrolysis of one ATP molecule (Yasuda et al. 1998; Rondelez et al. 2005). In the bacterial enzyme these consist of substeps, the first of 80° driven by ATP binding and the second of 40° driven by release of ADP

or Pi (Adachi et al. 2007), whose angular velocity is debated (Martin et al. 2014). These substeps differ from those of human F1, in which ATP binding to one β-subunit occurs at 0°, Pi release from another β-subunit at 65° and ATP hydrolysis on the third β-subunit at 90°, demonstrating that chemomechanical coupling angles of the γ subunit are tuned during evolution (Suzuki et al. 2014).

Rotary subunit movements within the whole bacterial H^+-ATP synthase were also monitored in real time and with subnanometre resolution by a single-molecule FRET (fluorescence resonance energy transfer) approach, which uses a double-labelled enzyme incorporated in liposomes driving either ATP hydrolysis or ATP synthesis (Diez et al. 2004; Ernst et al. 2012).

Critical residues in the catalytic sites are βLys162 and βThr163 of the P-loop, βGlu188 and αArg373 (bovine numbering), which are highly conserved (Fig. 1.5). The hydrolysis of an ATP molecule bound to the βDP-subunit proceeds via the in-line nucleophilic attack of the γ-phosphate by a water molecule activated by residue βGlu188. It has been proposed that in the bovine enzyme the αR373 plays a critical role in this step by correctly positioning the γ-phosphate of the nucleotide (Rees et al. 2012). The reaction advances via formation of a transition-state intermediate, as observed in the transition analog structure of bovine F_1 (Menz et al. 2001), followed by scission of the terminal phosphate and release of products.

In the bacterial enzyme the conserved arginine of α subunit (αR376 – E. coli numbering) seems to be important for conformational communication among the three catalytic sites, (Futai et al. 2012), which entails the tremendous acceleration of ATP hydrolysis rates upon binding of ATP at lower affinity to the second and more so the third catalytic sites.

It is important to notice that the catalytic process requires the presence of Mg^{2+}, which contributes with γ subunit in determining the asymmetry of the catalytic sites necessary for the binding-change mechanism (Weber et al. 1996). Bovine F_1 crystal structures showed that Mg^{2+}, interacts directly with βThr163, with ATP atoms βO_2 and γO_2, and through three water molecules with βArg189, βGlu192 and βAsp256 (Rees et al. 2012) (Figure 1.5).

On the available evidence it appears that during catalysis, in the bovine enzyme at least, both phosphate and the magnesium ion are released before ADP (Rees et al. 2012).

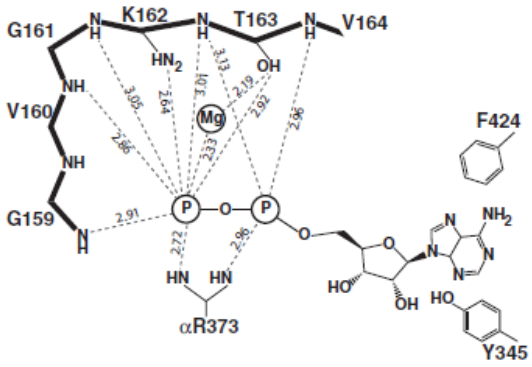

Figure 1.5: Localization of Mg ion in the catalytic sites of β_{DP} and β_E subunits in bovine ATP Synthase : Residues involved in the interaction with Mg2+ are depicted, distances are expressed in Å From (Rees et al. 2012).

Mg^{2+} can be replaced by other divalent cations including Ca^{2+}, the ionic radius being the chief factor determining their ability to activate the ATPase activity (Selwyn 1968). Intriguingly, Ca^{2+} ions, differently from other divalent cations with similar ionic radius, only support ATP hydrolysis, which is not coupled to proton translocation both in bacteria (Nathanson & Gromet-Elhanan 2000) and in mammals (Papageorgiou et al. 1998). In spite of this, CaATP was capable of supporting rotation of γ subunit attached to an actin filament in a similar way to MgATP, as demonstrated in a highly active hybrid F_1-ATPase consisting of α /β subunits from *Rhodospirillum rubrum* and γ subunit from spinach chloroplasts (Tucker et al. 2004). Replacement of the equivalent βT163 (bovine numbering) with serine in ATP synthase from *Rhodospirillum rubrum* produced a mutant unable to catalyze the proton-decoupled Ca^{2+}-dependent ATP hydrolysis while maintaining proton-coupled ATP synthesis as well as Mg^{2+}- and Mn^{2+}-dependent ATP hydrolysis (Nathanson & Gromet-Elhanan 2000). These observations suggest that Ca^{2+} mayinduce different conformational changes in the catalytic sites compared to Mg^{2+} (Bernardi et al. 2015).

1.2.5 ATP Synthase assembly process

The mitochondrial F_oF_1 complex is composed of both nuclear and mitochondrial gene products. In yeast the three Fo core proteins a, A6L and c, named Su6, Su8 and Su9 respectively, are encoded by mtDNA, while in mammals only subunits a and A6L are encoded by mitochondrial genome. This arrangement highlights the complexity of enzyme assembly, which requires accessory factors

whose definition is still under investigation (Wittig & Schägger, 2008). Altogether 9 factors have been identified in yeast, but, until now, the role of only five of them has been defined. Three factors mediate the F_1 formation (Atp11p, Atp12p and possibly Fmc1p) (Ackerman 2002; Lefebvre-Legendre et al. 2001) and two the Fo assembly (Atp10p and Atp22p) (Helfenbein et al. 2003; Rak et al. 2011). Recent findings in yeast have unveil that the coordinated expression of the ATP synthase genes depends on the cytosolic complex AME, which is made of two aminoacyl-t-RNA synthetases (cERS and cMRS) attached to the anchor protein Arcp1 (Frechin et al. 2014). In mammalian cells only two factors are known, which are orthologus to yeast F_1 assembly factors.

The assembly process is best characterized in yeast, where recent *in organello* pulse-labeling and pulse-chase experiments have enabled to identify three different assembly intermediates and to demonstrate that the whole enzyme is formed by two separate pathways that converge to form the ATP synthase from their respective end-products. One pathway leads to the formation of F_1, which was already known to assemble as an independent unit (Tzagoloff et al. 1969), and of the Su9- ring. These two sub-complexes subsequently combine to constitute the F_1/Su9-ring end-product. The other pathway leads to the formation of the Su6/Su8/stator sub-complex, which, in addition to Su6 and Su8, contains the chaperone Atp10p and additional still undefined proteins of the lateral stalk (Rak et al. 2011)

A similar assembly strategy has been proposed for human ATP synthase. Indeed, when expression of the lateral stalk d-subunit was knocked-down, human cells accumulated two subcomplexes, one containing the F_1-c-ring subcomplex and the other containing stator stalk components ("b-e-g" complex). F_1-c-ring was also formed when expression of mtDNA-coded a-subunit and A6L was suppressed, suggesting that the central rotor and the stator stalk are formed separately and they assemble later (Fujikawa et al. 2015).

It has been proposed that this bifurcated process may recapitulate some of the evolutionary events that gave rise to this enzyme. The F_1/Atp9p ring intermediate could be the product of an evolutionary event, which enabled a passive channel to be converted to an active ion transporter. The function of the ancestral protein from which the Atp6p/Atp8p/stator complex evolved is more difficult to envision. Its function may have been adapted to further modify the ATP-dependent ion pump into the present energy transforming machine (Rak et al. 2011).

1.2.6 Oligomers

ATP synthase is commonly purified as a functional monomer but this seems not to be its physiological state in mitochondrial membranes. Electron microscopic analyses of *Paramecium multimicronucleatum* mitochondria first showed F_1 complexes arranged as double rows of particles that wind around tubular cristae of the inner mitochondrial membrane (Allen et al. 1989). Subsequent studies in yeast demonstrated that these supra-molecular structures are formed by dimers of ATP synthase associated in oligomers that play a special role in defining mitochondrial morphology, being involved in cristae formation (Paumard et al. 2002). Additional proposed roles of the ATP synthase oligomers are higher efficiency (Bisetto et al. 2007; Strauss et al. 2008) and higher stability (Thomas et al. 2008a)

The structural role of ATP synthase has been further demonstrated by recent electron cryotomagraphy studies showing that in different types of mitochondria (bovine heart, potato and three fungi) ATP synthase dimers and oligomers are present exclusively on tightly curved cristae edges, where they interact within the IMM through the Fo subunits (Figure 1.6A) (Davies et al. 2011; Davies et al. 2012). These studies also revealed a fixed angle of 86° between the monomers (Davies et al. 2012), in contrast with previous single-particle electron microscopy images which indicated angles ranging from 40° (Couoh-Cardel et al. 2010; Minauro-Sanmiguel et al. 2005) to 70-90° (Dudkina et al. 2006; Thomas et al. 2008b). Based on this observation, the authors proposed that the shape of the F_oF_1 ATP synthase dimer was sufficient to deform the lipid bilayer and drive the self-assembly of the F_oF_1 ATP synthase dimers into rows (Davies et al. 2012). However, more recent studies based on single-particle cryo-EM map of detergent solubilised bovine F_oF_1 ATP synthase monomers (Baker et al. 2012) and on a combination of electron cryo-tomography, subtomogram averaging, and electron crystallographic image processing of intact bovine F_oF_1 ATP synthase in 2D membrane crystals (Jiko et al. 2015) proposed that the monomers alone can deform the lipid bilayer and that this membrane deformation is likely to be a prerequisite for the self-association of F_oF_1 ATP synthases into dimers and of dimers into rows. Interestingly, ATP synthase dimers have also been observed in chloroplasts of algae, where they appear to be more susceptible towards environmental effects, e.g. Pi concentration (Seelert & Dencher 2011), but not in bacteria.

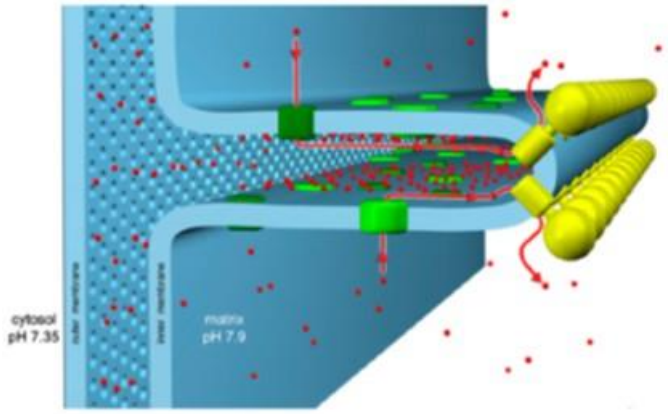

Figure 1.6 Disposition of ATP Synthase oligomers in mitochondrial cristae. The ATP synthase forms dimers rows (yellow) at the cristae tips, whereas the proton pumps of the electron transfer chain (green) reside predominantly in the adjacent membrane regions. From (Davies et al. 2011).

In yeast the structural properties of dimers have been characterized by genetic approaches and cross-linking analyses, which established preferential interactions within the IMM mainly through the Su6(a) (Wittig & Schägger 2008), Su4(b) (Spannagel et al. 1998), e (Everard-gigot et al. 2005) and g subunits (Bustos & Velours 2005) and also through subunit h(F6) and the yeast-specific subunit i (Fronzes et al. 2006). In keeping with its general occurrence, the involvement of subunit a (Wittig et al. 2010), e (Bisetto et al. 2008; Johann Habersetzer et al. 2013)and g (Habersetzer et al. 2013a) in ATP synthase dimer/oligomer formation has been demonstrated also in mammals. Moreover, a stabilizing effect on mammalian ATP synthase dimers has been reported for the inhibitor protein IF_1 (García et al. 2006; Campanella et al. 2008; Bisetto et al. 2013)and the matrix metalloprotein Factor B, which interacts with e and g subunits of F_O (Belogrudov 2009). In addition, a second interface (named the oligomerization interface) has been described in yeast; this interface was stabilized through e/e and g/g interactions allowing oligomer formation (Habersetzer et al. 2013b). However, the existence of an oligomerization interface has been criticized based on the above cited electron cryotomography data, which evidenced variable distance between dimers making direct protein contacts difficult (Davies et al. 2012).

Both in yeast (Habersetzer et al. 2013b; Wittig & Schägger 2008) and mammals (Bisetto et al. 2013; Wittig et al. 2010; Habersetzer et al. 2013a) the stabilizing contribution of the different subunits seems to be additive and low amounts of ATP synthase dimers and oligomers have been detected by native PAGE

also in mutants lacking one or more of the above mentioned subunits, such as ρ° cells depleted of a- and A6L-subunits (Wittig et al. 2010), and yeast (Paumard et al. 2002) and human (Habersetzer et al. 2013a) cells totally or partially depleted of e- and g-subunits. Surprisingly, down-regulation of e- and g-subunits in HEK and HeLa cells not only affected ATP synthase dimerization/oligomerization, but also the OXPHOS activity and the mitochondrial network (Habersetzer et al. 2013a).

1.2.7 ATP Synthase interactors

Beside the formation of oligomers, ATP synthase activity is optimized by biochemical events, such as by reversible association of regulatory peptides and by post-translational modifications (PTMs). A high number of modifications has been identified in the various subunits of ATP synthase, including phosphorylation, acetylation, trimethylation, nitration, s-nitrosylation and tryptophan oxidation (Covian & Balaban 2012). However, in most cases it remains unknown what are the signalling pathways responsible for these PTMs, in which tissues or biological conditions these modifications occur, how they impact on the biochemical activity of the target protein and of the holo-enzyme, and how much of the target protein can be modified (Bernardi et al. 2015).

The **endogenous inhibitor protein IF_1** is considered as a major determinant in the regulation of ATP synthase (Green & Grover 2000; Campanella et al. 2009). IF_1 is evolutionarily conserved from yeast to human and reversibly binds to F_1 with a 1:1 stoichiometry fully inhibiting the enzyme activity.

IF_1 is encoded in the *ATPIF1* gene and in humans three different isoforms of the protein due to alternative splicing of the IF_1 mRNA primary transcript have been described (Sánchez-Cenizo et al. 2010). In yeast, along with IF_1, two additional proteins, namely Stf1 and Stf2 (stabilizing factor 1 and 2) have been found, whose role is still debated (Venard et al. 2003).

The levels of IF_1- F_1 interactions are governed by the factors promoting release and rebinding, i.e. membrane potential and MgATP (Lippe et al. 1988). In addition, IF_1 binding is strongly favored by low pH. Indeed, in mammalian mitochondria low pH favours the formation of the inhibitory dimeric IF_1, while the increase in pH provokes the formation of tetramers hence masking the N-terminal inhibitory region of IF_1 (Cabezón et al. 2000). This regulation involves three key histidine and one glutamic acid (H49, H55, H56 and E26 – bovine numbering) (Bason et al. 2011).

Consistently, treatment of bovine IF_1 with the histidine reagent diethyl pyrocarbonate (DPC) prevented its binding to the inner membrane at acidic pH (Panchenko & Vinogradov 1985). In contrast, the yeast IF_1, which lacks the above mentioned histidine, can be found as an inhibitory monomer at low pH and as a non-inhibitory dimer at high pH (Robinson et al. 2013).

IF_1 blocks the rotation of the enzyme nanomotor by inserting its N-terminal inhibitory domain between the C-terminal domains of the α_{DP} and β_{DP} subunits and the coiled-coil region of the γ subunit. The mechanism of IF_1 inhibition is quite complex and fundamental insights have been recently obtained by point mutations and X-ray crystallography of bovine (Bason et al. 2011; Bason et al. 2014a) and yeast IF_1 (Robinson et al. 2013). Interestingly, the pathway from the initial interaction of IF_1 to F_1 to the final inhibited IF_1-F_1 complex implies that the rotor of the enzyme turns through two 120° steps hydrolyzing two ATP molecules, which are trapped in bovine IF_1 as Mg^{2+} -ADP complexes in both β_{DP} and β_{TP} subunits, while β_E is empty (Bason et al. 2011; Bason et al. 2014). In spite of a similar structure, the final inhibited IF_1-F_1 complex of yeast still contains an ADP molecule (without Mg^{2+} and Pi) in the catalytic site of β_E, indicating that IF_1 has arrested the catalytic cycle at a slightly different point (Robinson et al. 2013). Interestingly, the novel inhibitor ζ subunit of the F_OF_1-ATPase of *Paracoccus denitrificans* similarly blocks the intrinsic rotation of the nanomotor (García-Trejo et al. 2016).

At variance from IF_1 binding, the mechanism of IF_1 release from F_1 in response to the formation of a membrane potential is less clear; it has been proposed that the reversal of the direction of γ rotation to drive ATP synthesis destabilizes IF_1 binding, leading to its ejection (Bason et al. 2011; Bason et al. 2014).

The activity of IF_1 as an inhibitor of the ATP synthase is also regulated by PTMs. Indeed, phosphorylation of S39 in human IF_1 by the action of a mitochondrial cAMP-dependent protein kinase A hampers its interaction with the ATP synthase, indicating that only the dephosphorylated IF_1 interacts with the enzyme (García-Bermúdez et al. 2015).

IF_1 is considered responsible for the beneficial (at least partial) inhibition of F_oF_1 during ischemia both in *in vitro* experimental models as well as *in vivo* (Rouslin & Broge 1996; Di Pancrazio et al. 2004; Green & Grover 2000; Campanella et al. 2009). Unexpectedly, IF_1-knockout mice grew without defects, but their behavior against stressful situations have not been tested (Nakamura et al. 2013).

New emerging roles of IF_1 are related to metabolic reprogramming of cancer cells, where IF_1 overexpression causes inhibition of oxidative phosphorylation, triggering mitochondrial hyperpolarization and ROS production, which is able to reprogram the nucleus of the cell to confer cell resistance against oxidative stress (Sánchez-Aragó et al. 2012). Consistently, recent findings indicate that a high expression level of IF_1 is a bad predictor of survival and recurrence of the disease in liver, bladder, gastric and glioma cancer patients (Song et al. 2014; Yin et al. 2015; Wei et al. 2015; Wu et al. 2015). However, in breast and colon carcinomas the overexpression of IF_1 predicts much better patient's prognosis (Sánchez-Aragó et al. 2013), indicating that IF_1 overexpression affects carcinogenesis in a tissue specific manner.

Recently it has been reported that ATP synthase binds another regulatory protein, which interacts with the OSCP subunit of the lateral stalk: **Sirtuin3** (Vassilopoulos et al. 2014; Wu et al. 2013). It is possible that Sirtuin3 acts as sensing protein whose loss of function may induce ATP Synthase dysfunction and might indirectly compromise mitochondrial respiratory function capacity by affecting the formation of mitochondrial supercomplexes and their electron transfer function (Vassilopoulos et al. 2014). Also **p53** has been reported to interact with OSCP (Bergeaud et al. 2013), taking part in the assembly or stabilization of the mature F_oF_1 complex. This finding suggests that the mitochondrial fraction of p53, although very low, may be an important regulator of mitochondrial physiology potentially exerting tumor suppression (Bergeaud et al. 2013). However, interaction domains between Sirtuin3and p53 with OSCP have been not yet determined.

Another interactor that induces the enzyme inhibition is the **Protein Kinase Cδ** which binds to the d subunit of the F_oF_1 lateral stalk (Nguyen et al. 2010). Others interactors conversely improve the enzyme performance, such as **S100A1,** which interacts with the F_1 moiety in a Ca^{2+}-dependent manner in cardiomyocytes (Boerries et al. 2007; Kraus et al. 2010), and **Bcl-X_L** that also binds to F_1 and increases the aerobic ATP production in healthy neurons by decreasing the membrane leak conductance (Alavian et al. 2011). Indeed, neurons overexpressing Bcl-x_L, have higher ATP levels with respect to the cells in which endogenous Bcl-x_L is depleted or inhibited.

A new, intriguing interactor is the **CyPD**, a peptidyl-prolyl *cis-trans* isomerase which binds to the OSCP subunit inhibiting both the hydrolytic and synthetic activity of ATP synthase (Giorgio et al. 2013;). CyPD is the unique mitochondrial isoform of

CyPs in mammals (Giorgio et al. 2010), it is involved in protein folding (Fischer et al. 1989; Takahashi et al. 1989; Galat & Metcalfe 1995) and, most importantly, plays a crucial role in the regulation of the mitochondrial permeability transition pore (PTP), a conserved high-conductance channel located in the IMM (Bernardi et al. 2015). The identification of CyPD interaction with the OSCP subunit of ATP synthase was an essential step for the identification of the molecular nature of PTP. (*For a further description see paragraph 1.4.1).*

1.3 Permeability transition pore

The first description of permeability transition (PT) can be found in a 1976 manuscript published in The Journal of Biological Chemistry by Douglas Hunter, Robert Haworth and James Southard where they concluded that Ca^{2+} addition to isolated cow heart mitochondria induced a "...nonspecific increase in the permeability of the inner membrane, resulting in entry of sucrose into the matrix space and the observed configurational transition (swelling) of mitochondria" (Hunter et al. 1976). Further, they showed that this process required the energized uptake of Ca^{2+} through a ruthenium red-sensitive mechanism now known to be the mitochondrial calcium uniporter (MCU), the genetic identity of which was recently defined (De Stefani et al. 2011; Baughman et al. 2011); and that the PT resulted in uncoupling of oxidative phosphorylation. The same group followed this discovery with numerous reports detailing the nature of the PT and its role in physiology that have largely held to date. The authors concluded in subsequent studies that the channel is gated in a Ca^{2+}-specific manner and that its opening imparts permeability to solutes up to 1.5kDa in size (Hunter et al. 1976; Hunter & Haworth 1979).

The PTP hypothesis, despite being described in mitochondria from different species, was not greeted with enthusiasm by the scientific community, because it was in contrast with the chemiosmotic theory, which had just been recognized with the award of the Nobel Prize to Peter Mitchell in 1978 (Mitchell 1979).

An important turning point was the discovery that the PT can be desensitized by submicromolar concentrations of cyclosporine A (CsA). Fournier et al. first described the enhanced ability of CsA-treated mitochondria to accumulate high loads of Ca^{2+} (Fournier et al. 1987). CsA is well known to be a potent immunosuppressant able to inhibit calcineurin signaling after complex formation with CyPA (Clipstone & Crabtree 1992). Available evidence indicated that CsA affects the pore independently of calcineurin. Indeed, Pfeiffer's group proposed that CsA bound a modulatory entity

specific to pore formation (Broekemeier & Pfeiffer 1989), which was then identified as the matrix CyPD, whose enzymatic activity is inhibited by CsA with a matching inhibition of the PTP (Connern & Halestrap 1992; Nicolli, Nicolli, et al. 1996; Woodfield et al. 1997; Griffiths & Halestrap 1991)

These discoveries provided a protein regulator to the PTP (CyPD), and a drug (CsA) to test its occurrence in cells and living organisms. Through the use of CsA the occurrence of PTP opening in cell death (Crompton & Costi 1988) could be tested in a series of pioneering studies in hepatocytes subjected to oxidative stress (Broekemeier et al. 1992; Imberti et al. 1992) or anoxia (Pastorino et al. 1993), as well as in cardiomyocytes (Duchen et al. 1993) and isolated hearts (Griffiths & Halestrap 1995) exposed to ischemia followed by reperfusion. The realization that a whole spectrum of cell death modalities exists (Galluzzi et al. 2015) and that PTP is involved in several of them (Lemasters et al. 2002; Orrenius et al. 2015) resulted in a vastincrease of interest in the phenomenon of PT over the last 30 years, as testified by over 5,000 publications on regulation of the PTP and its role in cell death (Bernardi et al. 2015).

Another important point was the characterization of the biophysical properties of the PTP by using patch-clamping techniques. In the early 1990s Szabò and Zoratti found a large conductance channel located in the IMM referred to as the mitochondrial megachannel (MMC). This channel was inhibited by CsA and other PTP regulators (such as Mg^{2+} and ADP), therefore the authors hypothesized that the MMC and the PTP were expression of the same entity and were constituted by the same molecular components (Bernardi 1992; Szabó et al. 1992). The channel shows a maximum conductance in the range of 0.9 to 1.3 nS (Szabó & Zoratti 1991) and, in its fully open conformation, its apparent diameter is about 3 nm, thus able to allow diffusion of ions and of solutes with molecular masses up to 1.5 kDa .

MMC presents different conductance states and in particular one of these has a conductance that is half of the maximum, suggesting that the channel has a binary structure . Electrophysiology has greatly contributed to our understanding of the PTP (Szabo & Zoratti 2014).

1.3.1 Regulation of the PTP

The consequences of PTP opening depend on the open time of individual pores and on the number of open pores per mitochondrion at any given time. Measurements of the membrane potential resolved in individual mitochondria demonstrated transient and asynchronous cycles of depolarization-repolarization, which over time tended to become long-lasting (Hüser et al. 1998). When PTP opening is persistent, collapse of the proton gradient prevents ATP synthesis and ATP hydrolysis by the ATP synthase worsens ATP depletion. In mammalian mitochondria persistent PTP opening is also followed by equilibration of ionic gradients and solutes up to 1.5 kDa, which may cause swelling, cristae unfolding and eventually OMM rupture (Bernardi et al. 2015).

Numerous studies demonstrated that the pore open–closed transitions are highly regulated by multiple effectors the main of which are discussed below (Figure 1.7).

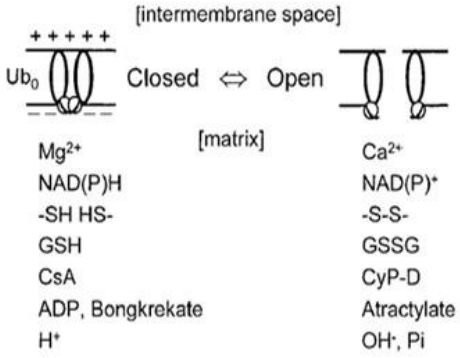

Figure 1.7 Matrix and membrane regulators of PT.
From (Bernardi 1999).

Ca^{2+} ions. As already mentioned, **matrix Ca^{2+}** plays a key role in the induction of the PTP, but the mechanism is still undefined. The threshold Ca^{2+} load required for PTP opening (the Calcium Retention Capacity,CRC) varies with the experimental conditions, in particular the presence of Pi (see below). **Matrix Mg^{2+}** desensitizes the PTP, and the effect is synergistic with that of **adenine nucleotides**. The desensitizing effect is also seen with other divalent cations that are transported by the MCU, indicating that the Ca^{2+} binding site in the matrix can be competitively inhibited by other Me^{2+} ions, such as Mn^{2+} and Sr^{2+} (Bernardi et al. 1992; Szabó et al. 1992). On the other hand, all these Me^{2+} ions, including Ca^{2+} itself, decrease the

probability of pore opening through an external binding site that does not require cation uptake (Bernardi et al. 1992).

Matrix inorganic phosphate is the most puzzling PTP effector. In mammalian mitochondria Pi is a classical inducer of the PTP, in spite of the fact that increasing concentrations of Pi decrease matrix free [Ca^{2+}] (Zoccarato & Nicholls 1982). On the other hand, Pi can inhibit the PTP in CyPD null mouse liver mitochondria, suggesting that the inducing effects of Pi may depend, in part at least, on CyPD (Basso et al. 2008; Azzolin et al. 2010). This result is particulary intriguing because Pi is an inhibitor rather than an inducer of the PT in yeast (Jung et al. 1997; Yamada et al. 2009) and in *Drosophila melanogaster*¸ where the PTP cannot be desensitized by CsA (von Stockum et al. 2011).

The PT is strictly modulated by **matrix pH**. The optimum matrix pH for PT occurrence is about 7.3, and both an increase and decrease lead to decreased probability of PTP opening (Figure 1.8). An acidic pH locks the pore in the closed conformation through reversible protonation of still-unidentified His residues that can be blocked by DPC, whilst the mechanism of inhibition by pH > 7.4 is still unknown (Nicolli et al. 1993; Petronilli et al. 1993). His126 of CyPA plays an important role both in ligand binding and in catalysis (Yu & Fesik 1994), but PTP modulation by matrix pH was not affected by genetic ablation of CyPD (i.e, in *Ppif*$^{-/-}$ mice) demonstrating that the PTP-regulatory His are located on the PTP (Basso et al. 2005). It should be mentioned that in energized mitochondria an acidic matrix pH can promote rather than desensitize the PTP because it increases the rate of Pi uptake, worsening tissue damage in ischemic and postischemic acidosis (Kristian et al. 2001).

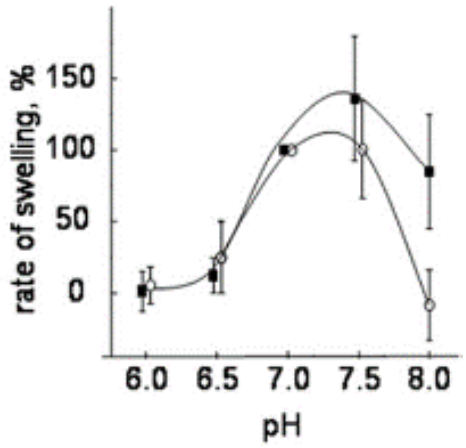

Figure 1.8 Effect of pH on the PTP: CyPD null (close symbol) and wild-type (open symbol) mouse liver mitochondria were treated at different pH and the rate of permeabilization was evaluated after Ca^{2+} addition .From (Basso et al. 2005).

The PTP is **voltage-dependent** in the sense that that inside-negative $\Delta\Psi m$ tends to stabilize the PTP in the closed conformation while the open state is favored by depolarization (Bernardi et al. 1992), as confirmed at the single channel level (Zoratti & Szabó 1994). The existence of a voltage sensor that may comprise critical Arg residues has been proposed, as suggested by modulation of the PTP voltage dependence by Arg-selective reagents (Eriksson et al. 1998; Johans et al. 2005). This mechanism could contribute to explain the effects of membrane-perturbing agents on the PTP. In general, amphipathic anions, such as fatty acids produced by phospholipase A2 (PLA2) (*e.g.* arachidonic acid) mimic a depolarization and favor the PT. Instead, polycations such as spermine, amphipathic cations such as sphingosine and trifluoroperazine, and positively charged peptides mimic a hyperpolarization and inhibit pore opening (see (Bernardi et al. 2006; Rasola & Bernardi 2007)for review). Control by the proton electrochemical gradient provided a conceptual framework to reconcile the PTP with chemiosmosis (Bernardi 1999).

The voltage-dependence in turn is modulated by **redox events.** Pore opening is strongly promoted by oxidation of pyridine nucleotides ($NADH/NAD^+$ and $NADPH/NADP^+$) (Costantini et al. 1996), and by a dithiol-disulfide interconversion at two distinct, matrix- and intermembrane space exposed sites. These can be discriminated by the use of proper oxidants and reductants. The membrane permeant dithiol reagent phenylarsine oxide (PhAsO) cross-links matrix-exposed internal cysteins (Cys), and this can be prevented by low concentrations of *N*-ethylmaleimide (NEM) (Petronilli et al. 1994) or monobromobimane (Costantini et al. 1995). A second redox-sensitive site whose oxidation increases the probability of PTP opening is affected by the membrane-impermeant oxidant copper-*o*-phenantroline [Cu(OP)2]; oxidation of this site is inhibited by dithiotreitol and β-mercaptoethanol but not by monobromobimane (Costantini et al. 1998).

It appears likely that oxidation of critical PTP thiols mediates the inducing effects of peroxides and redox-cycling agents, which are indeed prevented by low concentrations (Ki about 5 μM) of NEM and monobromobimane (Petronilli et al. 1994).

The PTP open probability increases with electron flux within complex I (Fontaine et al. 1998) and this finding led to the discovery that the PT is regulated by **quinones**: Ubiquinone 0 or decylubiquinone prevent pore opening and their inhibitory effects can be relieved by pore-inactive quinones (Walter et al. 2002).

Provided that Pi is present, also **rotenone** desensitizes the PTP. The potency of the drug has been correlated with the CyPD expression levels, the less CyPD mitochondria express, the more potent rotenone is in inhibiting the PTP (Li et al. 2012). It appears likely that PTP modulation by complex I is mediated, in part at least, by production of ROS. Indeed, oxidation of succinate, which induces reverse electron flow at complex I, greatly favors ROS production and PTP opening, both events being prevented by rotenone (Li et al. 2012).

The PTP is regulated by two inhibitors of the ANT: **bongkrekate** and **atractylate**. Both compounds inhibit the ANT yet have the same effect on pore opening, which is inhibited. This set of observations was one of the bases for the proposal that the PTP forms from the ANT (Woodfield et al. 1998), which was disproved later by genetic studies as discussed in the next paragraph. To explain the effects of these ANT inhibitors a modulation by the surface potential, which in turn may affect the PTP open-closed transition through the voltage sensor, has been proposed (Bernardi, 2015).

The PT is primarily an IMM event, as it also occurs in mitoplasts, i.e. in mitochondria stripped of the OMM (Šileikytė et al. 2011), yet the OMM plays a role in pore modulation. Indeed, PTP induction by high concentrations (0.5-1.0 mM) of NEM and other substituted maleimides and by hematoporphyrin plus high light doses, a treatment that leads to the production of singlet oxygen (Petronilli et al. 2009), requires an intact OMM (Šileikytė et al. 2014).

1.3.2CyPD

Cyclophilins (CyPs) can be identified in the genomes of mammals, plants, insects, fungi and bacteria; they all share a common domain of approximately 109 amino acids, the CyP-like domain, which is endowed with peptidyl-prolyl *cis–trans* isomerase (PPIase) activity (Wang & Heitman 2005). In humans 16 CyPs isoforms have been found (Wang & Heitman 2005), with cytosolic CyPA representing the most abundant one and CyPD the unique mitochondrial CyP isoform.

The evolutionary conservation of the PPIase activity among species suggested that this can be an important function of the CyPs. However, and somewhat surprisingly, *Saccharomyces cerevisiae* mutants lacking all 12 yeast CyPs were viable, and the phenotype of the dodecuplet mutant resulted from simple addition of the subtle phenotypes of each individual mutation (Dolinski et al. 1997). This striking

finding led the authors to propose that each CyP instead may regulate a restricted number of unique partner proteins (Dolinski et al. 1997). In keeping with this prediction, CyPs have been shown to be involved in a variety of pathophysiological processes including inflammation and vascular dysfunction (Jin et al. 2004; Kim et al. 2004; Kim et al. 2005; Arora et al. 2005), wound healing (Kong et al. 2007), innate immunity to HIV (Sokolskaja & Luban 2006), hepatitis C infection (Flisiak et al. 2007), host–parasite interactions (Bell et al. 2006) , tumor biology (Yao et al. 2005), besides the PTP regulation.

Cs (Cyclosporins) are cyclic undecapeptides known to bind CyPs and to inhibit their PPIase activity. CsA is the most studied (Borel et al. 1977); its ability to prevent the immune response has revolutionized medicine, allowing organ transplantion to become a standard therapeutic practice. As mentioned above, interaction of CsA with cytosolic CyPA generates a complex that acquires the ability to bind, and inhibit, the cytosolic, Ca^{2+}-activated phosphatase calcineurin (Liu et al. 1991). As a consequence of calcineurin inhibition, its substrate phospho-NFAT is no longer dephosphorylated and therefore unable to translocate to the nucleus and trigger the IL-2-dependent activation of the immune response against the transplant (Clipstone & Crabtree 1992; Walsh et al. 1992). Work with mutants of human CyPA has allowed a clear separationof the PPIase activity of the protein from CsA binding and calcineurin inhibition (Zydowsky et al. 1992).

As already mentioned, CyPD is the mitochondrial target for CsA and modulates the PTP by decreasing the Ca^{2+} load required for pore opening, an effect that is prevented in the presence of CsA (Crompton & Costi 1988; Connern & Halestrap 1992; Woodfield et al. 1997). This has been definitely proven by the crystal structure of human CyPD in complex with its inhibitor CsA obtained at 0.96 Å resolution (Kajitani et al. 2008) and by the genetic ablation of the *Ppif* gene (which encodes for CyPD) in the mouse (Baines et al. 2005; Basso et al. 2005; Nakagawa et al. 2005; Schinzel et al. 2005). CyPD-null mice showed no overt phenotype and no obvious changes in mitochondrial function. As expected, CyPD-null mitochondria were desensitized to Ca^{2+}, as opening of the PTP required about twice the Ca^{2+} load necessary in wild-type mitochondria, and were insensitive to CsA. Other than for the requirement of higher Ca^{2+} loads, the PTP response to a variety of modulators was similar in mitochondria from wild-type and CyPD null mice, thereby demonstrating that CyPD has all the key aspects of a PTP modulator but is not an essential structural component of the PTP. Consistently, the electrophysiological features of

the PTP from CyPD-null mitochondria were indistinguishable from those of wild-type individuals (De Marchi et al. 2006). Moreover, yeast and Drosophila PTPs are not modulated by CyP and are insensitive to CsA (Jung et al. 1997; von Stockum et al. 2011).

A major step in mechanistic understanding of the role of CyPD in PTP regulation has been the discovery that CyPD masks an inhibitory site for Pi (Figure 1.9). In fact, in the absence of Pi, the sensitivity to Ca^{2+} is identical in wild type and CyPD-null mitochondria (Basso et al. 2008).

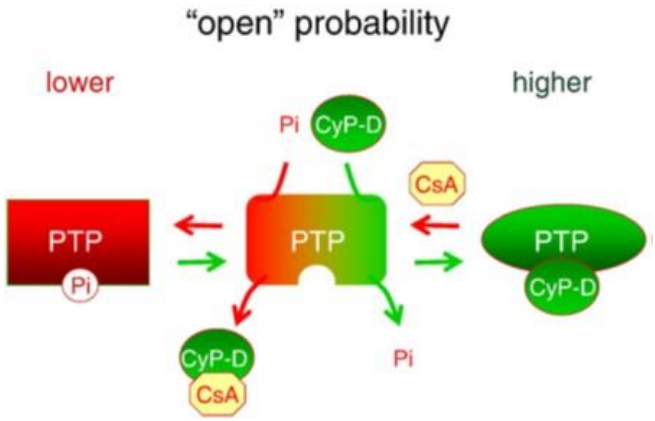

Figure 1.9. Modulation of the PTP by CyPD and Pi. The CyPD-bound form of the PTP shows a higher probability of opening; addition of CsA displays CyPD and unmasks an inhibitory Pi (Giorgio et al. 2010).

1.3.3CyPD involvement in pathology

The use of CyPD-null mice allowed to demonstrate that a wide variety of diseases, most notably ischemia-reperfusion injury of the heart and brain, muscular dystrophies and neurodegeneration, have their basis in mitochondrial pathogenesis and misregulation of the PTP (Giorgio et al. 2010). Baines and colleagues (2005) have found that CyPD null mice are protected from ischaemia-reperfusion *in vivo*, whereas CyPD overexpressing mice show mitochondrial swelling and spontaneous cell death. Consistently, mitochondria isolated from the livers, hearts and brains of *Ppif*$^{-/-}$ mice (*Ppif* encodes CyPD) are resistant to mitochondrial swelling and permeability transition *in vitro*. Moreover, primary hepatocytes and fibroblasts isolated from these mice are largely protected from Ca^{2+} overload and oxidative stress-induced cell death, but not from staurosporine- or TNFα- mediated cell death, or death induced by Bax. Consistent with these data, CyPD overexpression in B50 neuronal cells promoted PTP and necrotic cell death, although it inhibited apoptotic

cell death (Li et al. 2004).

Ppif$^{-/-}$ mice also display a striking resistance to the development of axonopathy in a model of autoimmune encephalomyelitis (Forte et al. 2007), and to disease progression after crossing with the superoxide dismutase 1 mice (Martin et al. 2009; Parone et al. 2013), suggesting that CyPD-dependent mechanism may be critical in the neurodegenerative aspects of de-myelinating and motor neuron diseases. Genetic ablation of CyPD rescues mitochondrial defects enhancing β-cell survival in diabetes (Fujimoto et al. 2010), preventing muscle apoptosis in collagen VI myopathic mice (Palma et al. 2009) and improving learning, memory and synaptic function in a mouse model of Alzheimer disease, where it also alleviated reduction of long-term potentiation mediated by the amyloid β peptide (Du et al. 2008).

1.3.4Molecular nature of the PTP

A set of observations, based primarily on biochemistry and electrophysiology studies, led to a model where the PTP would be a multiprotein complex spanning both mitochondrial membranes and comprising the ANT and the Pi carrier (PiC) of the IMM, matrix CyPD, as well as the voltage-dependent anion channel (VDAC), the translocator protein (TSPO, also known as peripheral benzodiazepine receptor), hexokinase (HK) and Bcl-2 proteins of the OMM (Zamzami & Kroemer 2001).

However, this model did not stand the test of genetics as a CsA-sensitive PT could be easily detected in the absence of ANT (Kokoszka et al. 2004), VDAC (Krauskopf et al.2006; Baines et al. 2007) as well as of TSPO (Šileikytė et al. 2014).

1.3.4.1ANT

The ANT is the most abundant IMM protein and catalyzes the exchange of ATP for ADP. In most mammals four isoforms are present, showing differential tissue distribution.

The hypothesis that ANT could be a structural component of the PTP was initially suggested by the effects of bongkrekic acid and atractylate on PT (Hunter & Haworth 1979; Schultheiss & Klingenberg 1984), as described above. Further investigations found that ANT reconstituted into liposomes exhibits high-conductance channel activity that is stimulated by Ca^{2+} and insensitive to CsA, like the MMC; unike the MMC, however, currents could only be inhibited by ADP and bongkrekate together, while ADP alone had a marginal effect (Brustovetsky & Klingenberg 1996). Moreover, binding of the ANT to a CyPD affinity matrix has been

reported and the authors proposed that the effects of both CsA and ADP on the PTP could be due to ANT interaction with CyPD. However, the relevance of CyPD-ANT interaction to PTP regulation remains unclear because CyPD bound equally well the ANT purified from rat liver or yeast (Woodfield et al. 1998) in spite of the fact that in yeast mitochondria the PT is not regulated by CyP or inhibited by CsA, (Jung et al. 1997).

A decisive proof against this theory was the generation of mice lacking *Ant1* and *Ant2* by the Wallace and Coworkers, who demonstrated that mitochondria isolated from double-null hepatocytes still exhibited PT induced by Ca^{2+}, sensitive to CsA and favoured by diamide and H_2O_2. These data clearly indicated that the ANT is not essential for PTP formation and is not the site of action of these oxidants, or the relevant partner for CyPD binding (Kokoszka et al. 2004); of note, mice (and all rodents) lack a gene for ANT3 and the fact that PTP from ANT1/ANT2-null mitochondria was resistant to atractylate and ADP excludes a compensatory (mis)targeting of ANT4 in liver (Bernardi, 2015).

1.3.4.2PiC

The PiC (SLC25A3 gene) is the primary transporter of inorganic phosphate (Pi) into the mitochondrial matrix by proton cotransport (or in exchange for hydroxyl ions) and in mammals is encoded by a single gene. PiC has been proposed to be either an effector of the PTP or, possibly, a structural component in cooperation with the ANT (Halestrap 2009). This hypothesis was mainly based on the observation that the CsA-sensitive binding of CyPD to the PiC and its modification by SH-reagents correlated with PTP opening and inhibition (Leung et al. 2008).

Genetic tests demonstrated that mitochondria where PiC expression was reduced by 60% showed no alteration in PTP function (Gutiérrez-Aguilar et al. 2014) and that in mitochondria with over 90% reduction in PiC levels the PTP could still form, and displayed marginally reduced sensitivity to activators (Kwong et al. 2014). Moreover, patch-clamp experiments with the reconstituted, functionally active PiC revealed conductance properties different that those of the MMC (Herick et al. 1997). These data indicate that PiC, like the ANT, cannot constitute a key structural element of the PTP.

1.3.4.3 Spastic paraplegia 7

A recent paper (Shanmughapriya et al. 2015) proposed thatthe spastic paraplegia 7 protein (SPG7 or paraplegin) is an essential component of the PTP. SPG7 is an AAA-type protease involved in the processing and quality control of a variety of mitochondrial proteins that forms oligomeric (normally hexameric) ring-shaped complexes (Casari et al. 1998). The candidacy of SPG7 emerged from an initial screening in which 128 possibly relevant genes were knocked down by appropriate shRNAs and the effects on the mitochondrial PT was evaluated. However, it should be noted that the selected genes also included some of the candidates ruled out by genetic tests, such as ANT2 and VDAC1. Moreover, no electrophysiological data have been provided, while these latter may be particularly relevant, because SPG7 has not yet been reported to form permanent pores .

1.3.4.4 VDAC

VDAC is a major OMM protein which functions as a general diffusion pore for small hydrophilic molecules; in mammals, distinct genes encode three variants of the protein, VDAC1, 2 and 3 (Raghavan et al. 2012). Various observations from different groups suggested that VDAC1 could be an essential component of the PTP. Purified VDAC1 incorporated into planar phospholipid bilayers forms channels with a pore diameter of 2.5-3.0 nm, whose electrophysiologial properties were similar to those of the PTP (Szabó et al. 1993; Szabó & Zoratti 1993). Moreover the VDAC channel properties were modulated by NADH (Zizi et al. 1994), Ca^{2+} (Gincel et al. 2001), glutamate (Gincel & Shoshan-Barmatz 2004) and hexokinase (Pastorino et al. 2002), all factors that also regulate the PTP. However, as for ANT, studies based on genetic ablations questioned this conclusion. Indeed mitochondria lacking all three VDAC isoforms compared to wild-type mitochondria showed the same properties in terms of pore opening (Baines et al. 2007)

1.3.4.5 TSPO

The translocator protein of 18 kDa, TSPO, , is a hydrophobic protein localized to the OMM with a cytoplasmic domain containing a cholesterol recognition region (Li et al. 2001). In several steroidogenic cell types it has been found that TSPO ligands stimulate steroid synthesis and promote translocation of cholesterol from the OMM to the IMM (Krueger & Papadopoulos 1992; Gavish et al. 1999). Consistently, TSPO was initially identified as the peripheral benzodiazepine receptor, which was presumed to have a key role in the hormonally induced entry of cholesterol into

steroidogenic cells (Besman et al. 1989). However, the ubiquitous expression of TSPO suggested that it could serve more general functions. Moreover, its role in cholesterol metabolism has been questioned in conditional *Tspo*$^{-/-}$ mice (Morohaku et al. 2014); consequently, the precise function of TSPO remainsto be established.

It was suggested that TSPO takes part to PTP formation due to its interaction with VDAC and ANT (McEnery et al. 1992). In addition, experiments with compounds specifically targeting TSPO suggested that its ligands influenced the opening of the PTP, such as the benzodiazepine Ro5-4864,the isoquinoline carboxamide PK-11195, and protoporphyrin IX, which are inducers of the PTP (Kinnally et al. 1993; Pastorino et al. 1994; Šileikytė et al. 2014). However, it has been recently found that the PTP properties are identical in TSPO null and wild type mitochondria, demonstrating that TSPO plays no role in the regulation or structure of the PTP (Šileikytė et al. 2014). Consistent with this conclusion, hearts lacking TSPO are as sensitive to ischemia-reperfusion injury as hearts from wild-type mice (Šileikytė et al. 2014), in contrast to mice missing CyPD (Baines et al. 2005). These results indicate that OMM regulation of PTP activity occurs though a mechanism that does not require TSPO and call into question a number of studies implicating TSPO in pathological processes mediated by the PTP (Bernardi et al. 2015).

1.3.5Alternative models for PTP formation

In 2002 a model was proposed where the PTP would originate from misfolded membrane proteins (He & Lemasters 2002), similarly to an earlier suggestion that the PT is due to oxidative damage of membrane proteins rather than a consequence of the opening of a pre-formed pore (Kowaltowski et al. 2001). This misfolding by oxidative stress and other perturbations would expose hydrophilic clusters enclosing aqueous channels that allow diffusion of low molecular weight solutes. Alterations of thiol groups, particularly cross-linking, may be critical for the initial misfolding of membrane proteins leading to clustering. Similarly, exogenous amphipathic peptides would also assemble into pore-forming clusters. After the initial formation of protein clusters, He and Lemasters propose that one or more chaperone-like proteins (such as CyPD) bind to the clusters to block pore conductance. Increased Ca^{2+} causes CyPD to perturb the protein cluster/chaperone complex causing the opening of a CsA-sensitive PTP. When the number of these protein clusters exceeds available chaperones opening of “unregulated” pores would occur, which would no longer be sensitive to CsA.

The model accounts for both CsA-sensitive and -insensitive pores, as well as for the lack of selectivity of the permeability pathway. On the other hand, it doesn't account for the regulatory role of membrane potential and matrix pH, whose effects are difficult to explain by heterogeneous misfolded proteins (Bernardi et al. 2006).

1.4 F_0F_1 ATP Synthase and the PTP

Recently our group has demonstrated that purified F_0F_1 ATP synthase dimers from bovine heart, (Giorgio et al. 2013), yeast (Carraro et al. 2014) and *Drosophila melanogaster* (von Stockum et al. 2015) form channels possessing many properties of the PTP after treatment with oxidants in the presence of Ca^{2+}.

Two sets of critical observations greatly contributed to these findings. The first was that CyPD binds to the OSCP subunit of the mammalian complex, resulting in partial enzyme inhibition; CsA displaces CyPD from OSCP resulting in enzyme reactivation (Giorgio et al. 2009). The second was that ATP synthase dimers, but not monomers, generate Ca^{2+}-dependent currents with features indistinguishable from those of the MMC, the electrophysiological equivalent of the PTP (Giorgio et al. 2013).

While these findings leave little doubt that the PTP forms from the ATP synthase, the mechanism of pore formation remains an open question. Our working hypothesis is that channel forms from dimers of ATP synthase after replacement of Mg^{2+} with Ca^{2+} at the F_1 catalytic sites, which induces specific conformational changes leading to the uncoupling of ATP hydrolysis from H^+ transport (Papageorgiou et al. 1998). Once the conformational change has occurred, permeation would take place at the interface between dimers. The ATP synthase would then return to its basal coupled state when the catalytic site is reoccupied by Mg^{2+}, consistent with the full reversibility of the PT.

1.4.1 CyPD interaction with mammalian F_oF_1 ATP Synthase

Initially, CyPD interaction with bovine heart ATP synthase has been demonstrated by blue native electrophoresis of mitochondrial proteins after low-detergent extraction, which is widely used for the identification of protein-protein interactions (Wittig et al. 2006), and immunoprecipitation of ATP synthase (Giorgio et al. 2009). Furthermore, cross-linking with the membrane-permeant cleavable bifunctional reagent dimethyl 3,3-dithiobis-propionimidate, which reacts with the primary amines of two interacting proteins at an average distance of about 8 Å (Green et al. 2001), evidenced that CyPD forms a cross-linked complex with the subunits OSCP, b, and d subunits in an apparent ratio of 1:1:1:1 (Giorgio et al. 2009), supporting the interaction of CyPD with the extrinsic part of the ATP synthase peripheral stalk.

Binding of CyPD to the enzyme complex is favored by Pi and competed by CsA. Importantly, CyPD binding has major functional consequences, with a decrease of both ATP synthetic and ATP hydrolytic activity that can be reversed by CsA-dependent CyPD displacement (Giorgio et al. 2009). Consistently, the stimulatory effect of CsA was lost in *Ppif*$^{-/-}$ mitochondria, indicating that it is mediated by CyPD, while assembly of the ATP synthase was unaffected by CyPD ablation (Giorgio et al. 2009), demonstrating that CyPD is not involved in the enzyme assembly process.

By immunoprecipitation of each of the lateral stalk subunits b,d and OSCP individually it was later established that OSCP is the direct interactor of CyPD (Figure 1.10) (Giorgio et al. 2013). Moreover, decreased expression of OSCP after treatment with specific siRNAs in human HQB17 cells led to a parallel decrease of CyPD binding to F-ATP synthase, and, most importantly, to a matching decrease of the threshold matrix Ca^{2+} required for PTP opening, suggesting that ablation of OSCP or CyPD binding to OSCP would induce equivalent effects causing increased probability of PTP opening. In this scenario OSCP would be a “negative” modulator influencing the probability of replacing Mg^{2+} with Ca^{2+} in the F_1 catalytic sites, while CyPD would be a “positive” effector, which does increase the apparent Ca^{2+} affinity of the PTP.

CyPD interaction with the OSCP subunit can be displaced by Bz-423. In addition, Bz-423 has a PTP-sensiting effect, in a striking analogy with CyPD, suggesting that their binding site may coincide. Bz-423 was originally characterized as an apoptosis-inducing agent acting through mitochondria (Blatt et al. 2002).

OSCP was identified as its target through the unbiased screening of a human phage display library (Johnson et al. 2005) and by NMR studies, which established that Bz-423 binds to a region comprising the helices 3 and 4 and induces conformational changes able to perturb the OSCP- F_1 interface resulting in enzyme inhibition (Stelzer et al. 2010).

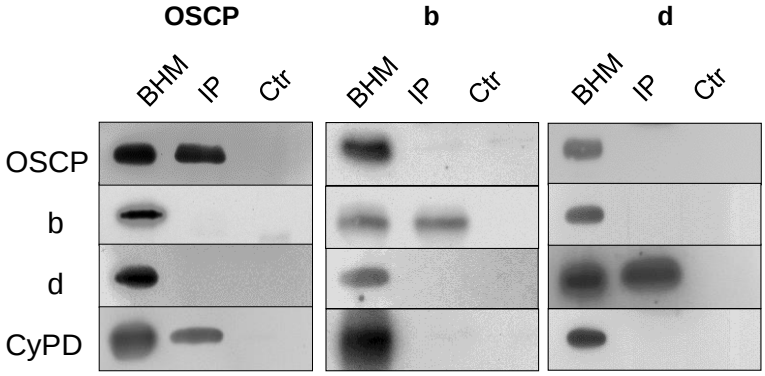

Figure 1.10 CyPD interaction whit OSCP. Immunoprecipitates of bovine heart mitochondria whit OSCP, b and d subunits are shown. From (Giorgio et al. 2013).

Consistently, helices 3 and 4 of OSCP form a low surface potential region and may therefore be a putative binding site of the basic CyPD on OSCP, whose interactions are mostly electrostatic in nature, being disrupted by increased ionic strength. However, the same study identified a second region of low surface potential located at OSCP residues His112, Glu115 comprised in helix 6, and Val116, Glu128 and Glu133 of the linker region (Figure 1.11) (Giorgio et al. 2013).

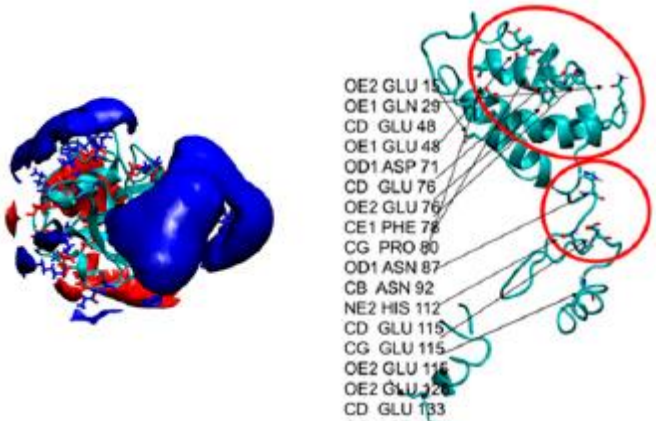

Figure 1.11 Surface potential and isopotential curves of CyPD and OSCP. A) Electrostatic isopotential curves on CyPd are displayed in blue (positive) and red (negative). **B**) Side chain atoms with the lowest average surface potential on OSCP. The two main regions of lowest surface potential are indicated.

1.4.2 ATP Synthase dimers form the PTP

The demonstration that in mammalian mitochondria Bz-423 induces the PTP, and that its binding site may coincide with that of CyPD on OSCP paved the way to the demonstration that ATP synthase can form channels with the features of the PTP-MMC.

To test this hypothesis digitonin mitochondrial extracts were separated through blue native electrophoresis (Wittig & Schägger 2009). ATP Synthase dimers and monomers were eluted and inserted into planar lipid membrane for subsequent electrophysiological characterization. Dimers and monomers were subjected to Western blot analysis, which excluded the presence of VDAC and ANT. Purified dimers, but not monomers, formed channels activated by Ca^{2+}, Bz-423 and oxidative stress with a unit conductance of about 500 pS. This is a value close to that of a "half-MMC" channel (De Marchi et al. 2008), suggesting that the maximum-size PTP may be formed by ATP synthase tetramers (Bernardi et al. 2015). The channels were inhibited by Mg^{2+}/ADP and by the ATP synthase inhibitor γ-imino ATP (a non hydrolyzable ATP analog). Consistent with the lack of CyPD and ANT in the preparations, channels were insensitive to CsA, bongkrekic acid and atractyloside (Giorgio et al. 2013). The channel-forming property was also found in preparations from *Saccharomyces cerevisiae,* which displayed Ca^{2+}-dependent currents of about 300 pS (Carraro et al. 2014) and *Drosophila melanogaster,* where the conductance was 53 pS, in keeping with earlier results on solute permeation (von Stockum et al. 2015). Importantly, yeast mutants lacking the ATP synthase e and g subunits involved in dimer formation, turned out to be resistant to Ca^{2+}-dependent PTP opening, supporting the dimer model (Carraro et al. 2014).

Channel formation by ATP synthase has been confirmed in human cells (Alavian et al. 2014) and is supported by a study where the c subunit was downregulated by siRNA in HeLa cells, which resulted in PTP inactivation (Bonora et al. 2013). These studies proposed that the Fo c-ring is a core component of the pore, an idea that was originally suggested by the observations that the PT could be induced by a phosphorylated peptide derived from the c subunit and by subunit c itself (Azarashvili et al. 2002; Azarashvili et al. 2014). Alavian et al. have observed that upon reconstitution into an artificial bilayer assemblies of tagged c subunits formed large Ca^{2+}-dependent pores with peak conductance up to 1.5-2 nS resembling the PTP, whose opening was blocked by addition of the F_1 β subunit, but not by subunits γ,/δ/ ε, which interact with the Fo c-ring in the native enzyme. The authors

suggested that the PTP channel forms within the c-ring itself after Ca^{2+}-dependent extrusion of F_1. However, if PTP opening depends on F_1 release, their data show that F_1 itself cannot reintegrate within F_O through subunits γ/δ/ε, each event of pore opening would denature the corresponding ATP synthase, while the PTP is fully reversible in mitoplasts (Szabò et al. 1992), intact mitochondria (Petronilli et al. 1994) as well as in reconstituted dimers of ATP synthase (Giorgio et al. 2013). Moreover, in the protocols of Alavian et al. channel openings strictly required CyPD, while neither the yeast nor the Drosophila PTPs are regulated by CyPs. Another critical point of this model is that both in mammals and in Drosophila the c-ring is composed by 8 subunits (Watt et al. 2010), making quite difficult to see how c-rings of the same size can form 500 pS channels in mammals and 53 pS channels in Drosophila. The lack of correlation between conductance of the channel and composition of the c-ring is also supported by measurements in yeast, where the c-ring has 10 subunits and the conductance is 300 pS (Carraro et al. 2014). In summary, the ensemble of these findings is not consistent with the idea that the PTP channel forms within the ring of c subunit. Furthermore, when present in "excess", c subunit forms hydrophobic aggregates with no increase of membrane permeability, as recently observed after silencing of the ε subunit in HEK293 cells, which blocked the biogenesis of ATP synthase with accumulation of subunit c (Havlíčková et al. 2010). Mitochondria in these cells were more coupled, which is unexpected if the c-ring can form high-conductance membrane channels.

AIM

PTP formation from ATP Synthase poses the challenging opportunity to determine the molecular mechanisms through which the enzyme complex shifts from an energy-conserving into an energy-dissipating device based on the structural and functional properties of ATP synthase.

pH plays a relevant role in the PTP modulation. The probability of PTP opening has an optimum at neutral matrix pH, while the pore is blocked at acidic matrix pH values. Inhibition is due to reversible protonation of histidyl residue(s) because diethylpyrocarbonate (DPC), a histidine-modifying reagent, prevents PTP inhibition by H^+ through carbethoxylation of histidyl residues. In addition, low pH promotes release of the PTP-modulator CyPD from the IMM through reversible protonation of histidyl residues still blocked by DPC.

The goal of the present work is to identify the mechanism(s) through pH affects the PTP. As CyPD interacts with the OSCP subunit of ATP synthase, the possibility that the histdine critical for pH modulation of PTP are located within OSCP will be evaluated. Moreover, the involvement of the histidine(s) responsible of the pH-dependent binding of the endogenous inhibitor IF1 will be considered. Finally, the pH influence on the structural stability of the ATP synthase dimers will be assessed.

2. Matherials and Methods

2.1 Isolation of bovine heart mitochondria

Bovine heart mitochondria were prepared following two procedures, as described below.

2.1.1 Isolation of heavy bovine heart mitochondria (HBHM)

Heavy bovine heart mitochondria were prepared from fresh hearts (Löw & Vallin 1963) obtained from the abattoir and packed in ice. All the following steps were run at 4°C. The meat was diced and fat and connective tissue were removed. Then the diced meat was suspended in buffer A (0.25M sucrose, 10mM Tris/HCl, pH 7.8) in a volume ratio of 1:3 and the pH decrease due to lactic acid release was neutralized by the addition of 2M Tris. Buffer A was removed by filtration through muslin clothes, the minced meat was re-suspended in buffer B (0.25M sucrose, 10mM Tris/HCl, 2mM EDTA and 1mM Tris/succinic acid, pH 7.8) and then homogenised in a Waring blender (Waring Products Division, New Hartford CT, U. S. A.) for 30sec. Cell debris was removed by low speed centrifugation at 1,000x*g* for 10min. The supernatant was filtered twice through muslin clothes and the mitochondria, now in suspension, were collected by high-speed centrifugation at 19.000x*g* for 20min. The pellets from each portion were re-suspended, combined and homogenised in a Potter homogeniser. After a final high-speed centrifugation step (39.000x*g* for 15min), the supernatant was decanted and the pellets stored at -80°C.

2.1.2Isolation of functional mouse liver (MLM) and bovine heart mitochondria (BHM)

To obtain small quantities of well coupled mitochondria, the method of (Costantini et al. 1995) was used. All steps were run at 4°C. Wild type or *Ppif*$^{-/-}$ mouse livers were removed and placed in a glass beaker containing ice-cold buffer C (0.25 M sucrose, 10 mM Trs/HCl, 0.1 mM EGTA pH 7.4), cut into small pieces with scissors. rinsed with ice-cold buffer C (to remove as much blood as possible) and passed through a pre-chilled Potter homogenizer. In the case of bovine heart, the ventricular tissue was freed from fat and connective tissue before being cut into small pieces with scissors. rinsed with ice-cold buffer C (to remove as much blood as possible) and passed through a pre-chilled Potter homogenizer. The homogenate was centrifuged at 700x*g* for 10 minutes (4°C) to remove unbroken cells and nuclei. The supernatant containing mitochondria and other organelles was centrifuged at 7.000x*g* for 10 minutes at the same temperature. The mitochondrial pellet was carefully suspended in ice-cold buffer C

and spun at 9.000x*g* for 5 minutes at 4°C. The mitochondrial pellet was suspended in buffer C to give a protein concentration of about 60-80 mg/ml and immediately used.

2.2 Preparation of submitochondrial particles from HBHM

Ultrasonic disintegration of mitochondria produces inverted submitochondrial particles, in which the substrate binding sites for both the ATP synthase and the respiratory chain are on the outside. Different types of submitochodrial particles can be prepared depending on the medium used during the ultrasonic disintegration.

2.2.1 MgATP submitochondrial particles (MgATP-SMP)

In this type of membrane preparation the interaction between the F1 and the Fo domains is well coupled (Löw & Vallin 1963). HBHM stored at -80°C were thawed under cold tap water and suspended at 15 mg/ml with buffer A. $MgCl_2$ and ATP were added to reach a final concentration of 15mM and 1mM respectively. Aliquots of 3ml were exposed to sonic oscillation for four 30 sec cycles separated by 30 sec intervals in a Labsonic oscillator. The entire treated batch was centrifuged at 19.000x*g* for 20 min at 4°C , followed by a second centrifugation of the supernatant for 30m at 100.000x*g*. The pellet was suspended in a small amount of 0,25M Sucrose, 10mM Tris/HCl, pH 7.3 and the protein content was determined according to the Lowry method. Typically, the yield of particles was 17-22% of the mitochondrial protein (Löw & Vallin 1963).

2.2.2 EDTA submitochondrial particles (EDTA-SMP)

In this type of membrane preparation the interaction between the F_1 and the Fo domains is specifically altered, moreover the IF_1 content is reduced (Rouslin et al. 1995). Thawed HBHM were suspended in 0.25M sucrose to give a protein concentration of 20mg/ml. EDTA was added at the suspension to obtain a final concentration of 2mM, and the pH was adjusted to about 8.5-8.8 values with NaOH. Then the suspension was exposed to ultrasonic energy, as described above, and diluted 1:1 with 0.25 M sucrose. The sample was centrifuged at 19.000x*g* for 20 min at 4°C and the supernatant centrifuged again at 100,000x*g* for 30min. The final pellet was supended in 0.25M sucrose, 10mM Tris/HCl, pH 7.3 and the protein content estimated according to the Lowry method.

2.3 IF_1 extraction

For IF_1 extraction, MgATP-SMP were used as source materials. These particles were suspended in 0.25M Sucrose, 10mM Tris and 2 mM EDTA pH at a protein concentration of 20mg/ml and heated in a glass tube for 4 min at 75°C with occasional shaking. The denatured proteins were removed by centrifugation at 100.000x*g* for 10 min at 20°C. The supernatant was removed carefully, its volume measured and added with 125 mg *per* ml of ammonium sulfate and 5,5 ml *per* ml of ice-cold anhydrous ethanol. The suspension was mixed for 2 min and centrifuged at 100.000x*g* for 10 min at 20°C. The pellet (mainly containing IF1) was suspended in 2ml of 10mM Tris pH 7.4 and concentrated through the Vivaspin®Centrifugal concentrator for 20min at 8.000x*g*. The resulting supernatant was quantified by the Lowry method.

2.4 Protein estimation

The Lowry method (Lowry. et al., 1951) is particularly suitable for membrane protein estimation thanks to the presence of a detergent. The method consists of two steps:

1. The starting interaction between the proteins and cuprous ions in a basic solution;

2. The reduction of phosphotungstic and phosphomolybdic acid to blue tungstate and blue molybdate by the complex Cu-proteins and by tryptophan and tyrosine residues present in the proteins.

The reaction is followed spectrophotometrically at 750nm. Aliquots of mitochondria or submitochondrial particles were suspended in 0.2 ml of 10% (w/v) sodium deoxycolate (Na-DOC) solution in 0.01N NaOH and shaken. Then, 1 ml of reagent A (50 parts of 2% (w/v) Na_2CO_3 in 0.1N NaOH and 1 part of 0.5% (w/v) $CuSO_4$ $4H_2O$ in 1% (w/v) of Na-K tartrate) were added. After an incubation of 10min at 25°C, 50 µl of reactive B (1:1 Folin-Ciocalteau and H_2O) were added and the samples were shaken. The following incubation was carried on for 30min at room temperature and then the absorbance at 750nm was measured. 2-64 µg of bovine serum albumin (BSA) was used to establish standard calibration curves for each assay.

2.5 Measurement of ATP hydrolysis

The ATP hydrolysis rate was determined using an ATP regenerating system as shown in the scheme (Rosing et al. 1975).

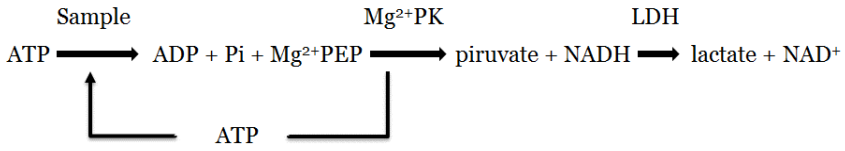

When the mitochondrial samples are added to the assay buffer, the decrease of absorbance due to NADH oxidation is directly proportional to the amount of hydrolysed ATP. As ATP is continuously regenerated, the rate of ATP hydrolysis remains constant over time.

The assay buffer consists of 30mM sucrose, 50mM Tris/HCl pH 7.4, 50mM KCl, 2mM EGTA, 4mM $MgCl_2$ and 2mM phospho-enol pyruvate (PEP), 2mM ATP/Tris pH 7.4, 0.3mM NADH; 4U/ml pyruvate kinase (PK) plus 3U/ml lactate dehydrogenase (LDH) (Das & Harris 1990). The assay was carried out at 37°C adding appropriate aliquots of MLM or BHM or MgATP-SMP or EDTA-SMP (treated as specified below) to a final volume of 1ml using a plastic cuvette. In the case of samples containing mitochondria 10 µM alamethicin was also added. The decrease in absorbance of NADH at 340nm was measured over a period of 5 min. An extinction coefficient (ε) of 6220 M^{-1} cm^{-1} was used to calculate the specific activity.

2.5.1 Pre-treatments of mitochondria or submitochondrial particles

Freshly prepared MLM or MgATP-SMP were suspended at 1 mg/ml in a medium containing 0.25M Sucrose, 10mM MOPS, 5mM Succinate, 20 µM EGTA pH 7.4 with KOH (assay buffer) in the absence or presence of 10mM KH2PO4 (Pi) and incubated with or without 200-400 µM DPC or 100-200 µM NBD-Cl (in the dark) for 15 minutes at room temperature. Samples incubated with Pi were treated with 1,6 µM CsA for 15 min at room temperature before addition of DPC or NBD-Cl, while samples treated with 200 µM DPC in the absence of Pi were subsequently incubated with 1mM hydroxylamine for 20 min at room temperature.

EDTA-SMP were suspended at 0.25 mg/ml in a medium containing 50mM Sucrose, 10mM KCl, 1mM MgATP, 10mM MOPS at pH 6 and incubated for 10min at 37°C with 1 µg of IF_1 pre-treated with or without DPC, as described by Vinogradov (Panchenko & Vinogradov 1985). Before incubation with the EDTA-SMP the isolated

IF1 was diluted to 0.045 µg/µl with 50mM Sucrose, 10mM KCl, 10mM MOPS at pH 6 and incubated in the absence or presence of 1 mM DPC for 10 min at room temperature.

2.6 Immunoprecipitation of FoF1 ATP Synthase after mitochondria treatment with or without DPC and incubation at low/neutral pH

Immunoprecipitation has been performed by using a commercial immunocapture kit, i.e. the anti-ATP Synthase monoclonal Ab covalently linked to protein G-Agarose beads (ATP Synthase immunocapture kit from Abcam).

To test the effects of pH on CyPD-ATP synthase interaction, 0.6 mg of freshly prepared BHM (2.1.2) were suspended at 3 mg/ml in a buffer containing 0.25M sucrose, 10mM MOPS, 10 mM Pi, 5mM succinate, 20µM EGTA,pH 7.4 (MOPS buffer) or in 0.25 M sucrose, 10mM sodium acetate, 10 mM Pi, 20µM EGTA, pH 7.4 (acetate buffer) and treated with or without 200 µM DPC for 15 minutes at room temperature. Five millimolar of MOPS pH 6 or pH 7.4 was added to the samples suspended in MOPS buffer to adjust the pH value at 6.5 or 7.4, respectively.Ten millimolar of sodium acetate (pH 4.5) was added to the samples suspended in acetate buffer to adjust the pH at 5.

After centrifugation for 15 minutes at 20.000x*g* at 4°C the mitochondrial pellets were suspended at 12 mg/ml in MOPS buffer (containing 10mM of imidazole to quench the DPC reaction), added with 1% (w/v) digitonin and centrifuged 100.000x*g* for 25 minutes at 4°C. Supernatants were then incubated overnight under wheel rotation at 4°C in the presence of anti-ATP Synthase monoclonal Ab in a ratio of 20 µl/mg of protein. After gentle centrifugation, the beads were washed twice in a buffer containing 0,05% (w/v) dodecyl maltoside (DDM) in PBS (8.1mM Na_2HPO4, 1.9mM KH_2PO_4, 137mM NaCl, 2.7mM KCl pH 7.4). The elution was performed in SDS-PAGE loading buffer (20mM Tris/HCl, pH 6.8, 4% (w/v) SDS, 2% (v/v) β-mercaptoethanol, 20% (v/v) glycerol and 0.01% (w/v) bromophenol blue). The collected fractions were heated at 98°C for 5 min and subjected to 15% SDS-PAGE followed by Western blotting against CyPD and β subunit of ATP Synthase.

For the mass spectrometry analyses the immunoprecipitation protocol includes these modifications: mitochondria were incubated in MOPS buffer without Pi (pH 7.4) and treated with 1 mM DPC. The samples were eluted in a buffer

containing 2% (v/v) TCEP instead of β-mercaptoethanol and the 15% SDS-PAGE was followed by Coomassie staining.

To evaluate the effect of DPC on the IF1 binding to ATP Synthase, freshly prepared BHM were suspended in MOPS buffer pH 7.4 or acetate buffer pH 7.4, treated with DPC and adjusted to pH 7.4 or 6 as described above. After immunoprecipitation with anti-ATP Synthase monoclonal Ab and 15% SDS-PAGE the samples were probed for the presence of IF1 and β subunit of ATP Synthase by Western blotting.

2.7 SDS Polyacrylamide Gel Electrophoresis (SDS-PAGE)

Sodium dodecyl sulphate polyacrylamide gel electrophoresis (SDS-PAGE) (Laemmli U.K., 1970) was used to analyze all IP samples using 10x10x0,1cm gels. The 15% acrylamide concentration in the separating gel was chosen according to the molecular size of the proteins to be separated and a ratio of 37.5:1 (w/w) between acrylamide and N,N'-methylenebisacrylamide was maintained. This mixture was solubilized in 0.25M glycine, 0.025M Tris/HCl, pH 8.8 and 0.1% (w/v) SDS. The stacking gel was prepared using 4% (v/v) acrylamide in stacking buffer (0.125M Tris/HCl, pH 6.8, 0.1% (w/v) SDS). 0.1% ammonium persulfate and 0.0015% (v/v) TEMED were added to start gel polymerization. Electrophoresis was performed with a limiting voltage of 250V and a current of 15mA until the dye front reached at the bottom of the gel. The electrophoresis system was cooled using an internal fan to circulate water.

Protein molecular weights were estimated by running standard proteins of known molecular weights in separated lanes (Bio-Rad).

Gels were stained with Colloidal Blue staining Kit (Invitrogen). This kit allows detection of <10ng of protein and it is mass spectrometry compatible. Proteins were visible within 3h and background was eliminated with water. Alternatively, gels were subjected to Western blotting.

2.8 Blue native Gel electrophoresis (BN-PAGE)

Blue native-polyacrylamide gel electrophoresis (BN-PAGE) is a powerful electrophoresis method for isolation and characterization of large multi-protein complexes in their native state (Wittig et al. 2006). BN-PAGE employs Coomassie blue G-250 dyes to introduce charge shifts on proteins and in the absence of denaturing detergents allows first dimension separation according to the size and shape of the complex.

Freshly prepared EDTA-SMP were supended at 3mg/ml in MOPS buffer at pH 7.4 or 6.5 or in 0.25 M sucrose, 20mM sodium acetate, 20µM EGTA, pH 5.0 for 20 min at room temperature. Then the samples were centrifuged at 100.000x*g* for 30 min at 4°C and the pellets suspended at 10 mg/ml in 50mM NaCl, 30mM Tris and 5mM amminocaproic acid (pH 7.4). Digitonin was added at 1 mg of detergent/mg protein and the suspensions were immediately centrifuged at 100.000x*g* for 25 min at 4°C. 14µl of each supernatant were mixed with 1µl of sample buffer (5% Coomassie-Brilliant-blue G-250 in 1M amminocaproic acid) and loaded onto a 3-12% gradient gel (Invitrogen).

The electrophoresis was performed at 4°C. For the first step of electrophoresis, cathode buffer containing Coomassie-Brilliant blue G-250 was used and the voltage was set for 30min at 150V and then shifted to 250V. When the blue front had migrated to two thirds of the separation distance, the cathode buffer was replaced by a cathode buffer without Coomassie-Brilliant blue G-250. Cathode buffers were prepared according to the manufactore's protocol (Invitrogen) At the end the gels were stained or incubated in a specific solution to measure the ATPase activity of ATP Synthase. Bands corresponding to monomeric and dimeric form of ATP synthase were cut out and loaded onto a SDS-gel.

2.8.1 In-gel ATPase activity staning

Because no denaturants are present in native PAGE, subunit interactions within a multimeric protein are generally retained and many proteins have been shown to be enzymatically active. After migration in BN-PAGE the ATP Synthase complex was identified by in-gel staining of the ATPase activity using the qualitative method of (Zerbetto et al. 1997). The activity was measured by plunging the gel into a solution containing 35mM Tris, 270mM glycine, 14mM Mg SO_4, 0.2% (w/v) $Pb(NO_3)_2$, 8mM ATP (pH 7.4) at 37°C. ATP Synthase appears as a white band due to the $Pb_3(PO_4)_2$ precipitation.

2.9 Western blot analysis

Proteins separated *via* SDS-PAGE were transferred to a 0.2µm pore size nitrocellulose membrane (Bio-Rad) using a semi-dry blotting apparatus (Amersham Biosciences TE 22 Tank Transfer Unit)

The transfer was performed at 2.5 mA/cm² for 1 h in a transfer buffer comprising 25mM Tris, 192mM glycine, 20% (v/v) methanol. After staining with ATX Ponceau S red staining solution (Fluka Analytical) to check transfer efficiency, the nitrocellulose sheet was saturated with 3% (w/v) non-fat dry milk in PBS buffer plus 0.1% Tween 20 for 1 h at room temperature and then incubated overnight with the following antibodies:

- Anti β subunit (Abcam) 1:1000 in PBS-0.1% Tween20
- Anti CyPD (Calbiochem) 1:1000 in PBS-0.1% Tween20
- Anti IF1 (Abcam) 1:1000 in PBS-0.1% Tween20

Blots were then rinsed three times with PBS buffer plus Tween 20 and incubated for 1.30 h with peroxidase coupled to anti-mouse-IgG (1/5000) at room temperature. The membrane was washed again three time in PBS buffer plus 0.1% Tween 20 and developed with SuperSignal West Dura Extended Duration Substrat (Thermo Scientific) according to the manufacturer's protocol.

2.9.1Densitometric analysis

High resolution images of the films were acquired using the instrument SF Launcher and processed using the program ImageQuant TL.

2.10 Mass spectrometry analyses

Mass spectrometry approach was applied to detect the DPC modification of apomyoglobin, used as model protein, and of the ATP synthase OSCP subunit. Mass spectrometry analyses were done in collaboration with Dr. Barbara Spolaore, CRIBI Biotechnology Centre, University of Padova.

Horse heart apomyoglobin (ApoMb) was prepared by removal of the heme group from myoglobin (Ascoli et al. 1981). ApoMb was suspended at 1 mg/ml in MOPS buffer pH 7.4, treated with or without 5-fold molar excess of DPC for 10 min at 37°C. The DPC reaction was quenched with 10mM of imidazole (Zhou & Vachet 2012) and each suspension was divided in two parts: one part was incubated 4 hours at 37°C and the other overnight at 4°C. From all samples one aliquot of 50 µg was used to determine the percentage DPC modification by reversed phase HPLC (RP-HPLC) followed by ESI-MS (detailed procedures in paragraph 2.11.1.1 and 2.11.1.2)

From the samples incubated 4 h at 37°C , other two aliquots of 50µg each were obtained. One aliquot was immediately digested with 5ng/µl of trypsin (Promega, modified sequencing grade) for 3h at 37°C and subjected to RP-HPLC and ESI-MS. Another aliquot was instead suspended in SDS-PAGE loading buffer (20mM Tris/HCl, pH 6.8, 4% (w/v) SDS, 2% (v/v) TCEP, 20% (v/v) glycerol and 0.01% (w/v) bromophenol blue), heated at 98°C for 5 min and loaded into 15% SDS-PAGE. After the gel staining with Colloidal Blue staining kit (Invitrogen), the ApoMb band was excided, processed for in gel-digestion and analysed by ESI-MS (detailed procedures in paragraph 2.11.1.3 and 2.11.1.2, respectively) .

2.10.1 Reversed phase HPLC (RP-HPLC)

RP-HPLC consists of a non-polar stationary phase and an aqueous, moderately polar, mobile phase, in a high pressure system. The RP-HPLC analysis was performed with a liquid chromatograph instrument at high pressure, purchased from Agilent Technologies, model 1100 (Waldbronn, Germany). The column used was a Jupiter C4 (Phenomenex, Torrance, CA, USA), whose dimensions are 4.6 x 150 mm with a diameter particles of 5 µm. Chromatographic separations were performed at flow rate of 0.8 mL/min by a linear water/acetonitrile gradient from 5% acetonitrile containing 0.1% of trifluoroacetic acid (TFA) to 60% acetonitrile containing 0.085% of trifluoroacetic acid (TFA) in 30 minutes. The effluent was

monitored by recording the absorbance at 226 nm. The collected fractions were analysed by ESI-MS.

2.10.2ESI-MS

Mass determinations were obtained with an electrospray ionization (ESI) mass spectrometer Q-Tof Micro from Micromass (Manchester,UK). The measurements were conducted at a capillary voltage 3kV and a cone and extractor voltages of 30 and 1 V, respectively (positive ion mode). Instrument control, data acquisition and processing were achieved with Masslynx 4.0 software (Micromass).

2.10.2.1 In-gel digestion of proteins

Enzymatic digestion of proteins in gel requires the following steps (Shevchenko et al. 1996):

- Washing of gel pieces
  The protein bands were cut into roughly 1mm^3 cubes and transferred to a clean tube. The gel pieces were washed with water (5 times gel volume) for 15 minutes. Water was then substituted with the same volume of 50% acetonitrile. After two washings of 15 minutes each, the gel pieces were shrunk with neat acetonitrile. When the bands became white and sticky, acetonitrile was removed.

- Reduction and alkylation
  The gel particles were swelled in 10mM dithiothreitol, 0.1 M NH_4HCO_3 (pH 8.2) and incubated for 45 minute at 56°C. After cooling at room temperature, the liquid was replaced quickly with roughly the same volume of iodoacetamide solution (55mM iodoacetamide in 0.1 M NH_4HCO_3). The tubes were incubated for 30 minutes in the dark at room temperature before removal of the iodoacetamide solution.

- *Washing of gel pieces*
  The gel pieces were washed again with water and acetonitrile to remove completely the Coomassie staining.

- Tryptic digestion
  The gel particles were rehydrate on ice in 50mM NH_4HCO_3 and 5 ng/µl of trypsin (Promega, modified sequencing grade) was added. After 45 minutes the remaining supernatant was removed, replaced with 50mM NH_4HCO_3 without trypsin and incubated overnight at 37°C.

- Extraction of peptides from gel
  The tubes containing the gel pieces were centrifuged at 6.000x*g* for 3 minutes at room temperature and the supernatants with the peptides transferred to clean tubes. To extract more peptides from the gel, 0.1%(v/v) of formic acid was added for 15 minutes, followed by the addition of the same volume of neat acetonitrile and incubation was continued for 15 minutes. The tubes with the gel pieces were centrifuged at 6.000x*g* for 3 minutes and the supernatants recovered. This step was repeated two folds. Then the samples were dried using a Speed-Vac system (Savant).
  Protein digests were redissolved in 0,1% of formic acid and analysed by ESI-MS.

2.10.3MS analyses of OSCP

After immunoprecipitation of ATP Synthase from BHM (as described in 2.6), the samples were loaded into 15% SDS-PAGE and the OSCP band was excised, processed for in-gel digestion (as described in 2.11.1.3) and analysed by LC-MS/MS.

2.10.3.1 LC-MS/MS

Liquid chromatography (LC) coupled to tandem mass spectrometry (MS/MS) was used to increase the sensitivity of the analysis on the tryptic peptide of OSCP containing the unique histidine (95–113: LTNTPAVISAFSTMMSVHR).Protein digests suspended in 0,1% (v/v) formic acid, 3 % acetonitrile were analysed by LC-MS/MS with a 6520 Q-TOF mass spectrometer (Agilent Technologies)coupled online with a 1200 series HPLC system through a Chip Cube Interface (Agilent Technologies). Samples were loaded onto a Polaris-HR-Chip 3C18 (enrichment column of 360 nl; separating column 75 µm×150 mm; Polaris C18 180 Å, 3 µm; Agilent Technologies). Peptides were separated with a gradient from 5 to 50% of solvent B over 15 min and from 50% to 65% B in 3 min at a flow rate of 0.27 µl/min (solvent A: H20 with 0,1% formic acid; solvent B: acetonitrile with 0.1% formic acid). LC-MS/MS analyses were performed in a data dependent mode for protein

identification and in a targeted mode to acquire MS/MS spectra of the native and modified peptide 95–113 of OSCP. Raw data files were converted into Mascot Generic Format (MGF) files with MassHunter Qualitative Analysis Software (Agilent Technologies) for MASCOT search and manually analyzed using the same software.

MS/MS data were searched using the MASCOT search engine (version 2.3.01, Matrix Science) against the Mammalia sequences of the Swiss-Prot database (release 2013_04). The following parameters were used in the MASCOT search: Trypsin specificity; maximum number of missed cleavages:2; fixed modification: carbamidomethyl (Cys); variable modifications: oxidation (M), deamidated (NQ); peptide mass tolerance: ± 10 ppm; fragment mass tolerance: ± 0.05 Da; protein mass: unrestricted; mass values: monoisotopic.

2.11 Cell culture

All the experiments were carried out using HEK293T cell line (Human Hembrionic Kidney). Through the CRISP/Cas9 system the genomic codons specifying His at position 112 of OSCP subunit were replaced by alternate codons directing the specific replacement of His at this position with Gln. This genome modification of HEK293T was done in the laboratory of Prof. Micheal Forte, Vollum Institute, Oregon Health and Sciences University.

HEK293T cells were grown in a culture medium composed of DMEM (GIBCO) supplemented with 10% Foetal Bovine Serum (GIBCO), 100 U/ml penicillin and 100µg/ml streptomycin (Invitrogen). Cells were grown in T-75 250 ml Falcon flasks and incubated at 37°C in a 5% CO2 humidified incubator. Once the cells have reached 70-80% confluency, they were split and plated again on T-75 flasks. Cells were first washed with PBS, followed by trypsinization at 37°C, 5% CO2 using 0.05% Trypsin-EDTA in Phenol red (GIBCO). To stop the action of trypsin, DMEM was added and then the cells were centrifuged at 1.200x*g* for 5 min, resuspended in about 9 ml of DMEM, counted and re-plated at $3 \cdot 10^6$ cells for flask.

2.12 Oxygen consumption rate (OCR)

Oxygen consumption rate was measured using XF24 Extracellular Flux Analyzer (Seahorse Bioscience). This instrument measures in real time the extracellular flux changes of oxygen and protons in the medium immediately above adherent cells cultured in a microplate. Seahorse medium was used (DMEM-Sigma D5030- added with 25 mM glucose, 1 mM sodium pyruvate and 2 mM glutamine).

Cells that had been grown in flasks were trypsinized and counted, and then about 40,000 wild type cells per well and 50,000 OSCP His112Gln cells per well were seeded on appropriate 24-well plates (coated with 0.01% Poly-L-Lysine (Sigma)), each with 28mm² surface and containing about 900µl of DMEM. Cells were incubated at 37°C in a 5% CO2 humidified incubator for 24 hours. Different cell concentration was used to reach the same confluent monolayer. Each XF24-microplate was coupled to a disposable sensor cartridge, embedded with 24 pairs of probes for measuring oxygen concentration and pH. Assay were initiated by replacing the growth medium with 670 µl of Seahorse medium prewarmed at 37°C. Cells were incubated at 37°C for 30 min to allow temperature and pH equilibration. A titration with FCCP was performed for wild type and OSCP His112Gln cells in order to determine the optimal FCCP concentration (i.e., the concentration that stimulates respiration maximally), which was found to be 1µM for both cell types. After an OCR baseline was established, 70µl of each solution containing oligomycin, FCCP, rotenone and antimycin A were sequentially added to each well to reach a final concentration of 1µg/ml oligomycin, 0.1µM FCCP, 1µM rotenone and antimycin A.

2.13 Calcium retention capacity (test)

The Calcium retention capacity (CRC) is one of the most sensitive assay to assess the propensity of the PTP to opening (Fontaine et al. 1998). The test measures the amount of Ca^{2+} that mitochondria can accumulate and retain before the precipitous release that marks PTP opening. Extramitochondrial Ca2+ fluxes were measured fluorimetrically using Calcium Green-5N (excitation-emission λ: 505-535 nm), a low affinity membrane-impermeant probe which increases its fluorescence upon Ca^{2+} binding.

The cells were cultured for 48 hours to reach 70-80% confluency, then harvested by trypsinization and suspended in KCl buffer (130mM KCl, 10mM MOPS/Tris, 1mM phosphoric acid-Tris, 0.1 mM EGTA/Tris, pH 7.4). Cells were centrifugated at 1.200x*g* for 5 min, the pellet was resuspended in KCl buffer (EGTA was increased to 1 mM) to give a concentration of $2 \cdot 10^7$ cells per ml and treated with 100µM digitonin (Sigma) for 10 min on ice to permeabilize the plasma membrane. Excess of digitonin was eliminated by washing cells twice in KCl buffer and the cells were suspended to $10 \cdot 10^7$ cells per ml in CRC buffer (250mM sucrose, 10Mm MOPS/Tris, 10µM EGTA/Tris, 1mM phosphoric acid, 5mM glutamate and 2.5 mM malate, pH 7.4.). Then the cells were dispensed $1 \cdot 10^6$ cells/well to a 96-well black

assay plate (Falcon 353376) containing 0,2ml of CRC buffer supplemented with 0.5μM Calcium Green-5N in each well. The assay was done also in the presence of 2μM CsA. A train of 5 μM Ca^{2+} pulses was added at 4 minutes intervals and the fluorescence intensity was read on Fluoroskan Ascent FL (Thermo Scientific) plate reader.

2.14 Mitochondrial swelling

Changes in mitochondrial volume of permeabilized cells were followed in a 96 well clear assay plate (Falcon 353072) at a final volume of 0.2 ml. First, the cells were cultured and permeabilized in KCl buffer (deprived of 1mM phosphoric acid-Tris) as described above. Then cells were suspended in KSCN buffer (0.1M KSCN, 5mM MOPS/KOH, 10 μM EGTA/KOH) at pH 7.4 or KSCN buffer at pH 6.5 and dispensed $1{\cdot}10^6$ cells/well. Absorbance was first read for about 3 min at ƛ 540 nm to get the basal line-using a Multi-Skan EX (Thermo Scientific) plate reader. Then 0,1 mM Ca^{2+} was added to induce mitochondrial swelling and the absorbace changes were followed for 30 min. Ca^{2+} -dependent pore induction by DPC was assessed in KSCN buffer at pH 6.5. The test wells contained 0.5 mM DPC and the experiment was started as described before.

3. Results and Discussion

3.1 Modulation of the F_OF_1 ATP synthase by pH: role of His112 protonation of OSCP

As already mentioned, our group demonstrated that in mammalian mitochondria (i) CyPD interacts with the OSCP subunit of ATP synthase, resulting in partial enzyme inhibition; (ii) CyPD binding requires high Pi concentrations, while the CyPD inhibitor CsA displaces CyPD from OSCP, resulting in enzyme reactivation; (iii) CyPD-OSCP contacts are mostly electrostatic in nature, because they are disrupted by increased ionic strength and (iv) ATP synthase dimers generate Ca^{2+}-dependent currents with features indistinguishable from those of the PTP, suggesting that the PTP forms from a Ca^{2+}-dependent conformational change of F_OF_1 dimers (Giorgio et al. 2013). These findings imply that many modulators of the PTP may act on the ATP synthase.

The most potent inhibitors of the PTP are H^+ ions; indeed, the pore is potently inhibited at acidic matrix pH values *via* reversible protonation of still undefined histidine(s) that can be prevented by the histidine modifying reagent DPC (Nicolli et al. 1993). As PTP modulation by matrix pH was not affected by genetic ablation of CyPD (i.e, in *Ppif*$^{-/-}$ mice), the involvement of histidyl residues located on the PTP was postulated (Basso et al. 2005). In addition, low pH promotes release of CyPD from the IMM through reversible protonation of histidyl residues, which is also blocked by DPC (Nicolli, Basso, et al. 1996).

Based on these observations, the hypothesis has been advanced that the same histidine(s) located on ATP synthase may be responsible for both the pH effects on PTP/ATP synthase opening and for CyPD (un)binding to PTP/ATP synthase. To test this working hypothesis in the first part of this doctoral work experiments have been performed to: (i) define the pH profile of the ATP synthase-CyPD interaction and evaluate the involvement of histidine residue(s) by DPC treatment of bovine heart mitochondria; (ii) identify the ATP synthase histidine(s) modified by DPC using mass spectrometry; (iii) evaluate the effect of DPC on the enzymatic activity of ATP synthase. As the results obtained suggested that reversible protonation of the unique histidine of OSCP (His112 in bovine mitochondria) may play a critical role in modulation of the CyPD-ATP synthase interaction, its role in ATP synthase/PTP switch has further been addressed by mutagenesis, as described in the second part of this thesis.

3.1.1 Effects of pH and of the histidine modifying reagent DPC on the interaction between CyPD and F_oF_1 ATP Synthase in bovine heart mitochondria

To assess the pH profile of the CyPD-ATP synthase interaction freshly prepared respiring mitochondria from bovine heart were added with millimolar Pi concentrations, in order to favour CyPD binding to ATP synthase (Giorgio et al. 2009; Giorgio et al. 2013), and incubated with or without 200 μM DPC at pH 7.4, as in previous experiments (Nicolli et al. 1993). DPC reaction was quenched by adding an excess of imidazole (Mendoza & Vachet 2008) and mitochondria were treated with buffers of different pH (7.4, 6.5 and 5.0). After centrifugation, the mitochondrial pellets were suspended at pH 7.4, added with digitonin and incubated with anti-ATP synthase monoclonal Abs covalently linked to protein G-Agarose beads to immunoprecipitate the complex (immunocapture kit from Mitosciences). The IPs were subjected to 15% SDS-PAGE and immunoblotted with monoclonal antibody against CyPD and F1 β subunit. The parallel detection of CyPD and F1 β subunit allowed to express CyPD content as the CyPD/F1 ratio and to follow its variations under the different experimental conditions (Figure 3.1).

The results clearly indicate that acidic treatment of mitochondria causes CyPD release from ATP synthase, although the exact matrix pH value induced by the different buffers has not been determined. DPC did not affect CyPD binding at neutral/slightly acidic pH, while at low pH it prevented CyPD release. As DPC as such does not affect matrix pH, its effect can be traced to carbethoxylation of histidyl residues (Nicolli et al. 1993). This behavior perfectly matches the effect of DPC on CyPD-PTP interaction (Nicolli et al. 1996), demonstrating that, consistent with PTP formation by ATP synthase, CyPD binding to ATP synthase, which is mostly electrostatic in nature (Giorgio et al. 2013), is also modulated through protonation of one or more histidine(s). Considering that the OSCP subunit of the lateral stalk is the binding partner of CyPD on ATP synthase (Giorgio et al. 2013), the involvement of OSCP histidyl residue(s) has been evaluated by assessing whether they were modified by DPC treatment of mitochondria.

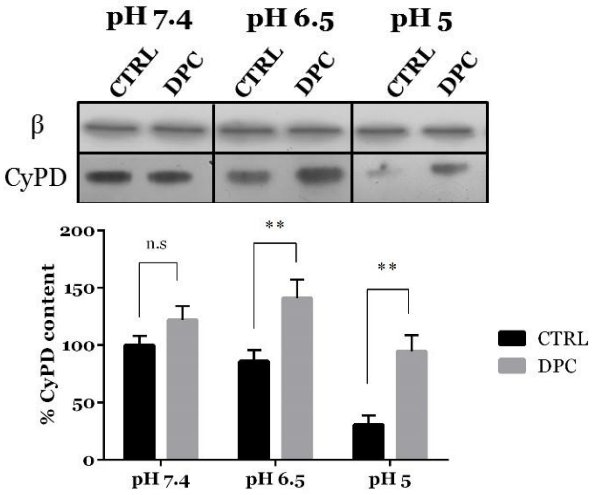

Figure 3.1 The histidine reagent diethylpyrocarbonate (DPC) prevents the release of CyPD from ATP synthase induced by acidic pH. Bovine heart mitochondria, were incubated at the indicated pH in the absence or presence of DPC, and ATP synthase was immunoprecipitated with an anti-ATP Synthase Ab followed by 15% SDS-PAGE. β subunit and CyPD content were detected by Western blotting. Each immunodetected band was analyzed by densitometry and the ratio between the peak area of CyPD and that of the corresponding β subunit was measured and expressed relative to the ratio obtained at pH 7.4 in the absence of DPC, which was taken as 100%. Values are average ± S.E. of three independent experiments .**P<0.01, n.s.= not significant (Student *t* test).

Analysis of OSCP sequence showed that OSCP has only one histidine, His 112 (bovine numbering), which is conserved among species (Figure 3.2A). This histidine appeared an interesting candidate for the pH modulation of the CyPD-ATP synthase interaction for several regions: (i) it is exposed to the matrix, as depicted in Figure 3.2B, potentially allowing its modification by DPC, which is known to react only with surface-accessible hystidyl nitrogen atoms (Hnízda et al. 2008); (ii) it is located in one of the lowest (i.e. most negative) surface potential regions (Figure 3.2C), that has been recognized as a putative CyPD binding regions due to the complementary electrostatic properties (Giorgio et al. 2013); (iii) it is located in the linker region between the N- and C-terminal domains of OSCP (Rees et al. 2009), which appears to be flexible, enabling bending of the peripheral stalk towards the top of F_1 in the intact ATP synthase (Zhou A et al. 2015); (iv) it has a low pKa of 5.7, which is a property of histidine(s) involved in conformational changes induced by their protonation (Edgcomb & Murphy 2002). pKa value has been obtained by pre-processing the structure of bovine OSCP (PDB code 2WSS, chain S) using the

program PDB2PQR (Dolinsky et al. 2007) and the CHARMM set of radii and charges. The resulting pqr file was used as input to the program Bluues (Fogolari et al. 2012) to compute all titratable residues pKa. The results were compared with those obtained with the program PROPKA (Olsson et al. 2011), which essentially identical results.

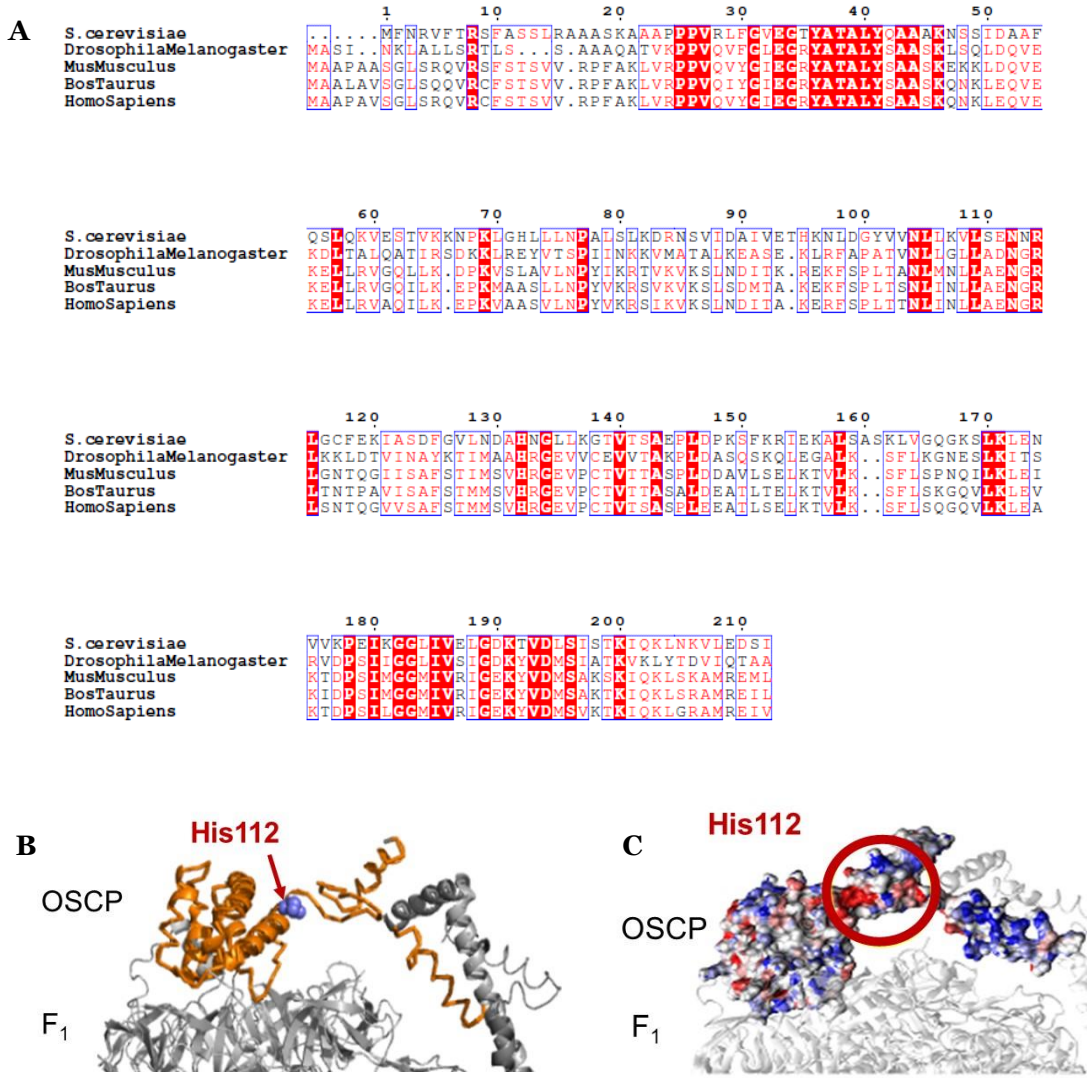

Figure 3.2 OSCP structure analysis. A) Sequence alignement of OSCP from different species. OSCP sequences were retrieved from Swiss-Prot database and the alignement performed with Clustal O (McWilliam et al. 2013). Numbering includes signal peptide. Conserved residues are highlighted in red and the unique conserved histidine is marked with an asterisk, which corresponds to position 112 of the bovine protein. **B)** View of the His112 of OSCP and the top of F1 domain based on the bovine crystal structure 2WSS (PDB entry). **C)** His 112 is located in one (highlighted by a red circle) of the two lowest potential regions on OSCP, which represent the putative binding regions of CyPD. The color code for the potential is: saturated red -8.0 kJ/(mol q), saturated blue 8.0 kJ/(mol q). F1 structure is shown in transparency. Surface potential is computed as previously described (Fogolari F. et al. 2012; Giorgio V. et al. 2013; Antoniel M. et al. 2014)

3.1.2Mass spectrometry analysis of the DPC-modified OSCP subunit of F_oF_1 ATP Synthase

It is well established that DPC labeling is very useful for studying protein structure and protein-protein interactions (Dage et al. 1998; Tsubaki et al. 2000; Qin et al. 2003). Due to DPC's molecular size, proteins are typically only labelled at amino acids that are exposed to the solvent on the protein surface (Hnízda et al. 2008). In particular, the reaction between DPC and histidine is accompanied by the formation of an ethoxyformyl group bound to the nitrogen atom of imidazole leading to a mass increase of 72 Da (Figure 3.3), so that the sites modified by DPC can be readily identified with high sensitivity by mass spectrometry (MS) because their signals are not diluted across many products (Foti et al. 1991; Zhou & Vachet 2012).

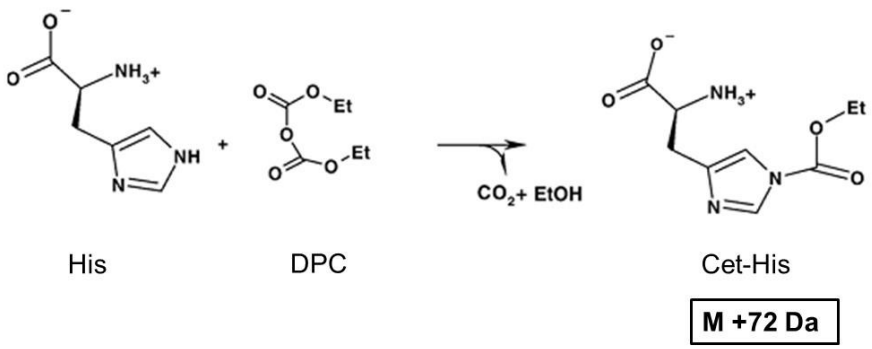

Figure 3.3 Modification of histidine by DPC and formation of carbethoxyhistidine (Cet-His) . From (Hnizda et al.2008).

Although very useful, the main limitation of using DPC is the relative instability of histidyl ethoxyformylation, which is particularly relevant at acidic and alkaline pH values (Melchior & Fahrney 1970). Moreover, thiol groups could capture a carbethoxy group from a modified histidine during SDS-PAGE (Zhou & Vachet 2012). Therefore, to set up the conditions of sample preparation for MS analysis of DPC-modified OSCP, a model protein, apomyoglobin (ApoMb), was used to check the stability of the DPC-modified histidines over time.

ApoMb, which contains 11 histidyl residues, is an extremely well-characterized protein commonly used in MS standardization (Zhou & Vachet 2012) and. The purified protein was treated with 5-fold molar excess of DPC for 10 minutes at 37 °C, the reaction was quenched with 10 mM imidazole and the sample was analysed by HPLC-MS after 4 hours incubation at 37°C, a time frame that does not

result in significantchanges in DPC-dependent histidine modification (Zhou & Vachet 2012). As expected, only His64 and His93 were modified, and the percentage modification was of about 30% as determined after overnight (O/N) incubation at 4°C, as well as after 4 hours incubation at 37°C followed by in solution tryptic digestion or in gel tryptic digestion. In this latter condition, Tris(2-carboxyethyl)phosphine hydrochloride (TCEP) was used as a thiol-free reducing agent during SDS-PAGE (Table 2). These results demonstrated that DPC modification remained rather stable under all the tested conditions, making this approach for MS analysis of DPC-modified OSCP.

Table 2. Comparison of DPC modification percentages[a] of ApoMb under different conditions

Residue	4 h 37° C	4 h 37° C Tryptic digestion	4 h 37° C In-gel digestion	O/N 4° C
His64	23,9	27,7	25,3	31
His93	29	31	28	34,2

[a] Modification percentages were calculated as ratio between peak intensity of carbethoxyhistidine and total histidine.

Mitochondria were then incubated in the absence or presence of DPC, as in Figure 3.1 and the ATP synthase immunoprecitates were subjected to 15% SDS-PAGE and stained with Coomassie Colloidal Blue. The bands at the molecular mass expected of the OSCP subunit were excised and processed by in-gel trypsin digestion. The resulting peptide mixtures were analysed by LC-MS/MS and MS/MS data were checked using the MASCOT search engine (Matrix Science Ltd, London, UK) against the Mammalian sequences of the Swiss-Prot database. The results showed a very high sequence coverage, confirming that the bands extracted from the gels correspond to OSCP subunit of bovine heart ATP synthase (Table 3).

Visual inspection of the ESI-MS spectrum acquired in the LC-MS/MS analysis of the OSCP tryptic peptide 95-113 (which contains His112) showed a mass shift of 72 Da compared to the sample not treated with DPC, consistent with His112

modification by DPC (Figure 3.4). Further analysis of the ESI-MS/MS spectra of the 95-113 peptides revealed that all the y ions in the DPC-modified peptide exhibit a mass shift of 72 Da, confirming the carbethoxylation of the unique His112 of OSCP (Figure 3.5). Of note, y ions derive from fragmentation of the CO-NH bonds, which are the most common cleavage sites along the amino acid backbone, and retain the charge on the C-terminal fragments (Roepstorrf et al. 1984; Johnson et al. 1989).

Table 3. Results of the MASCOT search for the OSCP band.[a]

Protein	UniProtKB AC.	Mass (Da)	Protein score	Sequence cov. (%)[b]	Peptide sequences
ATP synthase subunit O, mitochondrial OS=Bos taurus	P13621	23419	505	72.1	14(6[c])

[a]LC-MS/MS data were acquired on the tryptic digest of the SDS-PAGE band corresponding to the theoretical molecular mass of OSCP separated from the ATP synthase IPs. LC-MS/MS analyses were performed on a 6520 Q-TOF mass spectrometer (Agilent Technologies) and the data were analysed by the MASCOT software against the Mammalia sequences of the Swiss-Prot database (release 2013_04). The following parameters were used in the MASCOT search: Trypsin specificity; maximum number of missed cleavages: 2; fixed modification: carbamidomethyl (Cys); variable modifications: oxidation (M), deamidated (NQ); peptide mass tolerance: ± 10 ppm; fragment mass tolerance: ± 0.05 Da; protein mass: unrestricted; mass values: monoisotopic; [b]Sequence coverage calculated on the mature protein; [c] Peptides sequenced with a significant score ($p<0.05$).

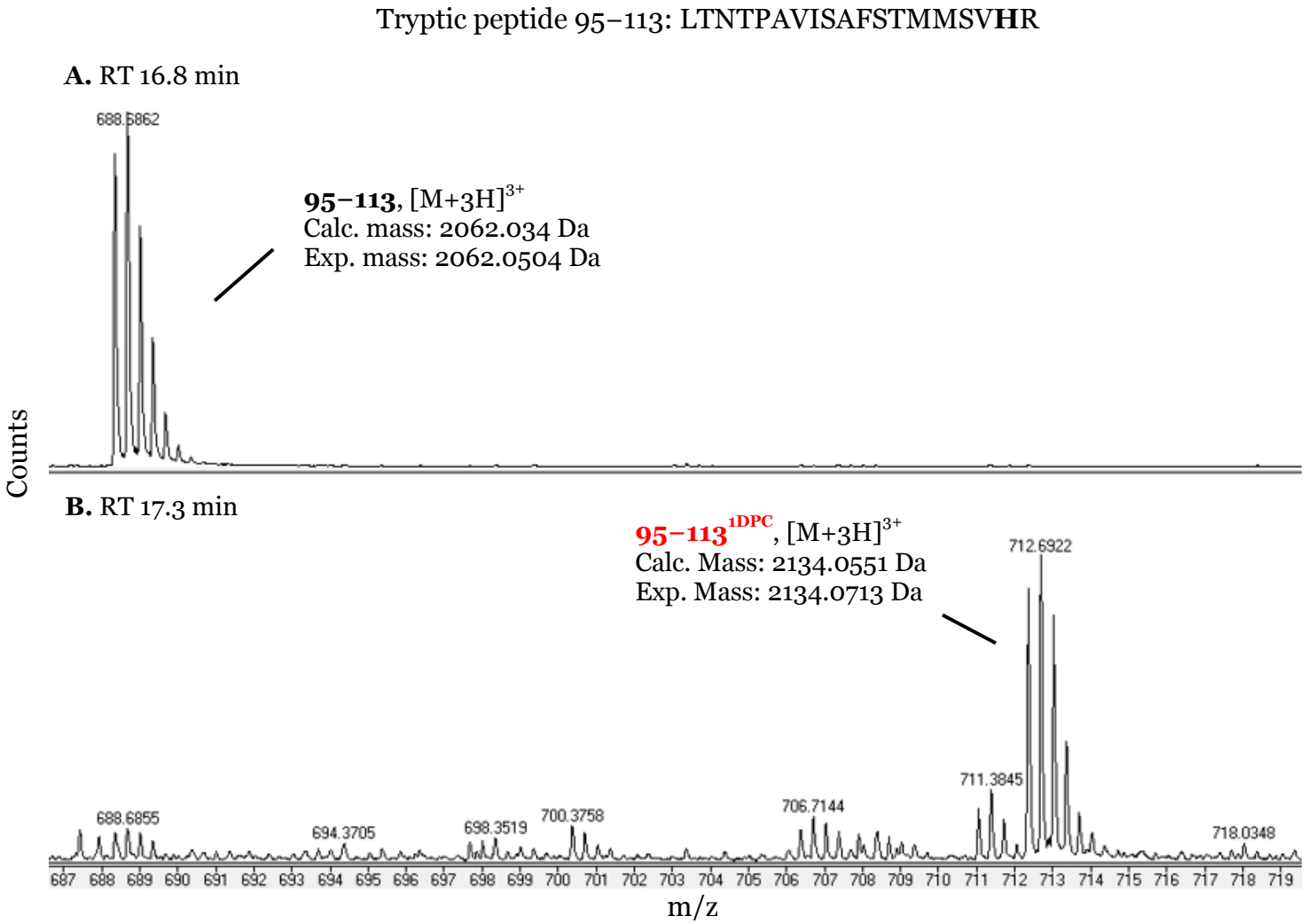

Figure 3.4. ESI-MS spectra acquired in the LC-MS/MS analysis of the tryptic digest of OSCP derivatised with DPC. The m/z region of the spectra in which the +3 molecular ions of peptide 95–113 (A, RT 16.8 min) and 95–113^{1DPC} (B, RT 17.3 min) were detected are shown.

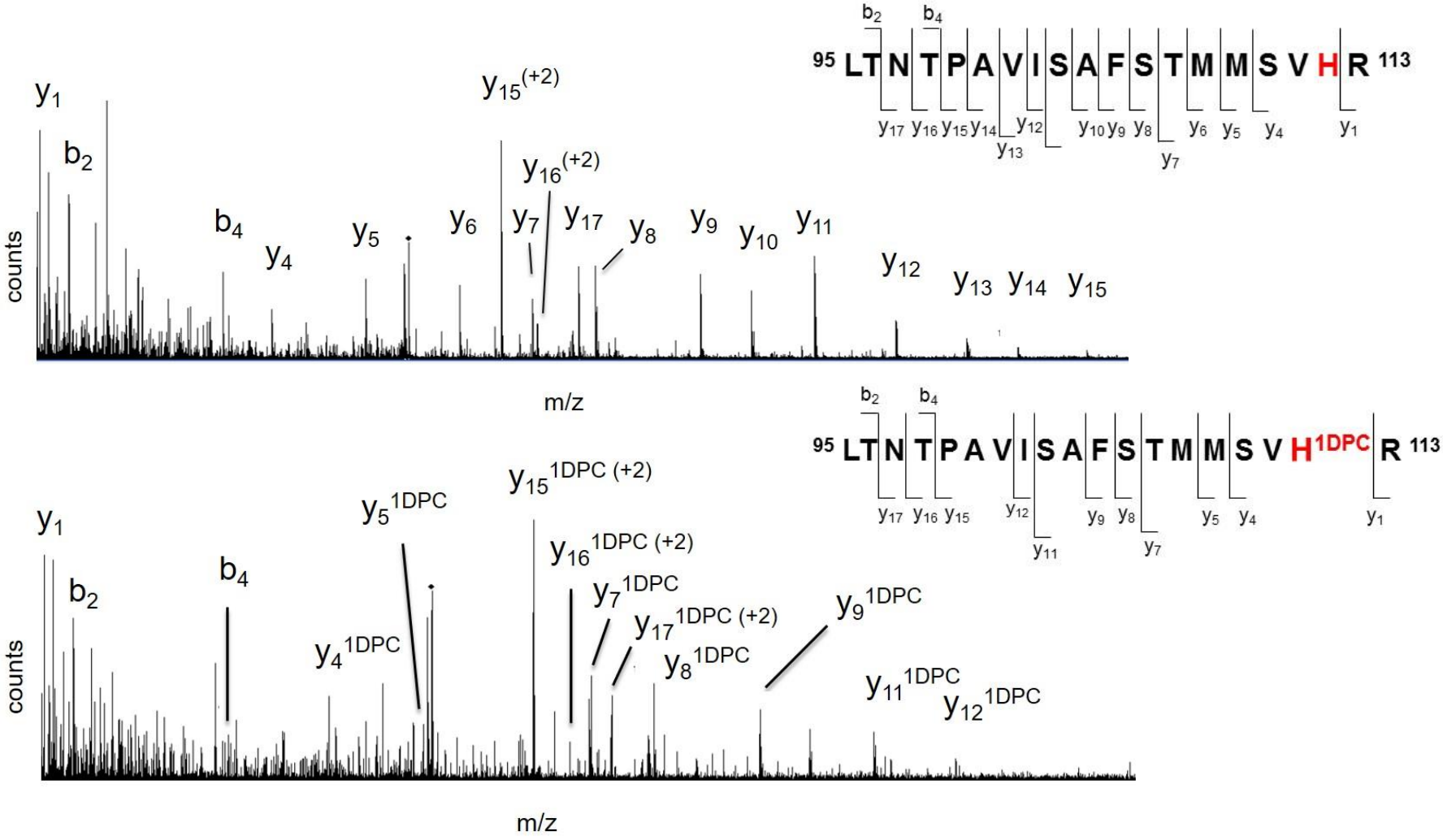

Figure 3.5.Region 170-280 m/z of the MS/MS mass spectra of peptide 95–113 of OSCP and OSCP modified at level of His112 with DPC. Fragments of the series b and y that were identified in the MS/MS spectra are indicated on the sequence of the peptides. His112 is indicated in bold as H and H^{1DPC} for the modified peptide. In the MS/MS spectra, ions assigned to fragments of the series y and b are indicated. All y ions show, in the modified peptide, a mass shift of +72 Da which is consistent with carbethoxylation of the unique His112.

3.2 Effect of DPC on the ATP hydrolytic activity of F_oF_1 ATP synthase

As already mentioned, CyPD binding to OSCP has major functional consequences, with a decrease of the ATP hydrolytic activity catalysed by ATP synthase that can be reversed by CsA-dependent CyPD displacement. Consistently, the ATPase activity of CyPD null mice mitochondria was 50% higher than that of wild type mitochondria, and CsA had no effect on the rate of ATP hydrolysis (Giorgio et al. 2009). As DPC treatment of mitochondria caused the modification of the unique histidyl residue of OSCP possibly involved in the CyPD binding, the effect of DPC on the enzyme activity was evaluated under conditions that affect CyPD binding to ATP synthase.

Assay of ATP hydrolysis was performed in Mg^{2+}-ATP submitochondrial particles from bovine heart (MgATP-SMP), wherebound CyPD can be displaced by CsA (Nicolli, Basso, et al. 1996). This membrane preparation, where the F1 catalytic moiety of ATP synthase is exposed to the solvent, is particularly useful inkinetic assays where putative enzyme modulators are tested. Briefly, MgATP-SMP were suspended in a medium containing 10 mM Pi (Pi), to favor CyPD binding, or without Pi (w/o Pi), treated with 200 μM or 400 μM DPC and the oligomycin-sensitive ATP hydrolysis rate was determined in the presence of an ATP-regenerating system (Harris & Bashford 1987). As shown in figure 3.6A, DPC inhibits the hydrolytic activity of ATP synthase in a dose-dependent manner, reaching a maximum value of about 30%, that is consistent with the inhibition value obtained with other inhibitors that target OSCP, such as Bz-423 (Johnson et al. 2005; Giorgio et al. 2013). However, DPC affected the ATPase activity only in the absence of Pi, while in the presence of Pi ATP synthase was protected from DPC inhibition. Moreover, DPC inhibition was reverted by hydroxylamine, strongly suggesting that its effect can be specifically traced to carbethoxylation of histidyl residues, which is readily reversed in the presence of nucleophiles, rather than to reaction with tyrosyl or sulfhydryl groups Nicolli et al. 1993 (Mendoza & Vachet 2008) (Figure 3.6B).

We also tested the effect of DPC in the presence of Pi and CsA, which displaces CyPD from ATP synthase even in the presence of Pi. Interestingly, under these conditions DPC inhibited the ATP hydrolytic activity, strongly suggesting that the “protective” effect of Pi on DPC inhibition is due to CyPD binding to OSCP rather

than to a direct effect of Pi on ATP Synthase (Figure 3.7A). Consistently, CsA was ineffective against inhibition of MgATP-SMP by 4-chloro-7-nitrobenzofurazan (NBD-Cl) (Perez et al. 1986), which reacts specifically with Tyr-311 of βE subunit (Orriss et al. 1998) and is protected by the binding of Pi to the F1 catalytic sites (Figure 3.7B).

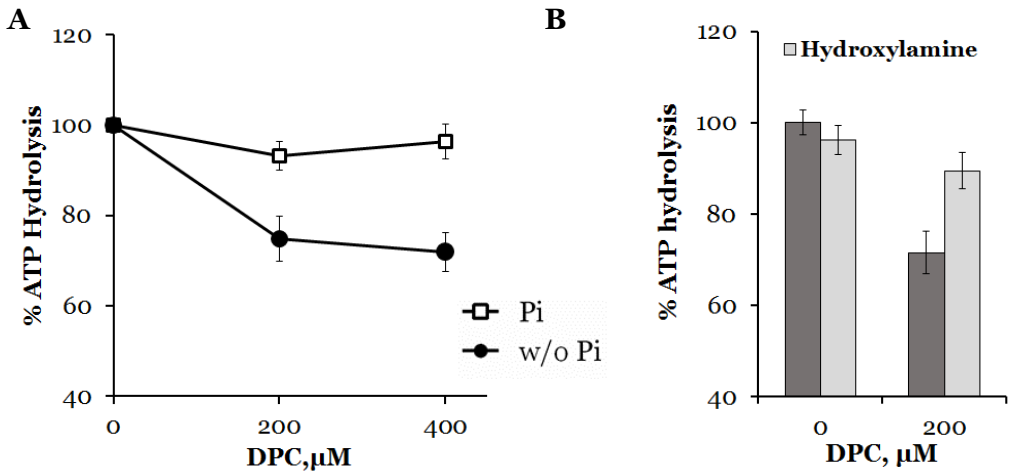

Figure 3.6. Effect of Pi and hydroxylamine on DPC-dependent ATP synthase inhibition. A) MgATP-SMP were incubated with the indicated concentrations of DPC in the presence (Pi) or absence (w/o) of 10 mM Pi and the rate of oligomycin-sensitive ATP hydrolysis at 37 °C was measured. **B)** MgATP-SMP were treated with 200 µM DPC in the absence of Pi, followed by their incubation with 1 mM hydroxylamine before the measurement of the ATP hydrolytic activity. Data are average ± S.E. of 4 independent experiments.

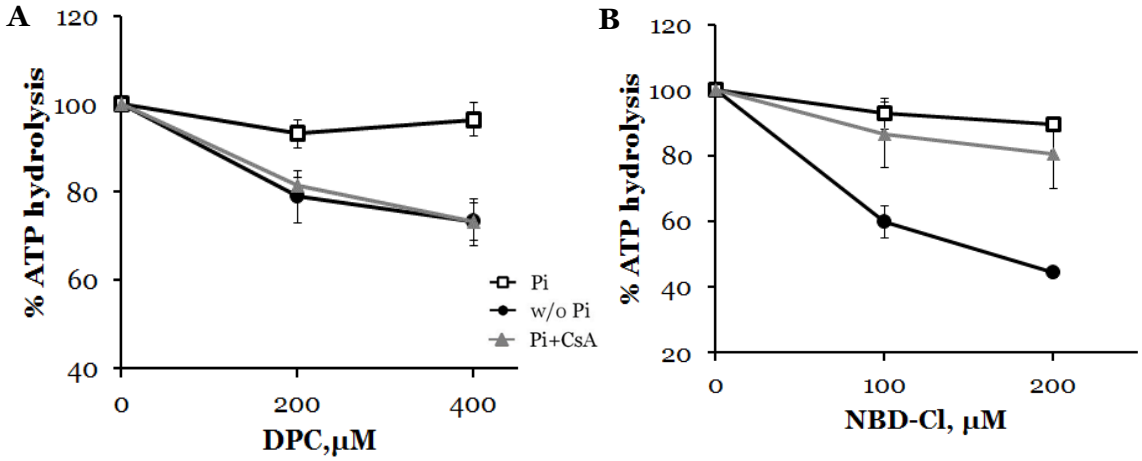

Figure 3.7. Effect of Pi and CsA on ATP Synthase inhibition by DPC and NBD-Cl. MgATP-SMP were incubated with the indicated concentrations of DPC **(A)** or NBD-Cl **(B)** in the absence of Pi (w/o Pi), in the presence of 10 mM Pi (Pi) or in the presence of 10 mM Pi and 1.6 µM CsA (Pi+CsA). The rate of oligomycin-sensitive ATP hydrolysis at 37 °C was measured. Data are average ± S.E. of 4 independent experiments.

To further test the involvement of CyPD in the protection against DPC inhibition, mitochondria from CyPD null mice were treated with DPC in the presence or absence of Pi. As expected, ablation of CyPD abolished the protective role of Pi against DPC inhibition (Figure 3.8A). Conversely, in the same mitochondria Pi protection against NBD-Cl was totally ineffective (Figure 3.8B).

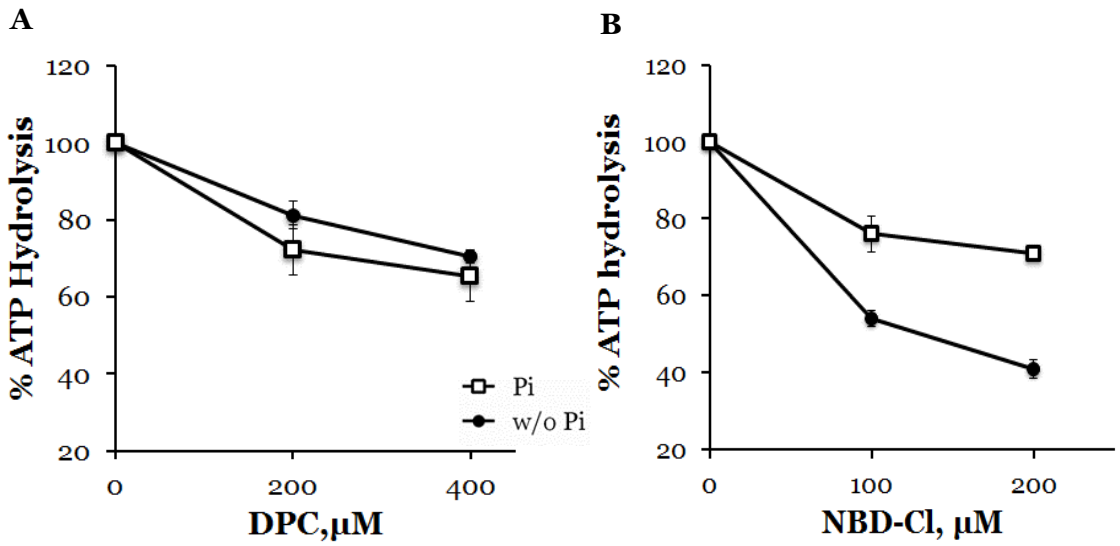

Figure 3.8. Effect of Pi and CsA on ATP Synthase inhibition by DPC and NBD-Cl in CyPD-null mitochondria. Freshly prepared liver mitochondria from *Ppif*$^{-/-}$mice were incubated in the presence (Pi) or absence (w/o Pi) of xx mM Pi and treated with the indicated concentrations of DPC (A) or NBD-Cl (B). After incubation with 10 µM alamethicin ATP Synthase hydrolytic activity was measured. Reported values are average± S.E. of 3 independent experiments.

In summary, the ensemble of these findings suggest that the partial inhibition of ATPase activity by DPC may be a consequence of carbethoxylation of the OSCP His112, which is not accessible to the solvent when CyPD is bound to ATP synthase. Indeed, DPC inhibited the ATPase activity exclusively in the presence of CsA (which releases CyPD from OSCP) or in mitochondria from *Ppif*$^{-/-}$ mice (where CyPD has been genetically ablated). Consistent with this model, DPC does not influence CyPD binding at neutral pH, because His112 is not exposed. Conversely, lowering pH (i) favors CyPD release due to protonation of His112 and (ii) at the same time, it allows DPC reaction with His112, allowing CyPD (re)binding. These data therefore strongly support the hypothesis that OSCP His112 is part of the binding site of CyPD on the protein. This region also comprises Glu115, Glu128 and Glu133, which confer a low potential surface (Giorgio et al. 2013).

As already mentioned, bioinformatic analyses suggested a secondputative binding region of CyPD on OSCP located at residues Glu48, Asp71, Glu76, Phe78 (bovine numbering). This region overlaps with helices 3 and 4, the binding site of the PTP inducer Bz-423 (Giorgio et al. 2013). When the effect of Bz-423 on the association of CyPD was tested, both in mouse and bovine ATP synthase a concentration-dependent displacement was observed that is indeed consistent with competition for a common binding site (Giorgio et al. 2013). On the other hand, an NMR study established that Bz-423 binding to OSCP helices 3 and 4 induces conformational changes at helices 1,5 and 6 perturbing the OSCP-F1 interface and resulting in enzyme inhibition (Stelzer et al. 2010). As His112 is very close to helix 6 (Rees et al. 2009), it may be speculated that Bz-423 competition with CyPD is not directly due to a common binding site on helices 3 and 4, but rather to Bz-423-dependent conformational rearrangements of the domain comprising His112.

3.3 Effects of pH on the PTP in OSCP His 112 mutants

The results presented so far suggest (i) that protonationof the His 112 of OSCP favours CyPD release from ATP Synthase (which would lead to PTP inhibition by acidic pH), and (ii) that DPC-dependent His112 carbethoxylation prevents CyPD release (which would allow PTP opening in spite of the acidic pH). In order to investigate whether a mechanistic relationship exists between CyPD binding to ATP synthase and propensity of the PTP to open OSCP His112 was been replaced with a residue that is not subjected to reversible protonation.

By applying the CRISPR/Cas9 technology a OSCP H112Q variant was introduced in the genome of HEK cells by the laboratory of Prof. Micheal Forte, Vollum Institute, Oregon Health and Sciences University. This amino acid substitution was chosen based onusing the PAM120 database, built by comparing evolutionarily close sequences that are highly similar (Wilbur 1985).The His → Gln mutation was found to be very frequent and should be the most conservative because it removes the charge and the pH equilibrium, but maintains hydrogen-bonding capability. Another frequent mutation was His → Tyr but this was not preferred for the possible occurrence of tyrosine phosphorylation events

To assess whether ATP Synthase activity was affected by the mutation we assessed oxygen consumption rate (OCR) with the sensitive Seahorse technology (Wu et al. 2007). In a typical experiment, basal respiration largely reflects mitochondrial oxygen consumption linked to ATP synthesis, as shown by its inhibition with oligomycin. Addition of the protonophore FCCP then allows to determine the maximal respiratory rate, and the subsequent addition of rotenone (selective inhibitor of respiratory complex I) and antimycin A (inhibitor of complex III) allows to define the small fraction of residual non mitochondrial respiration

Wild type cells (WT) and cells carrying the OSCP His112Gln mutation (H>Q cells) displayed exactly the same respiratory pattern (Figure 3.9), indicating that respiratory function and mitochondrial ATP production are unaffected by the mutation, consistent with its conservative nature of the mutation and to the location of His112 in the flexible linker region between the N- and C-terminal domains of OSCP. This is at variance with the yeast OSCP Gly → Asn mutation at position 166, which is located in the structured C-terminal domain that contacts with F6 and b of the lateral stalk, so that the mutation causes impaired coupling of ATP synthase complexes, which were more susceptible to dissociation of F1 from Fo (Boyle et al. 2000).

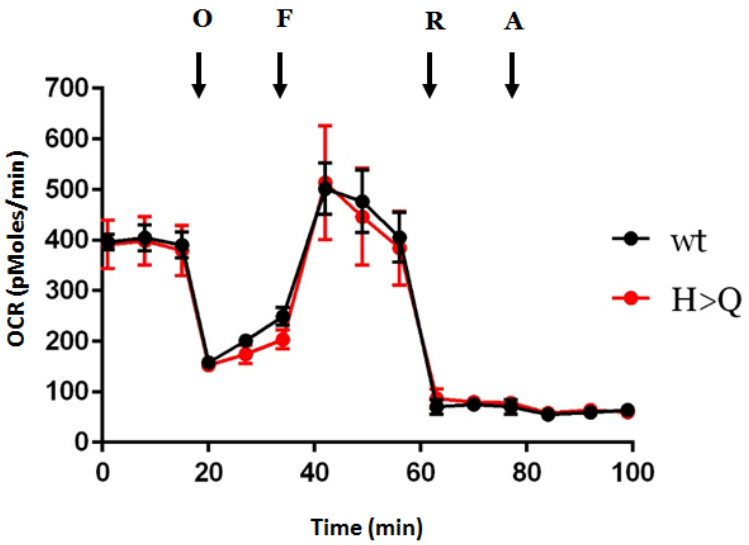

Figure 3.9 Activity of FoF1 ATP Synthase in wild type HEK cells and in HEK cells carrying the OSCP His112Gln mutation (H>Q). ATP Synthase activity was measured by the Seahorse technique as detailed in Materials and Methods. Where indicated (arrows) oligomycin (O), FCCP (F), rotenone (R), and antimycin A (A) were added. The traces are representative of 3 experiments.

The ability of WT and mutated cells to undergo PT was evaluated with the sensitive CRC test. Briefly, digitonin permeabilized cells were suspended in sucrose assay buffer that also contains Calcium Green-5N, a probe that increases its fluorescence emission upon calcium binding, and subjected to a train of Ca^{2+} pulses. PTP opening is marked by a process of precipitous Ca^{2+} release.

H>Q cells readily took up a train of Ca^{2+} pulses in a process that was sensitive to CsA. The Ca^{2+} load required to trigger PTP opening was indistinguishable from that of wild type cells (Figure 3.10A and B), meaning that, at neutral pH, PTP function is maintained in the cells carrying the OSCP His112Gln mutation.

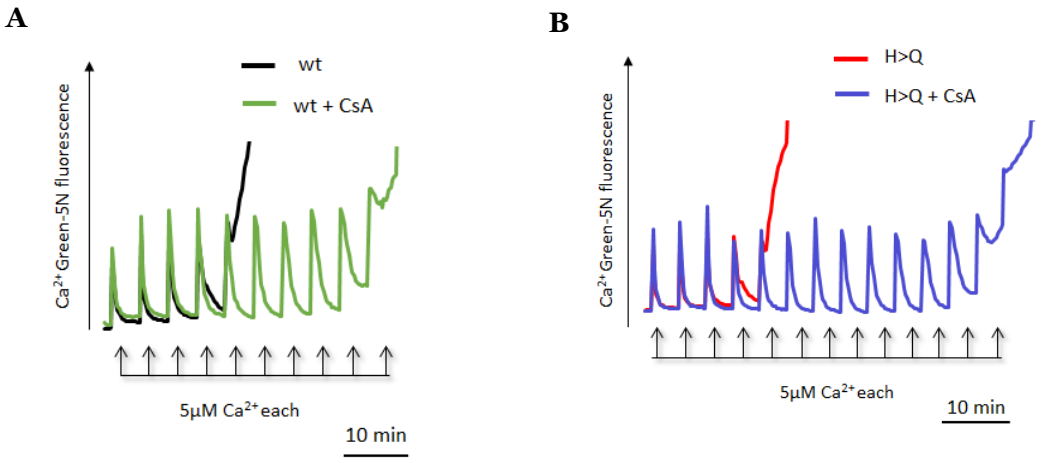

Figure 3.10 Ca^{2+} sensitivity of the PT in wild type HEK cells (A) and in HEK cells carrying the OSCPHis112Gln mutation (H>Q) (B). The PTP function is assessed through CRC assay in the absence and presence of CsA (see Materials and Methods). The traces are representative of 4 experiments.

To assess the pH sensitivity of the PT, permeabilized cells were suspended in KSCN buffers in the absence of respiratory substrates at different pH, in order to achieve constant values of matrix pH, as in (Nicolli et al. 1993). Under these conditions diffusion of the lipophilic SCN^- anion within mitochondria provides the driving force for electrophoretic Ca^{2+} accumulation (Selwyn et al. 1970). Ca^{2+} influx collapses SCN^- diffusion potential and prevents development of a large membrane potential that would counteract the increase of PTP opening (Bernardi et al. 1992; Petronilli et al. 1993). Since the permeability for SCN^- and Ca^{2+} is higher than that for H^+, it is possible to achieve Ca^{2+}-dependent PTP opening in absence of respiration and of net H^+ movements (Nicolli et al, 1993) and the PT can be measured as the rate of swelling (decrease in absorbance at 540nm).

As expected, in wild type cells PTP opened at pH 7.4, while at pH 6.5 there is a strong inhibitory effect of matrix H^+ on its opening (Figure 3.11 A). Conversely, in H>Q cells Ca^{2+} addition induces mitochondrial swelling at both neutral and acidic pH (Figure 3.11 B), indicating that the PTP of these cells is insensitive to inhibition at acidic pH.

DPC was expectedly effective in allowing PTP opening at acidic pH in wild type cells (Figure 3.12A), as originally observed in isolated mitochondria (Nicolli et al. 1993). On the other hand in H>Q cells DPC had no effect both at neutral and acidic pH. Therefore, these experiments conclusively show that His112 of OSCP

mediates the inhibitory effect of acidic pH on the PTP (Bernardi et al. 1992; Nicolli et al., 1993) and that it is the target of DPC (Figure 3.12B). Further experiments are in progress in HEK cells carrying the OSCP His112Tyr mutation, which is also very frequent. Indeed, OSCPTyr112 is not susceptible to protonation at low pH, because its pKa is much higher than OSCPHis112.

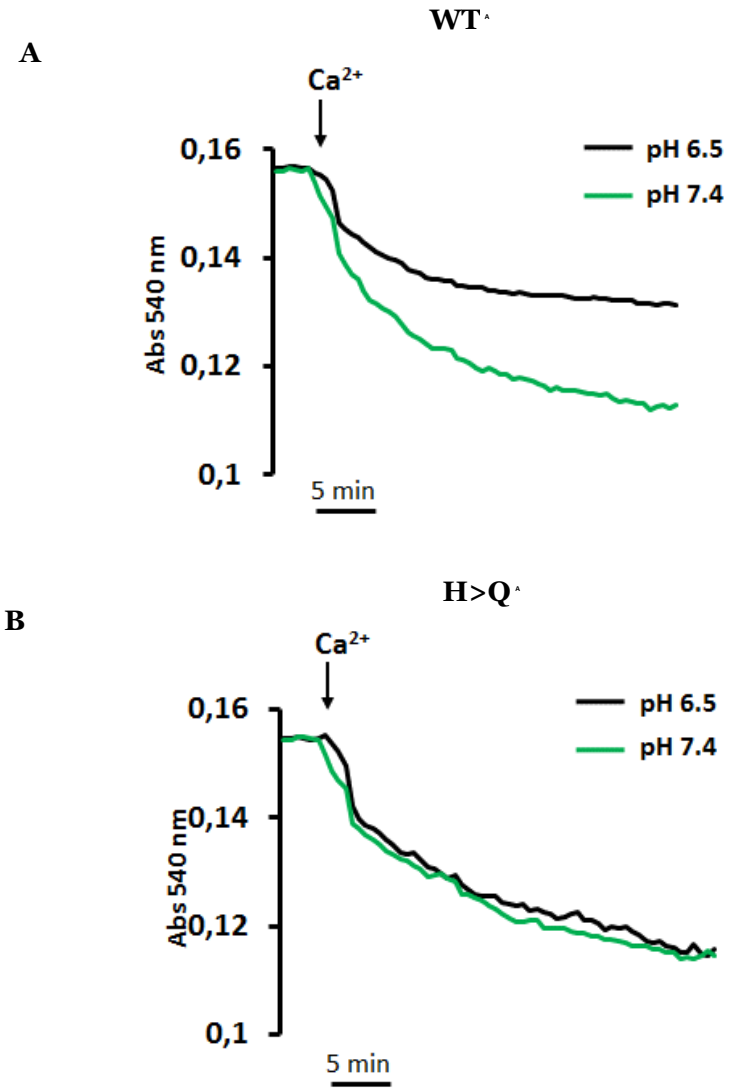

Figure 3.11 pH-dependent modulation of PTP opening in wild type HEK cells (A) and in HEK cells carrying the OSCP His112Gln mutation (H>Q) (B). Permeabilized cells were suspended in KSCN buffers at pH 7.4 or pH 6.5 and the PTP opening was measured as the rate of swelling (decrease in absorbance at 540nm), as outlined in Materials and Methods. Traces are representative of 3 experiments.

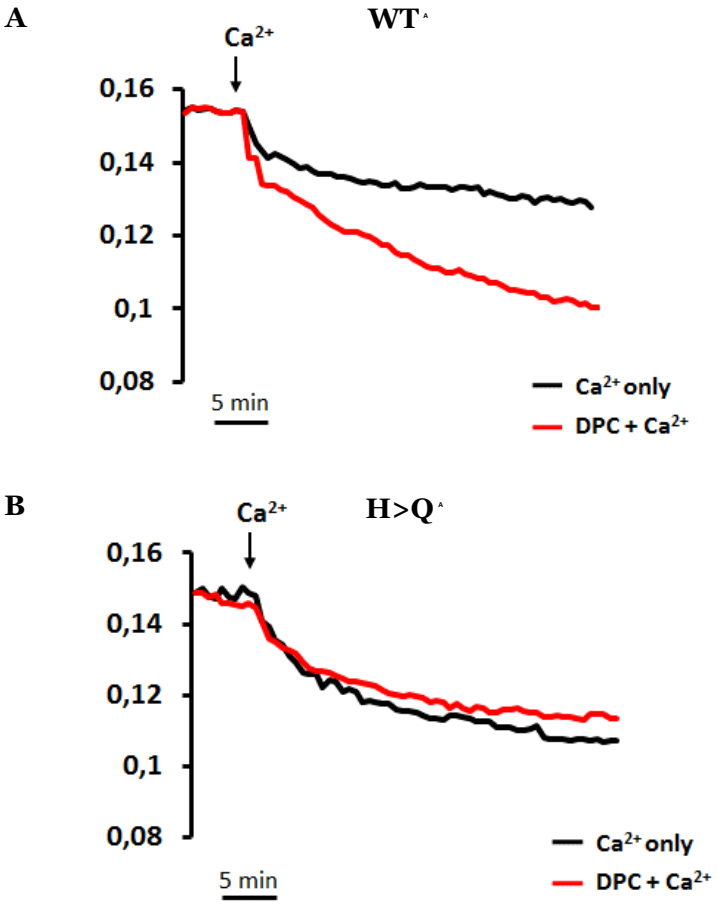

Figure 3.12. Effect of DPC on the PTP opening in wild type HEK cells (A) and in HEK cells carrying the OSCP His112Gln mutation (H>Q) (B). Permeabilized cells were suspended in KSCN buffers at pH 6.5 and the PTP opening was measured as the rate of swelling (decrease in absorbance at 540nm), as in Figure 3.11. Traces are representative of 3 experiments.

In summary, these results point at His112 of OSCP as the critical residue of the F_oF_1 ATP synthase responsible for the sensitivity of the PTP to acidic matrix pH. OSCP makes contacts with both F_1 and the peripheral stalk and the linker region comprising His112 appears involved in the bending of the entire peripheral stalk towards the top of F_1 in the intact ATP synthase (Zhou et al. 2015). It is tempting to speculate that His112 protonation may cause conformational changes within OSCP that affect accessibility of the Me^{2+} binding sites in β subunits and/or the state of the lateral stalk, blocking switch of ATP synthase switch to the PTP. OSCP His112 also appears critical for pH modulation of CyPD binding, at least in mammalian cells. Evaluation of the pH and DPC sensitivity of the CyPD binding to ATP synthase in mutated HEK cells, which is in progress, will help shed further light on the fascinating problem of modulation of the PTP by H^+.

3.4 Assessment of the interaction between inhibitor protein (IF_1) and F_oF_1 ATP Synthase

Inhibition of the at acidic pH may also suggest involvement of the inhibitor protein IF_1, whose binding to F_1 is favored by low pH with formation of the inhibitory dimeric form of IF_1 (Cabezon et al. 2000). Indeed, in the inhibited IF_1-F_1 complex two Mg^{2+}-ADP molecules are trapped in the catalytic sites of both β_{DP} and β_{TP} subunits (Bason et al. 2011; Bason et al. 2014b), which may affect the hypothetical replacement of Mg^{2+} with Ca^{2+} at the F_1 catalytic sites that we postulate to be required for the switch of ATP synthase to PTP. On the other hand, the inhibited IF_1-F_1 complex does not contain Pi, which is a PTP inhibitor at low concentration, suggesting that IF_1 binding might mask an inhibitory site favoring rather than preventing PTP opening.

Interestingly, in the 1980s it had been reported that DPC treatment of isolated IF_1 blocks its inhibitory activity towards submitochondrial particles deprived of endogenous IF_1 (Panchenko & Vinogradov 1985). Consistently, it was later established that IF_1 from mammalian mitochondria harbours a conserved histidine residue (His49), which requires a change in protonation to disassemble inactive IF_1 tetramers in two dimers allowing inhibition of ATPase activity by each dimer (Cabezón et al. 2003).

These observations might suggest that the effect of DPC on the PTP formation at low pH is, in part at least, related to the DPC modification of IF_1 impairing its inability to bind ATP synthase. We assessed whether DPC prevents the increased IF_1 binding to ATP synthase at acid pH in submitochodrial particles deprived of endogenous IF_1 and in whole mitochondria from bovine heart. Isolated IF_1 was treated with DPC and its ability to inhibit the ATP synthase activity tested as in (Panchenko & Vinogradov 1985). Whole mitochondria were treated with DPC prior to acidification and then subjected to ATP synthase immunoprecipitation to evaluate the amount of bound IF_1 by Western Blot against IF_1 and β subunit. As expected, DPC treatment of isolated IF_1 impaired its ability to inhibit ATP hydrolysis in submitochondrial particles (Figure 3.13A). Moreover, in whole mitochondria the amount of IF_1 bound to ATP synthase (expressed as IF1/β ratio), which is regulated by several factors (Lippe et al. 1988), increased at low pH in the absence but not in the presence of DPC (Figure 3.13B and C).

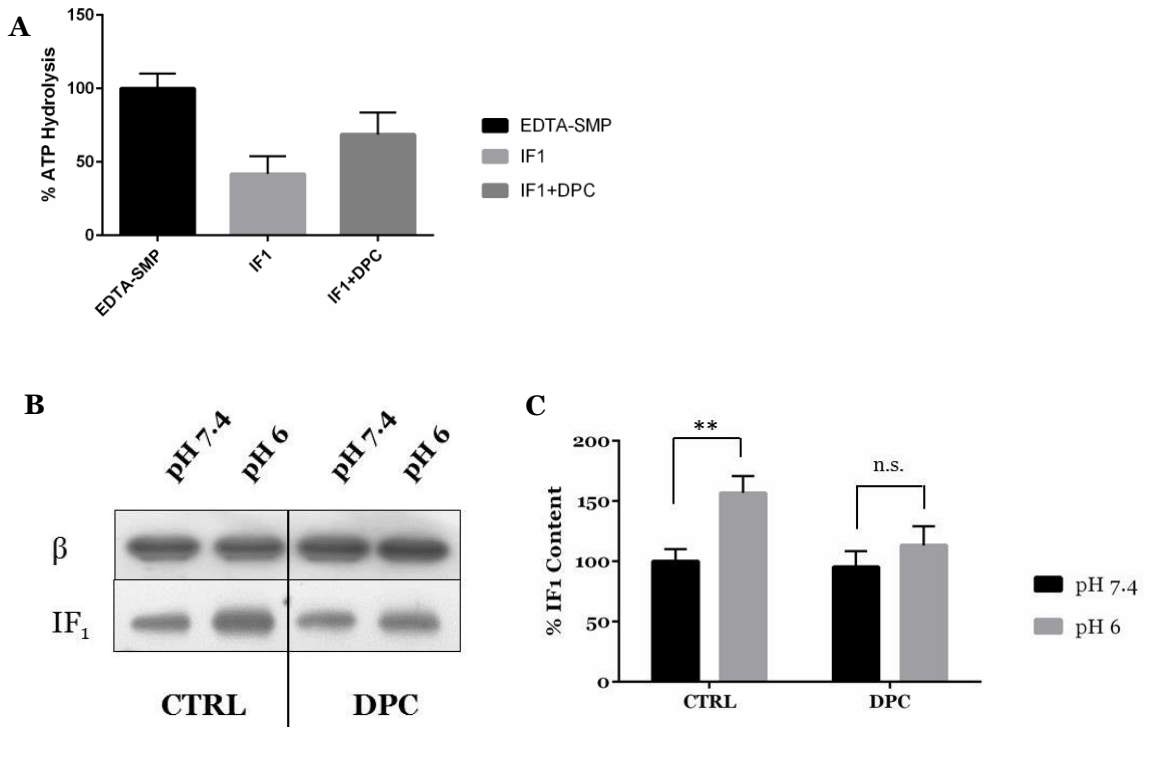

Figure 3.13. Effect of DPC on IF_1 binding to ATP Synthase
(**A**) Purified bovine heart IF1, incubated in the absence or presence of DPC, were added to the EDTA-SMP suspended at pH 6.5 before measuring their ATP hydrolysis activity as described in Methods. **B**) Freshly prepared bovine heart mitochondria were suspended at pH 7.4 or 6.0 and treated or not with DPC; ATP synthase was immunoprecipitated and the amount of IF1 and β subunit was detected by Immunoblot. **C**) Each immunodetected band was analyzed by densitometry and the ratio between the peak area of IF1 and that of the corresponding β subunit was measured and expressed relative to the ratio obtained at pH 7.4 in the absence of DPC, which was taken as 100%. Data are mean of 3 experiment ± SEM.**P <0.01, n.s.=not significant (Student *t* test).

These results appear promising but do not yet allow firm conclusions to be made. Although IF_1 silencing/overexpression could, at least in principle, establish if this factor has a role in PTP formation or modulation, conflicting results have been reported, demonstrating that modulation of the IF_1 expression differentially affects metabolism in normal (Bisetto et al. 2013) and tumor (Campanella et al. 2008) cells (Sánchez-Aragó et al. 2012). Single mutation of IF_1 at histidine residues appears a more promising approach to check if it is involved in the pH sensitivity of the PTP.

As already mentioned, in our hands only the dimeric form of ATP synthase is able to generate currents in electrophysiology experiments. The inhibition of PTP formation at low pH might be due to a structural instability of the dimers and the consequent dissociation into monomers. To test this hypothesis the stability of the dimers at different pH has been evaluated by blue native-PAGE assessing the ratio between the dimeric and

monomeric form both by Coomassie Blue and activity staining (Bisetto et al. 2007). Submitochondrial particles (EDTA-SMP) were suspended in buffers at different pH values, extracted using digitonin and subjected to blue native-PAGE. The dimer/monomer ratio revealed by Coomassie staining did not change, demonstrating that dimer stability is not affected by low pH (Figure 3.15A). Intriguingly, treatment at low pH selectively caused inhibition of the in-gel ATPase activity of the dimers, suggesting the occurrence of inhibitory binding to ATP synthase of IF_1 associated to the IMM (Figure 3.15B).

IF_1 content of both monomers and dimers was then evaluated by excising the bands from the native gel, followed by 2D SDS-PAGE and Western Blot analysis. As shown in Figure 3.15 C IF_1 content of monomers did not change in function of pH, while IF_1 seems to prefer the dimeric form of ATP synthase as binding partner at low pH. Therefore, decreased ATPase activity at low pH matches increased levels of bound IF_1 suggesting that it is not due to instability of the dimers.

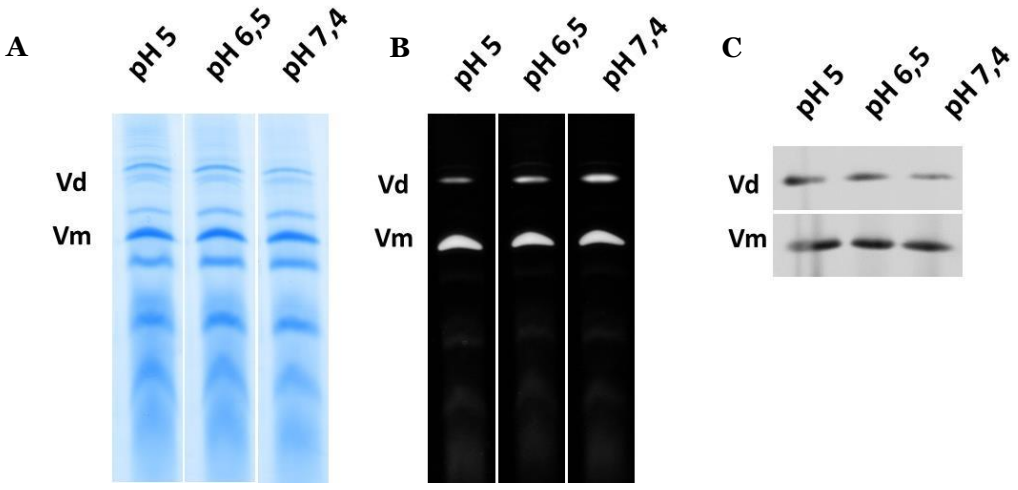

Figure 3.14. Blue native-PAGE of EDTA-SMP subjected to different pH-treatments. EDTA-SMP were suspended in buffers at the different pH and subjected to blue native PAGE stained by Coomassie staining (**A**) or in-gel ATPase activity (**B**). The bands of the ATP Synthase dimers (Vd) and monomers (Vm) were excised, their subunits were separated by 15% SDS-PAGE and the amount of IF1 was revealed by Western blotting (**C**). The patterns are representative of 4 experiments.

4. CONCLUSIONS

The results presented in this Thesis document the critical role of the unique OSCP histidine (His112) in the modulation of the CyPD-ATP Synthase interactions, strongly indicating that the region comprising His112 is the binding site of CyPD. Moreover, replacement of OSCP His112 with a Gln residue in HEK cells demonstrated that His112 mediates PTP inhibition by H^+, indicating that OSCP His112 is responsible for both pH modulation of PTP and CyPD binding to ATP synthase.

Treatment of bovine heart mitochondria with the histidine modifier reagent DPC (i) partially reduced IF1 binding at acidic pH, which is consistent with a critical role of IF1 histidyl residues for the inhibitory activity on the ATP synthase and (ii) prevented the release of CyPD from ATP synthase induced by acidic pH. While the first effect is probably not relevant to PTP modulation, the second effect led us to unravel the mechanism of PTP inhibition by acidic pH. This latter effect of DPC was reversed by hydroxylamine, indicating that it can be traced to carbethoxylation of histidyl residue(s). Consistently, both electrospray ionization mass spectrometry (ESI-MS) and mass tandem (LC-MS/MS) analyses confirmed the carbethoxylation of OSCP His112, which mediates partial inhibition of ATP synthaseonly when CyPD is not bound to the complex. Indeed, DPC inhibited ATPase activity only in mitochondria from CyPD null mice or in submitochondrial particles treated with CsA, i.e. a condition that promotes CyPD release from OSCP. In permeabilized HEK cells carrying the His112Gln mutation Ca^{2+} induced PTP opening both at neutral and acidic pH. This is at striking variance from wild-type HEK cells were Ca^{2+} does not induce PTP opening at acidic pH. These data demonstrate that protonation of OSCP His112 is responsible for PTP inhibition by H^+, and provide compelling evidence that ATP synthase and PTP are the same molecular entity.

5. References

Abrahams, J.P. et al., 1994. Structure at 2.8 A resolution of F1-ATPase from bovine heart mitochondria. *Nature*, 370(6491), pp.621–628.

Abrahams, J.P. et al., 1996. The structure of bovine F1-ATPase complexed with the peptide antibiotic efrapeptin. *Proceedings of the National Academy of Sciences of the United States of America*, 93(18), pp.9420–4.

Adachi, K. et al., 2007. Coupling of rotation and catalysis in F(1)-ATPase revealed by single-molecule imaging and manipulation. *Cell*, 130(2), pp.309–21.

Alavian, K.N. et al., 2014. An uncoupling channel within the c-subunit ring of the F1FO ATP synthase is the mitochondrial permeability transition pore. *Proceedings of the National Academy of Sciences of the United States of America*, 111(29), pp.10580–5.

Alavian, K.N. et al., 2011. Bcl-xL regulates metabolic efficiency of neurons through interaction with the mitochondrial F1FO ATP synthase. *Nature cell biology*, 13(10), pp.1224–33.

Allen, R.D., Schroeder, C.C. & Fok, A.K., 1989. An investigation of mitochondrial inner membranes by rapid-freeze deep-etch techniques. *The Journal of cell biology*, 108(6), pp.2233–40.

Antoniel, M. et al., 2014. The oligomycin-sensitivity conferring protein of mitochondrial ATP synthase: emerging new roles in mitochondrial pathophysiology. *International journal of molecular sciences*, 15(5), pp.7513–36.

Arora, K. et al., 2005. Extracellular cyclophilins contribute to the regulation of inflammatory responses. *Journal of immunology (Baltimore, Md. : 1950)*, 175(1), pp.517–22.

Ascoli, F., Fanelli, M.R. & Antonini, E., 1981. Preparation and properties of apohemoglobin and reconstituted hemoglobins. *Methods in enzymology*, 76, pp.72–87.

Azarashvili, T. et al., 2014. Potential role of subunit c of F0F1-ATPase and subunit c of storage body in the mitochondrial permeability transition. Effect of the phosphorylation status of subunit c on pore opening. *Cell Calcium*, 55(2), pp.69–77.

Azarashvili, T.S. et al., 2002. Phosphorylation of a peptide related to subunit c of the F0F1-ATPase/ATP synthase and relationship to permeability transition pore opening in mitochondria. *Journal of bioenergetics and biomembranes*, 34(4), pp.279–84.

Azzolin, L. et al., 2010. The mitochondrial permeability transition from yeast to mammals. *FEBS letters*, 584(12), pp.2504–9.

Baines, C.P. et al., 2005. Loss of cyclophilin D reveals a critical role for mitochondrial permeability transition in cell death. *Nature*, 434(7033), pp.658–662.

Baines, C.P. et al., 2007. Voltage-dependent anion channels are dispensable for mitochondrial-dependent cell death. *Nature Cell Biology*, 9(5), pp.550–555.

Baker, L. a et al., 2012. Arrangement of subunits in intact mammalian mitochondrial ATP synthase determined by cryo-EM. *Proceedings of the National Academy of Sciences of the United States of America*, 109(29), pp.11675–80.

Baker, M.J. et al., 2007. Mitochondrial protein-import machinery: correlating structure with function. *Trends in cell biology*, 17(9), pp.456–64.

Bason, J. V et al., 2011. Binding of the inhibitor protein IF(1) to bovine F(1)-ATPase. *Journal of molecular biology*, 406(3), pp.443–53.

Bason, J. V et al., 2014. Pathway of binding of the intrinsically disordered mitochondrial inhibitor protein to F1-ATPase. *Proceedings of the National Academy of Sciences of the United States of America*, 111(31), pp.11305–10.

Basso, E. et al., 2008. Phosphate is essential for inhibition of the mitochondrial permeability transition pore by cyclosporin A and by cyclophilin D ablation. *The Journal of biological chemistry*, 283(39), pp.26307–11.

Basso, E. et al., 2005. Properties of the permeability transition pore in mitochondria devoid of Cyclophilin D. *The Journal of biological chemistry*, 280(19), pp.18558–61.

Baughman, J.M. et al., 2011. Integrative genomics identifies MCU as an essential component of

the mitochondrial calcium uniporter. *Nature*, 476(7360), pp.341–5.

Bell, A., Monaghan, P. & Page, A.P., 2006. Peptidyl-prolyl cis-trans isomerases (immunophilins) and their roles in parasite biochemistry, host-parasite interaction and antiparasitic drug action. *International journal for parasitology*, 36(3), pp.261–76.

Belogrudov, G.I., 2009. Recent advances in structure-functional studies of mitochondrial factor B. *Journal of bioenergetics and biomembranes*, 41(2), pp.137–43.

Bergeaud, M. et al., 2013. Mitochondrial p53 mediates a transcription-independent regulation of cell respiration and interacts with the mitochondrial F_1 F0-ATP synthase. *Cell cycle (Georgetown, Tex.)*, 12(17), pp.2781–93.

Bernardi, P. et al., 2015. From ATP to PTP and Back: A Dual Function for the Mitochondrial ATP Synthase. *Circulation research*, 116(11), pp.1850–62.

Bernardi, P., 1999. Mitochondrial transport of cations: channels, exchangers, and permeability transition. *Physiological reviews*, 79(4), pp.1127–55.

Bernardi, P., 1992. Modulation of the Mitochondrial Cyclosporin A-sensitive Permeability Transition Pore by the Proton Electrochemical Gradient. , 267(13), pp.8834–8839.

Bernardi, P. et al., 1992. Modulation of the mitochondrial permeability transition pore. Effect of protons and divalent cations. *The Journal of biological chemistry*, 267(5), pp.2934–9.

Bernardi, P. et al., 2006. The mitochondrial permeability transition from in vitro artifact to disease target. *The FEBS journal*, 273(10), pp.2077–99.

Besman, M.J. et al., 1989. Identification of des-(Gly-Ile)-endozepine as an effector of corticotropin-dependent adrenal steroidogenesis: stimulation of cholesterol delivery is mediated by the peripheral benzodiazepine receptor. *Proceedings of the National Academy of Sciences of the United States of America*, 86(13), pp.4897–901.

Bisetto, E. et al., 2008. Functional and stoichiometric analysis of subunit e in bovine heart mitochondrial F(0)F(1)ATP synthase. *Journal of bioenergetics and biomembranes*, 40(4), pp.257–67.

Bisetto, E. et al., 2007. Mammalian ATPsynthase monomer versus dimer profiled by blue native PAGE and activity stain. *Electrophoresis*, 28(18), pp.3178–3185.

Bisetto, E. et al., 2013. Proteomic analysis of F1F0-ATP synthase super-assembly in mitochondria of cardiomyoblasts undergoing differentiation to the cardiac lineage. *Biochimica et biophysica acta*, 1827(7), pp.807–16.

Blatt, N.B. et al., 2002. Benzodiazepine-induced superoxide signals B cell apoptosis: mechanistic insight and potential therapeutic utility. *The Journal of clinical investigation*, 110(8), pp.1123–32.

Boerries, M. et al., 2007. Ca2+ -dependent interaction of S100A1 with F1-ATPase leads to an increased ATP content in cardiomyocytes. *Molecular and cellular biology*, 27(12), pp.4365–4373.

Bonora, M. et al., 2013. Role of the c subunit of the FO ATP synthase in mitochondrial permeability transition. *Cell cycle (Georgetown, Tex.)*, 12(4), pp.674–83.

Borel, J.F. et al., 1977. Effects of the new anti-lymphocytic peptide cyclosporin A in animals. *Immunology*, 32(6), pp.1017–25.

Bowler, M.W. et al., 2007. Ground state structure of F1-ATPase from bovine heart mitochondria at 1.9 A resolution. *The Journal of biological chemistry*, 282(19), pp.14238–42.

Boyer, P.D., 1993. The binding change mechanism for ATP synthase--some probabilities and possibilities. *Biochimica et biophysica acta*, 1140(3), pp.215–50.

Boyle, G.M. et al., 2000. Modulation at a distance of proton conductance through the Saccharomyces cerevisiae mitochondrial F1F0-ATP synthase by variants of the oligomycin sensitivity-conferring protein containing substitutions near the C-terminus. *Journal of bioenergetics and biomembranes*, 32(6), pp.595–607.

Braig, K. et al., 2000. Structure of bovine mitochondrial F(1)-ATPase inhibited by Mg(2+) ADP b

Broekemeier, K.M. et al., 1992. Cyclosporin A protects hepatocytes subjected to high Ca2+ and oxidative stress. *FEBS letters*, 304(2-3), pp.192–4.

Broekemeier, K.M. & Pfeiffer, D.R., 1989. Cyclosporin A-sensitive and insensitive mechanisms produce the permeability transition in mitochondria. *Biochemical and biophysical research communications*, 163(1), pp.561–6.

Brustovetsky, N. & Klingenberg, M., 1996. Mitochondrial ADP/ATP carrier can be reversibly converted into a large channel by Ca2+. *Biochemistry*, 35(96), pp.8483–8488.

Burkovski, A., Lill, H. & Engelbrecht, S., 1994. Complementation of Escherichia coli uncD mutant strains by a chimeric F1-beta subunit constructed from E. coli and spinach chloroplast F1-beta. *Biochimica et biophysica acta*, 1186(3), pp.243–6.

Bustos, D.M. & Velours, J., 2005. The modification of the conserved GXXXG motif of the membrane-spanning segment of subunit g destabilizes the supramolecular species of yeast ATP synthase. *The Journal of biological chemistry*, 280(32), pp.29004–10.

Cabezon, E. et al., 2000. Modulation of the oligomerization state of the bovine F1-ATPase inhibitor protein, IF1, by pH. *The Journal of biological chemistry*, 275(33), pp.25460–4.

Cabezón, E. et al., 2000. Dimerization of bovine F1-ATPase by binding the inhibitor protein, IF1. *The Journal of biological chemistry*, 275(37), pp.28353–5.

Cabezón, E. et al., 2003. The structure of bovine F1-ATPase in complex with its regulatory protein IF1. *Nature structural biology*, 10(9), pp.744–50.

Campanella, M. et al., 2009. IF1, the endogenous regulator of the F(1)F(0)-ATPsynthase, defines mitochondrial volume fraction in HeLa cells by regulating autophagy. *Biochimica et biophysica acta*, 1787(5), pp.393–401.

Campanella, M. et al., 2008. Regulation of mitochondrial structure and function by the F1Fo-ATPase inhibitor protein, IF1. *Cell metabolism*, 8(1), pp.13–25.

Capaldi, R. a & Aggeler, R., 2002. Mechanism of the F(1)F(0)-type ATP synthase, a biological rotary motor. *Trends in biochemical sciences*, 27(3), pp.154–60.

Carraro, M. et al., 2014. Channel formation by yeast F-ATP synthase and the role of dimerization in the mitochondrial permeability transition. *The Journal of biological chemistry*, 289(23).

Carroll, J. et al., 2009. Measurement of the molecular masses of hydrophilic and hydrophobic subunits of ATP synthase and complex I in a single experiment. *Analytical biochemistry*, 395(2), pp.249–55.

Casari, G. et al., 1998. Spastic paraplegia and OXPHOS impairment caused by mutations in paraplegin, a nuclear-encoded mitochondrial metalloprotease. *Cell*, 93(6), pp.973–83.

Chen, R. et al., 2007. Association of two proteolipids of unknown function with ATP synthase from bovine heart mitochondria. *FEBS letters*, 581(17), pp.3145–8.

Clipstone, N.A. & Crabtree, G.R., 1992. Identification of calcineurin as a key signalling enzyme in T-lymphocyte activation. *Nature*, 357(6380), pp.695–7.

Collinson, I.R. et al., 1994. ATP synthase from bovine heart mitochondria: identification by proteolysis of sites in F0 exposed by removal of F1 and the oligomycin-sensitivity conferral protein. *The Biochemical journal*, 303 (Pt 2, pp.639–45.

Connern, C.P. & Halestrap, A.P., 1992. Purification and N-terminal sequencing of peptidyl-prolyl cis-trans-isomerase from rat liver mitochondrial matrix reveals the existence of a distinct mitochondrial cyclophilin. *The Biochemical journal*, 284 (Pt 2, pp.381–5.

Costantini, P. et al., 1996. Modulation of the mitochondrial permeability transition pore by pyridine nucleotides and dithiol oxidation at two separate sites. *The Journal of biological chemistry*, 271(12), pp.6746–51.

Costantini, P. et al., 1995. Selective inhibition of the mitochondrial permeability transition pore at the oxidation-reduction sensitive dithiol by monobromobimane. *FEBS letters*, 362(2), pp.239–42.

Costantini, P., Colonna, R. & Bernardi, P., 1998. Induction of the mitochondrial permeability

transition by N-ethylmaleimide depends on secondary oxidation of critical thiol groups. Potentiation by copper-ortho-phenanthroline without dimerization of the adenine nucleotide translocase. *Biochimica et biophysica acta*, 1365(3), pp.385–92.

Couoh-Cardel, S.J. et al., 2010. Structure of dimeric F1F0-ATP synthase. *The Journal of biological chemistry*, 285(47), pp.36447–55.

Covian, R. & Balaban, R.S., 2012. Cardiac mitochondrial matrix and respiratory complex protein phosphorylation. *American journal of physiology. Heart and circulatory physiology*, 303(8), pp.H940–66.

Crompton, M. & Costi, A., 1988. Kinetic evidence for a heart mitochondrial pore activated by Ca2+, inorganic phosphate and oxidative stress. A potential mechanism for mitochondrial dysfunction during cellular Ca2+ overload. *European journal of biochemistry / FEBS*, 178(2), pp.489–501.

Dage, J.L., Sun, H. & Halsall, H.B., 1998. Determination of diethylpyrocarbonate-modified amino acid residues in alpha 1-acid glycoprotein by high-performance liquid chromatography electrospray ionization-mass spectrometry and matrix-assisted laser desorption/ionization time-of-flight-mass spectro. *Analytical biochemistry*, 257(2), pp.176–85.

Das, a M. & Harris, D. a, 1990. Regulation of the mitochondrial ATP synthase in intact rat cardiomyocytes. *The Biochemical journal*, 266(2), pp.355–61.

Dautant, A., Velours, J. & Giraud, M.-F., 2010. Crystal structure of the Mg·ADP-inhibited state of the yeast F1c10-ATP synthase. *The Journal of biological chemistry*, 285(38), pp.29502–10.

Davies, K.M. et al., 2011. Macromolecular organization of ATP synthase and complex I in whole mitochondria. *Proceedings of the National Academy of Sciences of the United States of America*, 108(34), pp.14121–6.

Davies, K.M. et al., 2012. Structure of the yeast F 1 F o -ATP synthase dimer and its role in shaping the mitochondrial cristae. , (4).

Davies, K.M. & Daum, B., 2013. Role of cryo-ET in membrane bioenergetics research. *Biochemical Society transactions*, 41(5), pp.1227–34.

Diez, M. et al., 2004. Proton-powered subunit rotation in single membrane-bound F0F1-ATP synthase. *Nature structural & molecular biology*, 11(2), pp.135–41.

Dolinski, K. et al., 1997. All cyclophilins and FK506 binding proteins are, individually and collectively, dispensable for viability in Saccharomyces cerevisiae. *Proceedings of the National Academy of Sciences of the United States of America*, 94(24), pp.13093–13098.

Dolinsky, T.J. et al., 2007. PDB2PQR: expanding and upgrading automated preparation of biomolecular structures for molecular simulations. *Nucleic acids research*, 35(Web Server issue), pp.W522–5.

Du, H. et al., 2008. Cyclophilin D deficiency attenuates mitochondrial and neuronal perturbation and ameliorates learning and memory in Alzheimer's disease. *Nature Medicine*, 14(10), pp.1097–1105.

Duchen, M.R. et al., 1993. On the involvement of a cyclosporin A sensitive mitochondrial pore in myocardial reperfusion injury. *Cardiovascular research*, 27(10), pp.1790–4.

Dudkina, N. V et al., 2006. Characterization of dimeric ATP synthase and cristae membrane ultrastructure from Saccharomyces and Polytomella mitochondria. *FEBS letters*, 580(14), pp.3427–32.

Edgcomb, S.P. & Murphy, K.P., 2002. Variability in the pKa of histidine side-chains correlates with burial within proteins. *Proteins*, 49(1), pp.1–6.

Eriksson, O., Fontaine, E. & Bernardi, P., 1998. Chemical modification of arginines by 2,3-butanedione and phenylglyoxal causes closure of the mitochondrial permeability transition pore. *The Journal of biological chemistry*, 273(20), pp.12669–74.

Ernst, S. et al., 2012. Elastic deformations of the rotary double motor of single F(o)F(1)-ATP synthases detected in real time by Förster resonance energy transfer. *Biochimica et biophysica acta*, 1817(10), pp.1722–31.

Everard-gigot, V. et al., 2005. Functional Analysis of Subunit e of the F 1 F o -ATP Synthase of the Yeast Saccharomyces cerevisiae : Importance of the N-Terminal Membrane Anchor Region. , 4(2), pp.346–355.

Fillingame, R.H., Jiang, W. & Dmitriev, O.Y., 2000. The oligomeric subunit C rotor in the fo sector of ATP synthase: unresolved questions in our understanding of function. *Journal of bioenergetics and biomembranes*, 32(5), pp.433–9.

Fischer, G., Berger, E. & Bang, H., 1989. Kinetic beta-deuterium isotope effects suggest a covalent mechanism for the protein folding enzyme peptidylprolyl cis/trans-isomerase. *FEBS letters*, 250(2), pp.267–70.

Flisiak, R., Dumont, J.-M. & Crabbé, R., 2007. Cyclophilin inhibitors in hepatitis C viral infection. *Expert opinion on investigational drugs*, 16(9), pp.1345–54.

Fogolari, F. et al., 2012. Bluues: a program for the analysis of the electrostatic properties of proteins based on generalized Born radii. *BMC bioinformatics*, 13 Suppl 4(Suppl 4), p.S18.

Fontaine, E. et al., 1998. Regulation of the permeability transition pore in skeletal muscle mitochondria. Modulation By electron flow through the respiratory chain complex i. *The Journal of biological chemistry*, 273(20), pp.12662–8.

Forte, M. et al., 2007. Cyclophilin D inactivation protects axons in experimental autoimmune encephalomyelitis, an animal model of multiple sclerosis. *Proceedings of the National Academy of Sciences of the United States of America*, 104(18), pp.7558–63.

Foti, S. et al., 1991. Fast-atom bombardment mass spectrometry of peptide derivatives with diethylpyrocarbonate. *Rapid Communications in Mass Spectrometry*, 5(7), pp.336–339.

Fournier, N., Ducet, G. & Crevat, A., 1987. Action of cyclosporine on mitochondrial calcium fluxes. *Journal of bioenergetics and biomembranes*, 19(3), pp.297–303.

Frechin, M. et al., 2014. Expression of nuclear and mitochondrial genes encoding ATP synthase is synchronized by disassembly of a multisynthetase complex. *Molecular cell*, 56(6), pp.763–76.

Fromme, P., Gräber, P. & Salnikow, J., 1987. Isolation and identification of a fourth subunit in the membrane part of the chloroplast ATP-synthase. *FEBS Letters*, 218(1), pp.27–30.

Fronzes, R. et al., 2006. The peripheral stalk participates in the yeast ATP synthase dimerization independently of e and g subunits. *Biochemistry*, 45(21), pp.6715–23.

Fujikawa, M. et al., 2015. Assembly of human mitochondrial ATP synthase through two separate intermediates, F1-c-ring and b-e-g complex. *FEBS letters*, 589(19 Pt B), pp.2707–12.

Fujimoto, K. et al., 2010. Targeting cyclophilin D and the mitochondrial permeability transition enhances beta-cell survival and prevents diabetes in Pdx1 deficiency. *Proceedings of the National Academy of Sciences of the United States of America*, 107(22), pp.10214–9.

Funatsu, T. et al., 1995. Imaging of single fluorescent molecules and individual ATP turnovers by single myosin molecules in aqueous solution. *Nature*, 374(6522), pp.555–9.

Futai, M. et al., 2012. Rotational catalysis in proton pumping ATPases: From E. coli F-ATPase to mammalian V-ATPase. *Biochimica et Biophysica Acta - Bioenergetics*, 1817(10), pp.1711–1721.

Galat, A. & Metcalfe, S.M., 1995. Peptidylproline cis/trans isomerases. *Progress in biophysics and molecular biology*, 63(1), pp.67–118.

Galluzzi, L. et al., 2015. Essential versus accessory aspects of cell death: recommendations of the NCCD 2015. *Cell death and differentiation*, 22(1), pp.58–73.

García, J.J. et al., 2006. The inhibitor protein (IF1) promotes dimerization of the mitochondrial F1F0-ATP synthase. *Biochemistry*, 45(42), pp.12695–703.

García-Bermúdez, J. et al., 2015. PKA Phosphorylates the ATPase Inhibitory Factor 1 and Inactivates Its Capacity to Bind and Inhibit the Mitochondrial H(+)-ATP Synthase. *Cell reports*, 12(12), pp.2143–55.

García-Trejo, J.J. et al., 2016. The Inhibitory Mechanism of the ζ Subunit of the F1FO-ATPase

Nanomotor of Paracoccus denitrificans and Related α-Proteobacteria. *The Journal of biological chemistry*, 291(2), pp.538–46.

Gavish, M. et al., 1999. Enigma of the peripheral benzodiazepine receptor. *Pharmacological reviews*, 51(4), pp.629–50.

Gincel, D. & Shoshan-Barmatz, V., 2004. Glutamate interacts with VDAC and modulates opening of the mitochondrial permeability transition pore. *Journal of bioenergetics and biomembranes*, 36(2), pp.179–86.

Gincel, D., Zaid, H. & Shoshan-Barmatz, V., 2001. Calcium binding and translocation by the voltage-dependent anion channel: a possible regulatory mechanism in mitochondrial function. *The Biochemical journal*, 358(Pt 1), pp.147–55.

Giorgio, V. et al., 2010. Cyclophilin D in mitochondrial pathophysiology. *Biochimica et Biophysica Acta - Bioenergetics*, 1797(6-7), pp.1113–1118.

Giorgio, V. et al., 2009. Cyclophilin D modulates mitochondrial F0F1-ATP synthase by interacting with the lateral stalk of the complex. *The Journal of biological chemistry*, 284(49), pp.33982–8.

Giorgio, V. et al., 2013. Dimers of mitochondrial ATP synthase form the permeability transition pore. *Proceedings of the National Academy of Sciences*.

Giraud, M.-F. et al., 2012. Rotor architecture in the yeast and bovine F1-c-ring complexes of F-ATP synthase. *Journal of structural biology*, 177(2), pp.490–7.

Green, D.W. & Grover, G.J., 2000. The IF(1) inhibitor protein of the mitochondrial F(1)F(0)-ATPase. *Biochimica et biophysica acta*, 1458(2-3), pp.343–55.

Green, N.S., Reisler, E. & Houk, K.N., 2001. Quantitative evaluation of the lengths of homobifunctional protein cross-linking reagents used as molecular rulers. *Protein science : a publication of the Protein Society*, 10(7), pp.1293–304.

Griffiths, E.J. & Halestrap, A.P., 1991. Further evidence that cyclosporin A protects mitochondria from calcium overload by inhibiting a matrix peptidyl-prolyl cis-trans isomerase. Implications for the immunosuppressive and toxic effects of cyclosporin. *The Biochemical journal*, 274 (Pt 2, pp.611–4.

Griffiths, E.J. & Halestrap, A.P., 1995. Mitochondrial non-specific pores remain closed during cardiac ischaemia, but open upon reperfusion. *The Biochemical journal*, 307 (Pt 1, pp.93–8.

Gutiérrez-Aguilar, M. et al., 2014. Genetic manipulation of the cardiac mitochondrial phosphate carrier does not affect permeability transition. *Journal of molecular and cellular cardiology*, 72, pp.316–25.

Habersetzer, J. et al., 2013. ATP synthase oligomerization: from the enzyme models to the mitochondrial morphology. *The international journal of biochemistry & cell biology*, 45(1), pp.99–105.

Habersetzer, J. et al., 2013. Human F1F0 ATP Synthase, Mitochondrial Ultrastructure and OXPHOS Impairment: A (Super-) Complex Matter? *PloS one*, 8(10), p.e75429.

Hackenbrock, C.R., 1966. Ultrastructural bases for metabolically linked mechanical activity in mitochondria. I. Reversible ultrastructural changes with change in metabolic steady state in isolated liver mitochondria. *The Journal of cell biology*, 30(2), pp.269–97.

Halestrap, A.P., 2009. What is the mitochondrial permeability transition pore? *Journal of molecular and cellular cardiology*, 46(6), pp.821–31.

Harris, D.A. & Bashford, C.L., 1987. *Spectrophotometry & Spectrofluorimetry: A Practical Approach*,

HavlíČková, V. et al., 2010. Knockdown of F1 epsilon subunit decreases mitochondrial content of ATP synthase and leads to accumulation of subunit c. *Biochimica et Biophysica Acta - Bioenergetics*, 1797, pp.1124–1129.

He, L. & Lemasters, J.J., 2002. Regulated and unregulated mitochondrial permeability transition pores: A new paradigm of pore structure and function? *FEBS Letters*, 512(1-3), pp.1–7.

Herick, K., Krämer, R. & Lühring, H., 1997. Patch clamp investigation into the phosphate carrier from Saccharomyces cerevisiae mitochondria. *Biochimica et biophysica acta*, 1321(3), pp.207–20.

Hnízda, A. et al., 2008. Reactivity of histidine and lysine side-chains with diethylpyrocarbonate -- a method to identify surface exposed residues in proteins. *Journal of biochemical and biophysical methods*, 70(6), pp.1091–7.

Hunter, D.R. & Haworth, R.A., 1979. The Ca2+-induced membrane transition in mitochondria. I. The protective mechanisms. *Archives of biochemistry and biophysics*, 195(2), pp.453–9.

Hunter, D.R., Haworth, R.A. & Southard, J.H., 1976. Relationship between configuration, function, and permeability in calcium-treated mitochondria. *The Journal of biological chemistry*, 251(16), pp.5069–77.

Hüser, J., Rechenmacher, C.E. & Blatter, L.A., 1998. Imaging the permeability pore transition in single mitochondria. *Biophysical journal*, 74(4), pp.2129–37.

Imberti, R. et al., 1992. Synergism of cyclosporin A and phospholipase inhibitors in protection against lethal injury to rat hepatocytes from oxidant chemicals. *Research communications in chemical pathology and pharmacology*, 78(1), pp.27–38.

Jiko, C. et al., 2015. Bovine F1Fo ATP synthase monomers bend the lipid bilayer in 2D membrane crystals. *eLife*, 4, p.e06119.

Jin, Z.-G. et al., 2004. Cyclophilin A is a proinflammatory cytokine that activates endothelial cells. *Arteriosclerosis, thrombosis, and vascular biology*, 24(7), pp.1186–91.

Johans, M. et al., 2005. Modification of permeability transition pore arginine(s) by phenylglyoxal derivatives in isolated mitochondria and mammalian cells. Structure-function relationship of arginine ligands. *The Journal of biological chemistry*, 280(13), pp.12130–6.

Johnson, K.M. et al., 2005. Identification and validation of the mitochondrial F1F0-ATPase as the molecular target of the immunomodulatory benzodiazepine Bz-423. *Chemistry & biology*, 12(4), pp.485–96.

Jung, D.W., Bradshaw, P.C. & Pfeiffer, D.R., 1997. Properties of a cyclosporin-insensitive permeability transition pore in yeast mitochondria. *The Journal of biological chemistry*, 272(34), pp.21104–12.

Kabaleeswaran, V. et al., 2009. Asymmetric structure of the yeast F1 ATPase in the absence of bound nucleotides. *The Journal of biological chemistry*, 284(16), pp.10546–51.

Kabaleeswaran, V. et al., 2006. Novel features of the rotary catalytic mechanism revealed in the structure of yeast F1 ATPase. *The EMBO journal*, 25(22), pp.5433–42.

Kagawa, R. et al., 2004. The structure of bovine F1-ATPase inhibited by ADP and beryllium fluoride. *The EMBO journal*, 23(14), pp.2734–44.

Kajitani, K. et al., 2008. Crystal structure of human cyclophilin D in complex with its inhibitor, cyclosporin A at 0.96-A resolution. *Proteins*, 70(4), pp.1635–9.

Kim, H. et al., 2005. Cyclophilin A may contribute to the inflammatory processes in rheumatoid arthritis through induction of matrix degrading enzymes and inflammatory cytokines from macrophages. *Clinical immunology (Orlando, Fla.)*, 116(3), pp.217–24.

Kim, S.-H. et al., 2004. Cyclophilin A as a novel biphasic mediator of endothelial activation and dysfunction. *The American journal of pathology*, 164(5), pp.1567–74.

Kinnally, K.W. et al., 1993. Mitochondrial benzodiazepine receptor linked to inner membrane ion channels by nanomolar actions of ligands. *Proceedings of the National Academy of Sciences of the United States of America*, 90(4), pp.1374–8.

Kokoszka, J.E. et al., 2004. The ADP/ATP translocator is not essential for the mitochondrial permeability transition pore. *Nature*, 427(6973), pp.461–5.

Kong, W. et al., 2007. Cyclophilin C-associated protein is up-regulated during wound healing. *Journal of cellular physiology*, 210(1), pp.153–60.

Kowaltowski, A.J., Castilho, R.F. & Vercesi, A.E., 2001. Mitochondrial permeability transition and

oxidative stress. *FEBS letters*, 495(1-2), pp.12–5.

Kraus, C. et al., 2010. S100A1 in cardiovascular health and disease: "Closing the gap between basic science and clinical therapy." *J Mol Cell Cardiol.*, 47(4), pp.445–455.

Krauskopf, A. et al., 2006. Properties of the permeability transition in VDAC1(-/-) mitochondria. *Biochimica et biophysica acta*, 1757(5-6), pp.590–5.

Kristian, T., Bernardi, P. & Siesjö, B.K., 2001. Acidosis promotes the permeability transition in energized mitochondria: implications for reperfusion injury. *Journal of neurotrauma*, 18(10), pp.1059–74.

Krueger, K.E. & Papadopoulos, V., 1992. Mitochondrial benzodiazepine receptors and the regulation of steroid biosynthesis. *Annual review of pharmacology and toxicology*, 32, pp.211–37.

Kühlbrandt, W., 2015. Structure and function of mitochondrial membrane protein complexes. *BMC biology*, 13, p.89.

Kunji, E.R.S., 2004. The role and structure of mitochondrial carriers. *FEBS letters*, 564(3), pp.239–44.

Kwong, J.Q. et al., 2014. Genetic deletion of the mitochondrial phosphate carrier desensitizes the mitochondrial permeability transition pore and causes cardiomyopathy. *Cell death and differentiation*, 21(8), pp.1209–17.

Lee, J. et al., 2015. Organization of Subunits in the Membrane Domain of the Bovine F-ATPase Revealed by Covalent Cross-linking. *The Journal of biological chemistry*, 290(21), pp.13308–20.

Lee, J.K., Belogrudov, G.I. & Stroud, R.M., 2008. Crystal structure of bovine mitochondrial factor B at 0.96-A resolution. *Proceedings of the National Academy of Sciences of the United States of America*, 105(36), pp.13379–84.

Lemasters, J.J. et al., 2002. Role of mitochondrial inner membrane permeabilization in necrotic cell death, apoptosis, and autophagy. *Antioxidants & redox signaling*, 4(5), pp.769–81.

Leung, A.W.C., Varanyuwatana, P. & Halestrap, A.P., 2008. The mitochondrial phosphate carrier interacts with cyclophilin D and may play a key role in the permeability transition. *The Journal of biological chemistry*, 283(39), pp.26312–23.

Li, B. et al., 2012. Inhibition of complex I regulates the mitochondrial permeability transition through a phosphate-sensitive inhibitory site masked by cyclophilin D. *Biochimica et biophysica acta*, 1817(9), pp.1628–34.

Li, H. et al., 2001. Cholesterol binding at the cholesterol recognition/ interaction amino acid consensus (CRAC) of the peripheral-type benzodiazepine receptor and inhibition of steroidogenesis by an HIV TAT-CRAC peptide. *Proceedings of the National Academy of Sciences*, 98(3), pp.1267–1272.

Li, Y. et al., 2004. Cyclophilin-D promotes the mitochondrial permeability transition but has opposite effects on apoptosis and necrosis. *The Biochemical journal*, 383(Pt 1), pp.101–9.

Lill, H. et al., 1993. Complementation of Escherichia coli unc mutant strains by chloroplast and cyanobacterial F1-ATPase subunits. *Biochimica et biophysica acta*, 1144(3), pp.278–84.

Lippe, G., Sorgato, M.C. & Harris, D.A., 1988. The binding and release of the inhibitor protein are governed independently by ATP and membrane potential in ox-heart submitochondrial vesicles. *Biochimica et biophysica acta*, 933(1), pp.12–21.

Liu, J. et al., 1991. Calcineurin is a common target of cyclophilin-cyclosporin A and FKBP-FK506 complexes. *Cell*, 66(4), pp.807–15.

Löw, H. & Vallin, I., 1963. Succinate-linked diphosphopyridine nucleotide reduction in submitochondrial particles. *Biochimica et Biophysica Acta*, 69, pp.361–374.

Mannella, C.A., 2000. Introduction: our changing views of mitochondria. *Journal of bioenergetics and biomembranes*, 32(1), pp.1–4.

De Marchi, U. et al., 2008. A maxi-chloride channel in the inner membrane of mammalian

mitochondria. *Biochimica et biophysica acta*, 1777(11), pp.1438–48.

De Marchi, U. et al., 2006. Electrophysiological characterization of the Cyclophilin D-deleted mitochondrial permeability transition pore. *Molecular membrane biology*, 23(6), pp.521–30.

Martin, J.L. et al., 2014. Anatomy of F1-ATPase powered rotation. *Proceedings of the National Academy of Sciences of the United States of America*, pp.1–6.

Martin, L.J. et al., 2009. The mitochondrial permeability transition pore in motor neurons: involvement in the pathobiology of ALS mice. *Experimental neurology*, 218(2), pp.333–46.

McEnery, M.W. et al., 1992. Isolation of the mitochondrial benzodiazepine receptor: association with the voltage-dependent anion channel and the adenine nucleotide carrier. *Proceedings of the National Academy of Sciences of the United States of America*, 89(8), pp.3170–3174.

McWilliam, H. et al., 2013. Analysis Tool Web Services from the EMBL-EBI. *Nucleic acids research*, 41(Web Server issue), pp.W597–600.

Melchior, W.B. & Fahrney, D., 1970. Ethoxyformylation of proteins. Reaction of ethoxyformic anhydride with alpha-chymotrypsin, pepsin, and pancreatic ribonuclease at pH 4. *Biochemistry*, 9(2), pp.251–8.

Mendoza, V.L. & Vachet, R.W., 2008. Protein surface mapping using diethylpyrocarbonate with mass spectrometric detection. *Analytical chemistry*, 80(8), pp.2895–904.

Menz, R.I., Walker, J.E. & Leslie, a G., 2001. Structure of bovine mitochondrial F(1)-ATPase with nucleotide bound to all three catalytic sites: implications for the mechanism of rotary catalysis. *Cell*, 106(3), pp.331–41.

Meyer, B. et al., 2007. Identification of two proteins associated with mammalian ATP synthase. *Molecular & cellular proteomics : MCP*, 6(10), pp.1690–9.

Minauro-Sanmiguel, F., Wilkens, S. & García, J.J., 2005. Structure of dimeric mitochondrial ATP synthase: novel F0 bridging features and the structural basis of mitochondrial cristae biogenesis. *Proceedings of the National Academy of Sciences of the United States of America*, 102(35), pp.12356–8.

Mitchell, P., 1979. Keilin's respiratory chain concept and its chemiosmotic consequences. *Science*, 206(4423), pp.1148–59.

Morohaku, K. et al., 2014. Translocator protein/peripheral benzodiazepine receptor is not required for steroid hormone biosynthesis. *Endocrinology*, 155(1), pp.89–97.

Nakagawa, T. et al., 2005. Cyclophilin D-dependent mitochondrial permeability transition regulates some necrotic but not apoptotic cell death. *Nature*, 434(7033), pp.652–658.

Nakamura, J., Fujikawa, M. & Yoshida, M., 2013. IF1, a natural inhibitor of mitochondrial ATP synthase, is not essential for the normal growth and breeding of mice. *Bioscience reports*.

Nakanishi-Matsui, M., Sekiya, M. & Futai, M., 2013. Rotating proton pumping ATPases: subunit/subunit interactions and thermodynamics. *IUBMB life*, 65(3), pp.247–54.

Nathanson, L. & Gromet-Elhanan, Z., 2000. Mutations in the beta-subunit Thr(159) and Glu(184) of the Rhodospirillum rubrum F(0)F(1) ATP synthase reveal differences in ligands for the coupled Mg(2+)- and decoupled Ca(2+)-dependent F(0)F(1) activities. *The Journal of biological chemistry*, 275(2), pp.901–5.

Nelson, N., 1992. Structure and function of V-ATPases in endocytic and secretory organelles. *The Journal of experimental biology*, 172, pp.149–53.

Nguyen, T.T. et al., 2010. Modulation of the protein kinase Cdelta interaction with the "d" subunit of F1F0-ATP synthase in neonatal cardiac myocytes: development of cell-permeable, mitochondrially targeted inhibitor and facilitator peptides. *The Journal of biological chemistry*, 285(29), pp.22164–73.

Nicolli, a, Nicolli, a, et al., 1996. Interactions of cyclophilin with the mitochondrial inner membrane and regulation of the permeability transition pore, and cyclosporin A- sensitive channel. *J Biol Chem*, 271(4), pp.2185–2192.

Nicolli, a, Basso, E., et al., 1996. Interactions of cyclophilin with the mitochondrial inner membrane and regulation of the permeability transition pore, and cyclosporin A-sensitive channel. *The Journal of biological chemistry*, 271(4), pp.2185–92.

Nicolli, a, Petronilli, V. & Bernardi, P., 1993. Modulation of the mitochondrial cyclosporin A-sensitive permeability transition pore by matrix pH. Evidence that the pore open-closed probability is regulated by reversible histidine protonation. *Biochemistry*, 32(16), pp.4461–5.

Ohsakaya, S. et al., 2011. Knockdown of DAPIT (diabetes-associated protein in insulin-sensitive tissue) results in loss of ATP synthase in mitochondria. *The Journal of biological chemistry*, 286(23), pp.20292–6.

Olsson, M.H.M. et al., 2011. PROPKA3: Consistent Treatment of Internal and Surface Residues in Empirical pKa Predictions. *Journal of chemical theory and computation*, 7(2), pp.525–37.

Oosawa, F. & Hayashi, S., 1986. The loose coupling mechanism in molecular machines of living cells. *Advances in biophysics*, 22, pp.151–83.

Orrenius, S., Gogvadze, V. & Zhivotovsky, B., 2015. Calcium and mitochondria in the regulation of cell death. *Biochemical and biophysical research communications*, 460(1), pp.72–81.

Orriss, G.L. et al., 1998. Bovine F1-ATPase covalently inhibited with 4-chloro-7-nitrobenzofurazan: the structure provides further support for a rotary catalytic mechanism. *Structure (London, England : 1993)*, 6(7), pp.831–7.

Palma, E. et al., 2009. Genetic ablation of cyclophilin D rescues mitochondrial defects and prevents muscle apoptosis in collagen VI myopathic mice. *Human molecular genetics*, 18(11), pp.2024–31.

Panchenko, M. V & Vinogradov, A.D., 1985. Interaction between the mitochondrial ATP synthetase and ATPase inhibitor protein. Active/inactive slow pH-dependent transitions of the inhibitor protein. *FEBS letters*, 184(2), pp.226–30.

Di Pancrazio, F. et al., 2004. In vitro and in vivo studies of F(0)F(1)ATP synthase regulation by inhibitor protein IF(1) in goat heart. *Biochimica et biophysica acta*, 1659(1), pp.52–62.

Papageorgiou, S., Melandri, a B. & Solaini, G., 1998. Relevance of divalent cations to ATP-driven proton pumping in beef heart mitochondrial F0F1-ATPase. *Journal of bioenergetics and biomembranes*, 30(6), pp.533–41.

Parone, P.A. et al., 2013. Enhancing Mitochondrial Calcium Buffering Capacity Reduces Aggregation of Misfolded SOD1 and Motor Neuron Cell Death without Extending Survival in Mouse Models of Inherited Amyotrophic Lateral Sclerosis. *Journal of Neuroscience*, 33(11), pp.4657–4671.

Pastorino, J.G. et al., 1993. Cyclosporin and carnitine prevent the anoxic death of cultured hepatocytes by inhibiting the mitochondrial permeability transition. *The Journal of biological chemistry*, 268(19), pp.13791–8.

Pastorino, J.G. et al., 1994. Protoporphyrin IX, an endogenous ligand of the peripheral benzodiazepine receptor, potentiates induction of the mitochondrial permeability transition and the killing of cultured hepatocytes by rotenone. *The Journal of biological chemistry*, 269(49), pp.31041–6.

Pastorino, J.G., Shulga, N. & Hoek, J.B., 2002. Mitochondrial binding of hexokinase II inhibits Bax-induced cytochrome c release and apoptosis. *The Journal of biological chemistry*, 277(9), pp.7610–8.

Paumard, P. et al., 2002. The ATP synthase is involved in generating mitochondrial cristae morphology. *The EMBO journal*, 21(3), pp.221–30.

Pebay-Peyroula, E. et al., 2003. Structure of mitochondrial ADP/ATP carrier in complex with carboxyatractyloside. *Nature*, 426(6962), pp.39–44.

Perez, J.A. et al., 1986. Characterisation of phosphate binding to mitochondrial and bacterial membrane -bound ATP synthase by studies of inhibition with 4-chloro-7-nitrobenzofurazan. , 198(1), pp.113–118.

Petronilli, V. et al., 1993. Physiological effectors modify voltage sensing by the cyclosporin A-sensitive permeability transition pore of mitochondria. *The Journal of biological chemistry*, 268(29), pp.21939–45.

Petronilli, V. et al., 2009. Switch from inhibition to activation of the mitochondrial permeability transition during hematoporphyrin-mediated photooxidative stress. Unmasking pore-regulating external thiols. *Biochimica et biophysica acta*, 1787(7), pp.897–904.

Petronilli, V. et al., 1994. The Voltage Sensor of the Mitochondrial Permeability Transition of Vicinal Thiols Pore Is Tuned by the Oxidation-Reduction State. , pp.16638–16642.

Prescott, M. et al., 1994. Properties of yeast cells depleted of the OSCP subunit of mitochondrial ATP synthase by regulated expression of the ATP5 gene. *Biochemistry and molecular biology international*, 34(4), pp.789–799.

Puri, N. et al., 2005. Expression of bovine F1-ATPase with functional complementation in yeast Saccharomyces cerevisiae. *The Journal of biological chemistry*, 280(23), pp.22418–24.

Qin, K. et al., 2003. The PrP-like protein Doppel binds copper. *The Journal of biological chemistry*, 278(11), pp.8888–96.

van Raaij, M.J. et al., 1996. The structure of bovine F1-ATPase complexed with the antibiotic inhibitor aurovertin B. *Proceedings of the National Academy of Sciences of the United States of America*, 93(14), pp.6913–7.

Raghavan, A. et al., 2012. Voltage-dependant anion channels: novel insights into isoform function through genetic models. *Biochimica et biophysica acta*, 1818(6), pp.1477–85.

Rak, M., Gokova, S. & Tzagoloff, A., 2011. Modular assembly of yeast mitochondrial ATP synthase. *The EMBO journal*, 30(5), pp.920–30.

Rasola, A. & Bernardi, P., 2007. The mitochondrial permeability transition pore and its involvement in cell death and in disease pathogenesis. *Apoptosis : an international journal on programmed cell death*, 12(5), pp.815–33.

Rees, D.M. et al., 2012. Structural evidence of a new catalytic intermediate in the pathway of ATP hydrolysis by F1-ATPase from bovine heart mitochondria. *Proceedings of the National Academy of Sciences of the United States of America*, 109(28), pp.11139–43.

Rees, D.M., Leslie, A.G.W. & Walker, J.E., 2009. The structure of the membrane extrinsic region of bovine ATP synthase. *Proceedings of the National Academy of Sciences of the United States of America*, 106(51), pp.21597–601.

Richter, M.L., Gromet-Elhanan, Z. & McCarty, R.E., 1986. Reconstitution of the H+-ATPase complex of Rhodospirillum rubrum by the beta subunit of the chloroplast coupling factor 1. *The Journal of biological chemistry*, 261(26), pp.12109–13.

Rizzuto, R. et al., 1998. Close contacts with the endoplasmic reticulum as determinants of mitochondrial Ca2+ responses. *Science (New York, N.Y.)*, 280(5370), pp.1763–6.

Robinson, A.J., Overy, C. & Kunji, E.R.S., 2008. The mechanism of transport by mitochondrial carriers based on analysis of symmetry. *Proceedings of the National Academy of Sciences of the United States of America*, 105(46), pp.17766–71.

Robinson, G.C. et al., 2013. The structure of F_1 -ATPase from Saccharomyces cerevisiae inhibited by its regulatory protein IF_1 . *Open biology*, 3(2), p.120164.

Rondelez, Y. et al., 2005. Highly coupled ATP synthesis by F1-ATPase single molecules. *Nature*, 433(7027), pp.773–7.

Rosing, J. et al., 1975. Nucleotide-binding properties of native and cold-treated mitochondrial ATPase. *Biochimica et biophysica acta*, 376(1), pp.13–26.

Rouslin, W. et al., 1995. ATPase activity, IF1 content, and proton conductivity of ESMP from control and ischemic slow and fast heart-rate hearts. *Journal of bioenergetics and biomembranes*, 27(4), pp.459–66.

Rouslin, W. & Broge, C.W., 1996. IF1 function in situ in uncoupler-challenged ischemic rabbit, rat, and pigeon hearts. *The Journal of biological chemistry*, 271(39), pp.23638–41.

Rubinstein, J.L. et al., 2005. ATP synthase from Saccharomyces cerevisiae: location of subunit h in the peripheral stalk region. *Journal of molecular biology*, 345(3), pp.513–20.

Rubinstein, J.L., Walker, J.E. & Henderson, R., 2003. Structure of the mitochondrial ATP synthase by electron cryomicroscopy. *The EMBO journal*, 22(23), pp.6182–92.

Rutter, G.A. & Rizzuto, R., 2000. Regulation of mitochondrial metabolism by ER Ca2+ release: an intimate connection. *Trends in biochemical sciences*, 25(5), pp.215–21.

Sánchez-Aragó, M. et al., 2013. Expression, regulation and clinical relevance of the ATPase inhibitory factor 1 in human cancers. *Oncogenesis*, 2(October 2012), p.e46.

Sánchez-Aragó, M. et al., 2012. IF1 reprograms energy metabolism and signals the oncogenic phenotype in cancer. *Cell cycle (Georgetown, Tex.)*, 11(16), pp.2963–4.

Sánchez-Cenizo, L. et al., 2010. Up-regulation of the ATPase inhibitory factor 1 (IF1) of the mitochondrial H+-ATP synthase in human tumors mediates the metabolic shift of cancer cells to a Warburg phenotype. *The Journal of biological chemistry*, 285(33), pp.25308–13.

Schinzel, A.C. et al., 2005. Cyclophilin D is a component of mitochondrial permeability transition and mediates neuronal cell death after focal cerebral ischemia. *Proceedings of the National Academy of Sciences of the United States of America*, 102(34), pp.12005–12010.

Schultheiss, H.P. & Klingenberg, M., 1984. Immunochemical characterization of the adenine nucleotide translocator. Organ specificity and conformation specificity. *European journal of biochemistry / FEBS*, 143(3), pp.599–605.

Seelert, H. & Dencher, N. a., 2011. ATP synthase superassemblies in animals and plants: Two or more are better. *Biochimica et Biophysica Acta - Bioenergetics*, 1807(9), pp.1185–1197.

Selwyn, M.J., 1968. Model reaction for mitochondrial adenosine triphosphatase. *Nature*, 219(5153), pp.490–3.

Selwyn, M.J., Dawson, A.P. & Dunnett, S.J., 1970. Calcium transport in mitochondria. *FEBS letters*, 10(1), pp.1–5.

Shanmughapriya, S. et al., 2015. SPG7 Is an Essential and Conserved Component of the Mitochondrial Permeability Transition Pore. *Molecular cell*, 60(1), pp.47–62.

Shevchenko, A. et al., 1996. Mass spectrometric sequencing of proteins silver-stained polyacrylamide gels. *Analytical chemistry*, 68(5), pp.850–8.

Sileikyte, J. et al., 2011. Regulation of the inner membrane mitochondrial permeability transition by the outer membrane translocator protein (peripheral benzodiazepine receptor). *The Journal of biological chemistry*, 286(2), pp.1046–53.

Šileikytė, J. et al., 2014. Regulation of the mitochondrial permeability transition pore by the outer membrane does not involve the peripheral benzodiazepine receptor (Translocator Protein of 18 kDa (TSPO)). *The Journal of biological chemistry*, 289(20), pp.13769–81.

Sokolskaja, E. & Luban, J., 2006. Cyclophilin, TRIM5, and innate immunity to HIV-1. *Current opinion in microbiology*, 9(4), pp.404–8.

Song, R. et al., 2014. Reciprocal activation between ATPase inhibitory factor 1 and NF-κB drives hepatocellular carcinoma angiogenesis and metastasis. *Hepatology (Baltimore, Md.)*, 60(5), pp.1659–73.

Spannagel, C. et al., 1998. Evidence of a subunit 4 (subunit b) dimer in favor of the proximity of ATP synthase complexes in yeast inner mitochondrial membrane. *Biochimica et biophysica acta*, 1414(1-2), pp.260–264.

De Stefani, D. et al., 2011. A forty-kilodalton protein of the inner membrane is the mitochondrial calcium uniporter. *Nature*, 476(7360), pp.336–40.

Stelzer, A.C. et al., 2010. NMR studies of an immunomodulatory benzodiazepine binding to its molecular target on the mitochondrial F(1)F(0)-ATPase. *Biopolymers*, 93(1), pp.85–92.

Stock, D. et al., 2000. The rotary mechanism of ATP synthase. *Current opinion in structural biology*, 10(6), pp.672–9.

Stock, D., Leslie, A.G. & Walker, J.E., 1999. Molecular architecture of the rotary motor in ATP

synthase. *Science (New York, N.Y.)*, 286(5445), pp.1700–5.

von Stockum, S. et al., 2015. F-ATPase of Drosophila melanogaster forms 53-picosiemen (53-pS) channels responsible for mitochondrial Ca2+-induced Ca2+ release. *The Journal of biological chemistry*, 290(8), pp.4537–44.

von Stockum, S. et al., 2011. Properties of Ca(2+) transport in mitochondria of Drosophila melanogaster. *The Journal of biological chemistry*, 286(48), pp.41163–70.

Strauss, M. et al., 2008. Dimer ribbons of ATP synthase shape the inner mitochondrial membrane. *The EMBO journal*, 27(7), pp.1154–60.

Suzuki, T. et al., 2014. Chemomechanical coupling of human mitochondrial F1-ATPase motor. *Nature chemical biology*, 10(11), pp.930–6.

Szabó, I., Bernardi, P. & Zoratti, M., 1992. Modulation of the mitochondrial megachannel by divalent cations and protons. *The Journal of biological chemistry*, 267(5), pp.2940–6.

Szabó, I., De Pinto, V. & Zoratti, M., 1993. The mitochondrial permeability transition pore may comprise VDAC molecules. II. The electrophysiological properties of VDAC are compatible with those of the mitochondrial megachannel. *FEBS letters*, 330(2), pp.206–10.

Szabo, I. & Zoratti, M., 2014. Mitochondrial channels: ion fluxes and more. *Physiological reviews*, 94(2), pp.519–608.

Szabó, I. & Zoratti, M., 1991. The giant channel of the inner mitochondrial membrane is inhibited by cyclosporin A. *The Journal of biological chemistry*, 266(6), pp.3376–3379.

Szabó, I. & Zoratti, M., 1993. The mitochondrial permeability transition pore may comprise VDAC molecules. I. Binary structure and voltage dependence of the pore. *FEBS letters*, 330(2), pp.201–5.

Takahashi, N., Hayano, T. & Suzuki, M., 1989. Peptidyl-prolyl cis-trans isomerase is the cyclosporin A-binding protein cyclophilin. *Nature*, 337(6206), pp.473–5.

Thomas, D. et al., 2008a. Supramolecular organization of the yeast F1Fo-ATP synthase. *Biology of the cell / under the auspices of the European Cell Biology Organization*, 100(10), pp.591–601.

Thomas, D. et al., 2008b. Supramolecular organization of the yeast F1Fo-ATP synthase. *Biology of the cell*, 100(10), pp.591–601.

Tsubaki, M. et al., 2000. Diethyl pyrocarbonate modification abolishes fast electron accepting ability of cytochrome b561 from ascorbate but does not influence electron donation to monodehydroascorbate radical: identification of the modification sites by mass spectrometric analysi. *Biochemistry*, 39(12), pp.3276–84.

Tucker, W.C. et al., 2004. Observation of calcium-dependent unidirectional rotational motion in recombinant photosynthetic F1-ATPaSe molecules. *Journal of Biological Chemistry*, 279(46), pp.47415–47418.

Ueno, H. et al., 2005. ATP-driven stepwise rotation of FoF1-ATP synthase. *Proceedings of the National Academy of Sciences of the United States of America*, 102(5), pp.1333–8.

Vassilopoulos, A. et al., 2014. SIRT3 deacetylates ATP synthase F1 complex proteins in response to nutrient- and exercise-induced stress. *Antioxidants & redox signaling*, 21(4), pp.551–64.

Venard, R. et al., 2003. Investigation of the role and mechanism of IF1 and STF1 proteins, twin inhibitory peptides which interact with the yeast mitochondrial ATP synthase. *Biochemistry*, 42(24), pp.7626–36.

Walker, J.E. et al., 1991. Identification of the subunits of F1F0-ATPase from bovine heart mitochondria. *Biochemistry*, 30(22), pp.5369–78.

Walker, J.E., 1985. Primary structure and subunit stoichiometry of F1-ATPase from bovine mitochondria. *Journal of Molecular Biology*, 184(4), pp.677–701.

Walker, J.E. et al., 1985. Primary structure and subunit stoichiometry of F1-ATPase from bovine mitochondria. *Journal of molecular biology*, 184(4), pp.677–701.

Walker, J.E., Saraste, M. & Gay, N.J., 1984. The unc operon. Nucleotide sequence, regulation and

structure of ATP-synthase. *Biochimica et biophysica acta*, 768(2), pp.164–200.

Wallace, D.C., 1999. Mitochondrial diseases in man and mouse. *Science*, 283, pp.1482–1488.

Wallace, D.C., Brown, M.D. & Lott, M.T., 1999. Mitochondrial DNA variation in human evolution and disease. *Gene*, 238(1), pp.211–30.

Walsh, C.T., Zydowsky, L.D. & McKeon, F.D., 1992. Cyclosporin A, the cyclophilin class of peptidylprolyl isomerases, and blockade of T cell signal transduction. *The Journal of biological chemistry*, 267(19), pp.13115–8.

Walter, L. et al., 2002. Regulation of the mitochondrial permeability transition pore by ubiquinone analogs. A progress report. *Free radical research*, 36(4), pp.405–12.

Wang, P. & Heitman, J., 2005. The cyclophilins. *Genome biology*, 6(7), p.226.

Watt, I.N. et al., 2010. Bioenergetic cost of making an adenosine triphosphate molecule in animal mitochondria. *Proceedings of the National Academy of Sciences of the United States of America*, 107(39), pp.16823–7.

Weber, J., 2006. ATP synthase: subunit-subunit interactions in the stator stalk. *Biochimica et biophysica acta*, 1757(9-10), pp.1162–70.

Weber, J., Bowman, C. & Senior, A.E., 1996. Specific tryptophan substitution in catalytic sites of Escherichia coli F1-ATPase allows differentiation between bound substrate ATP and product ADP in steady-state catalysis. *Journal of Biological Chemistry*, 271(31), pp.18711–18718.

Weber, J. & Senior, A.E., 2003. ATP synthesis driven by proton transport in F1F0-ATP synthase. *FEBS Letters*, 545(1), pp.61–70.

Wei, S. et al., 2015. Silencing of ATPase Inhibitory Factor 1 Inhibits Cell Growth via Cell Cycle Arrest in Bladder Cancer. *Pathobiology : journal of immunopathology, molecular and cellular biology*, 82(5), pp.224–32.

Westermann, B., 2008. Molecular machinery of mitochondrial fusion and fission. *The Journal of biological chemistry*, 283(20), pp.13501–5.

Wilbur, W.J., 1985. On the PAM matrix model of protein evolution. *Molecular biology and evolution*, 2(5), pp.434–47.

Wittig, I. et al., 2010. Assembly and oligomerization of human ATP synthase lacking mitochondrial subunits a and A6L. *Biochimica et biophysica acta*, 1797(6-7), pp.1004–11.

Wittig, I., Braun, H.-P. & Schägger, H., 2006. Blue native PAGE. *Nature protocols*, 1(1), pp.418–28.

Wittig, I. & Schägger, H., 2008. Structural organization of mitochondrial ATP synthase. *Biochimica et biophysica acta*, 1777(7-8), pp.592–8.

Wittig, I. & Schägger, H., 2009. Supramolecular organization of ATP synthase and respiratory chain in mitochondrial membranes. *Biochimica et biophysica acta*, 1787(6), pp.672–80.

Woodfield, K. et al., 1998. Direct demonstration of a specific interaction between cyclophilin-D and the adenine nucleotide translocase confirms their role in the mitochondrial permeability transition. *The Biochemical journal*, 336 (Pt 2, pp.287–90.

Woodfield, K.Y., Price, N.T. & Halestrap, A.P., 1997. cDNA cloning of rat mitochondrial cyclophilin. *Biochimica et biophysica acta*, 1351(1-2), pp.27–30.

Wu, J. et al., 2015. ATPase inhibitory factor 1 is a potential prognostic marker for the migration and invasion of glioma. *Oncology letters*, 10(4), pp.2075–2080.

Wu, M. et al., 2007. Multiparameter metabolic analysis reveals a close link between attenuated mitochondrial bioenergetic function and enhanced glycolysis dependency in human tumor cells. *American journal of physiology. Cell physiology*, 292(1), pp.C125–36.

Wu, Y.-T. et al., 2013. Regulation of mitochondrial F(o)F(1)ATPase activity by Sirt3-catalyzed deacetylation and its deficiency in human cells harboring 4977bp deletion of mitochondrial DNA. *Biochimica et biophysica acta*, 1832(1), pp.216–27.

Yamada, A. et al., 2009. Ca2+-induced permeability transition can be observed even in yeast

mitochondria under optimized experimental conditions. *Biochimica et biophysica acta*, 1787(12), pp.1486–91.

Yao, Q. et al., 2005. Roles of cyclophilins in cancers and other organ systems. *World journal of surgery*, 29(3), pp.276–80.

Yasuda, R. et al., 1998. F1-ATPase is a highly efficient molecular motor that rotates with discrete 120 degree steps. *Cell*, 93(7), pp.1117–24.

Yin, T. et al., 2015. ATPase inhibitory factor 1 is a prognostic marker and contributes to proliferation and invasion of human gastric cancer cells. *Biomedicine & pharmacotherapy = Biomédecine & pharmacothérapie*, 70, pp.90–6.

Yoshida, M., Muneyuki, E. & Hisabori, T., 2001. ATP synthase--a marvellous rotary engine of the cell. *Nature reviews. Molecular cell biology*, 2(9), pp.669–77.

Yu, L. & Fesik, S.W., 1994. pH titration of the histidine residues of cyclophilin and FK506 binding protein in the absence and presence of immunosuppressant ligands. *Biochimica et biophysica acta*, 1209(1), pp.24–32.

Zamzami, N. & Kroemer, G., 2001. The mitochondrion in apoptosis: how Pandora's box opens. *Nature reviews. Molecular cell biology*, 2(1), pp.67–71.

Zerbetto, E., Vergani, L. & Dabbeni-Sala, F., 1997. Quantification of muscle mitochondrial oxidative phosphorylation enzymes via histochemical staining of blue native polyacrylamide gels. *Electrophoresis*, 18(11), pp.2059–64.

Zhou, A. et al., 2015. Structure and conformational states of the bovine mitochondrial ATP synthase by cryo-EM. *eLife*, 4.

Zhou, Y. & Vachet, R.W., 2012. Increased protein structural resolution from diethylpyrocarbonate-based covalent labeling and mass spectrometric detection. *Journal of the American Society for Mass Spectrometry*, 23(4), pp.708–17.

Zizi, M. et al., 1994. NADH regulates the gating of VDAC, the mitochondrial outer membrane channel. *The Journal of biological chemistry*, 269(3), pp.1614–6.

Zoccarato, F. & Nicholls, D., 1982. The role of phosphate in the regulation of the independent calcium-efflux pathway of liver mitochondria. *European journal of biochemistry / FEBS*, 127(2), pp.333–8.

Zoratti, M. & Szabó, I., 1994. Electrophysiology of the inner mitochondrial membrane. *Journal of bioenergetics and biomembranes*, 26(5), pp.543–53.

Zydowsky, L.D. et al., 1992. Active site mutants of human cyclophilin A separate peptidyl-prolyl isomerase activity from cyclosporin A binding and calcineurin inhibition. *Protein science : a publication of the Protein Society*, 1(9), pp.1092–9.

6. ANNEX

PUBLICATIONS

1. **Antoniel M**, Giorgio V, Fogolari F, Glick GD, Bernardi P, Lippe G.
   The oligomycin-sensitivity conferring protein of mitochondrial ATP synthase: emerging new roles in mitochondrial pathophysiology.
   Int J Mol Sci. 2014 Apr 30;15(5):7513-36. doi: 10.3390/ijms15057513.

2. Giorgio V, von Stockum S, **Antoniel M**, Fabbro A, Fogolari F, Forte M, Glick GD, Petronilli V, Zoratti M, Szabó I, Lippe G, Bernardi P.
   Dimers of mitochondrial ATP synthase form the permeability transition pore.
   Proc Natl Acad Sci USA. 2013 Apr 9;110 (15):5887-92. doi : 10.1073/pnas.1217823110.

Int. J. Mol. Sci. **2014**, *15*, 7513-7536; doi:10.3390/ijms15057513

OPEN ACCESS
International Journal of
Molecular Sciences
ISSN 1422-0067
www.mdpi.com/journal/ijms

Review

The Oligomycin-Sensitivity Conferring Protein of Mitochondrial ATP Synthase: Emerging New Roles in Mitochondrial Pathophysiology

Manuela Antoniel [1,2], Valentina Giorgio [1], Federico Fogolari [3], Gary D. Glick [4], Paolo Bernardi [1] and Giovanna Lippe [2,*]

[1] Department of Biomedical Sciences, University of Padova, via Ugo Bassi 58/B, 35121 Padua, Italy; E-Mails: manuela.antoniel@studenti.unipd.it (M.A.); vgiorgio@bio.unipd.it (V.G.); bernardi@bio.unipd.it (P.B.)

[2] Department of Food Science, University of Udine, via Sondrio 2/A, 33100 Udine, Italy

[3] Department of Biomedical Sciences, University of Udine, p.le Kolbe, 33100 Udine, Italy; E-Mail: federico.fogolari@uniud.it

[4] Department of Chemistry, Graduate Program in Immunology, University of Michigan, Ann Arbor, MI 48109, USA; E-Mail: gglick@umich.edu

* Author to whom correspondence should be addressed; E-Mail: Giovanna.lippe@uniud.it; Tel.: +39-0432-558139; Fax: +39-0432-558130.

Received: 30 March 2014; in revised form: 18 April 2014 / Accepted: 21 April 2014 / Published: 30 April 2014

Abstract: The oligomycin-sensitivity conferring protein (OSCP) of the mitochondrial F_OF_1 ATP synthase has long been recognized to be essential for the coupling of proton transport to ATP synthesis. Located on top of the catalytic F_1 sector, it makes stable contacts with both F_1 and the peripheral stalk, ensuring the structural and functional coupling between F_O and F_1, which is disrupted by the antibiotic, oligomycin. Recent data have established that OSCP is the binding target of cyclophilin (CyP) D, a well-characterized inducer of the mitochondrial permeability transition pore (PTP), whose opening can precipitate cell death. CyPD binding affects ATP synthase activity, and most importantly, it decreases the threshold matrix Ca^{2+} required for PTP opening, in striking analogy with benzodiazepine 423, an apoptosis-inducing agent that also binds OSCP. These findings are consistent with the demonstration that dimers of ATP synthase generate Ca^{2+}-dependent currents with features indistinguishable from those of the PTP and suggest that ATP synthase is directly involved in PTP formation, although the underlying mechanism remains to be established.

In this scenario, OSCP appears to play a fundamental role, sensing the signal(s) that switches the enzyme of life in a channel able to precipitate cell death.

Keywords: mitochondria; oligomycin-sensitivity conferring protein (OSCP); cyclophilin D (CyPD); F_OF_1 ATP synthase dimer; permeability transition pore (PTP)

1. Introduction

Mitochondria are cytoplasmic double-membrane-delimited organelles of variable size, with a diameter between 0.5 and 5 μm, which are organized in a dynamic network [1] and are responsible of the aerobic production of ATP by the oxidative phosphorylation system (OXPHOS). In addition, mitochondria participate in intermediary metabolism and are involved in the early stages of cell death, where the Ca^{2+}-dependent permeability transition pore (PTP) plays a key role [2]. OXPHOS catalyzes the oxidation of fuel molecules and the concomitant synthesis of ATP via five complexes located in the inner mitochondrial membrane (IMM), which is highly folded into cristae. Briefly, Complexes I, III and IV of the respiratory chain catalyze a sequential series of redox reactions, resulting in the reduction of oxygen to water; at the same time, they pump protons across the IMM into the intermembrane space (IMS), generating a proton electrochemical gradient that provides the driving force for the synthesis of ATP from ADP and inorganic phosphate (Pi) within Complex V (or F_OF_1 ATP synthase).

Intriguingly, recent data suggest that Complex V has a second function, as it is able to generate Ca^{2+}-dependent currents with features indistinguishable from those of the PTP, as assessed after isolation in the form of dimers, which represent its physiological state in the IMM [3]. The enzyme of life appears therefore to be directly involved in PTP formation to stimulate cell death [4]. The OSCP (oligomycin-sensitivity conferring protein) subunit of ATP synthase appears to play a unique role, being the site of interaction of cyclophilin (CyP) D, a matrix protein that favors PTP opening, as will be discussed below. CyPD is also the downstream effector of kinase signaling pathways, which target the PTP, such as hexokinase II and the Akt-ERK-GSK3 axis, whose dysregulation is a hallmark of several neoplastic cell models [5]. Post-translational modifications (PTMs) of OSCP have also been reported [6–8], but their functional implications are still to be defined. These observations suggest that CyPD-OSCP interaction mediates a survival or death signal modulating the PTP closure/opening, although the underlying mechanism remains to be establish.

The IMM also contains many transporters or carriers that translocate nucleotides, inorganic ions and metabolites, including phosphate, thereby determining the compartmentalization of the metabolic functions of mitochondria. The mitochondrial proteome ranges between about 800 (yeast) and 1500 (human) different proteins [9], with relevant differences between organs [10]. Although the majority of mitochondrial proteins is encoded in the nucleus and post-translationally imported into the organelle by a complex protein-import machinery [11], some subunits of the OXPHOS (13 in humans) are encoded by the mitochondrial genome (mtDNA), which is present in several copies per organelle and is exclusively maternally inherited.

Defects in mitochondrial DNA (mtDNA) have been associated with mitochondrial diseases, which encompass a wide variety of degenerative diseases and may also play a role in aging and cancer [12]. Complex V deficiency due to mutations in the mtDNA-encoded subunits a and A6L is a very rare OXPHOS deficiency. Phenotypic variations in disease severity depend mainly on the fraction of mutated mtDNA percent (*i.e.*, the level of heteroplasmy), as observed in Maternally inherited Leigh syndrome (MILS) and neuropathy, ataxia and retinis pigmentosa (NARP) syndrome, caused by subunit a (*MT-ATP6*) mutations. Mitochondrial diseases due to genetic defects in the nuclear genes affecting one structural subunit, one assembly and one ancillary factor have also been described [13]. Deficiency in ATP synthesis appears to be the main pathogenic factor, although other mechanisms are involved, such as the generation of reactive oxygen species (ROS) [14–16]. On the other hand, the novel function of ATP synthase in PTP formation makes this picture much more complex, considering the role played by PTP and by its dysregulation in a variety of diseases characterized by altered cell death, which include ischemia-reperfusion injury of the heart and brain, muscular dystrophies, neurodegeneration and cancer [5,17].

2. ATP Synthase Structure

The mitochondrial ATP synthase is a 600-kDa multisubunit complex. Its molecular structure and catalytic mechanism were understood by the seminal work of the Nobel Laureates, Mitchell, Boyer and Walker [18–20], which revealed its complexity and the functional steps driving the synthesis of ATP. In addition to the IMM, ATP synthase is present in the thylakoid membrane of chloroplasts, and in the plasma membrane of bacteria and mammalian cells, although with opposite orientation [21,22]. It is well conserved, considering its structural complexity and the early divergence of bacteria, plants and animals [23]. Proton translocation and synthesis of ATP from ADP and Pi are coupled by a unique mechanism: subunit rotation. The electrochemical energy contained in the proton gradient is converted into mechanical energy in the form of subunit rotation and back into chemical energy as ATP [24–27]. The enzyme is also able to work in the direction of ATP hydrolysis, sustaining the formation of the proton gradient, when there is a loss of membrane potential. In both directions, Mg^{2+} is essential for catalysis, and it can be replaced by other divalent cations, such as Mn^{2+} and Co^{2+}. Intriguingly, Ca^{2+} ions, which induce PTP formation, only sustain ATP hydrolysis by F_1, which is not coupled to proton translocation both in bacteria [28] and in mammals [29].

Traditionally, ATP synthase is divided into two subcomplexes, the membrane-embedded F_O subcomplex, through which the protons flow, and the soluble F_1 subcomplex. The latter is always composed of three copies of each of subunits α and β (which carry the nucleotide binding sites) and one each of subunits γ, δ and ε (which constitute the central stalk of the complex). Subunit γ rotation within $\alpha_3\beta_3$ takes each of the three β subunits through the conformations, β_{DP}, β_{TP} and β_E, thereby synthesizing three Mg^{2+}-ATP molecules during each 360° rotation [30].

The inhibitor protein, IF_1, binds to F_1, at a α/β interface, under energy deficiency [31,32], *i.e.*, at low pH and membrane potential, when the enzyme hydrolyzes rather than synthesizes ATP. Therefore, IF_1, which is evolutionarily conserved from yeast to mammals, is considered responsible for the beneficial (at least partial) inhibition of F_OF_1 during ischemia both in *in vitro* experimental models, as well as *in vivo* [33], as also demonstrated by our group in anaesthetized open-chest goat heart [34].

Unexpectedly, IF_1-knockout mice grew without defects, but their behavior against stressful situations have not been tested [35].

In the simplest form of the enzyme, such as that of bacteria, like *Escherichia coli*, F_O consists of three different subunits, a, b and c, with stoichiometry $ab_2c_{9–12}$ [23]. Subunits a and c form the proton channel, while subunit b links the proton channel to F_1. The animal mitochondrial F_O sector has a more complicated structure, since ten subunits have been identified, a, b, c, F_6, d, e, A6L, f, g and OSCP [36]. The a, b and c subunits share great similarity with the bacterial subunits, except for subunit c stoichiometry which comprises only eight copies, thus reducing the bioenergetic cost of ATP synthesis [37], whereas the remaining subunits are unique to the mitochondrial complex (Table 1). The membrane-embedded part of F_O comprising subunits e, f, g and A6L is connected to F_1 by a complex peripheral stalk, composed by one copy each of subunit b, d, F_6 and OSCP, which is important to prevent the co-rotation of α and β subunits with γ and, therefore, the loss of enzyme efficiency. OSCP is a 213-amino acid protein (including the 23 amino acid mitochondrial leader sequence) located on the top of F_1 [38], which is analogous to *E. coli* δ-subunit and is highly conserved among mammals [39]. Besides these subunits, in beef, rat and man, two hydrophobic proteins, namely a 6.8-kDa proteolipid (called MLQ) [40,41], and α1 acid glycoprotein/diabetes-associated protein in insulin-sensitive tissue (called AGP/DAPIT) [42], are associated with the F_O. All together, the mitochondrial membrane domain is constituted by approximately 30 trans-membrane α-helices [43] (Figure 1).

Table 1. Equivalence of subunits of ATP synthase from different sources [1].

Mitochondria		***E. coli*,**	**Chloroplast, cyanobacteria [2]**
Bovine	**Yeast**	***P. modestum* and *A. woodii***	**and rhodobacteria [3]**
α	α	α	α
β	β	β	β
γ	γ	γ	γ
δ	δ	ε	ε
ε	ε	-	-
OSCP	OSCP	δ	δ
b	4 or b	B [4]	b and b' (I and II)
A6L	8	-	-
F6	h	-	-
a	6 or a	a	a (IV)
c	9 or c	c	c (III)
d	d	-	-
e	e	-	-
f	f	-	-
g	g	-	-
-	i/j	-	-
-	k	-	-
MLQ	-	-	-
AGP/DAPIT	-	-	-

[1] Subunit equivalence is based on sequence homology; [2] *Synechococcus*; [3] *Rhodospirillum rubrum* and *Rhodopseudomonas blastica*; [4] ATP synthase from *E. coli* and *P. modestum* have two copies of the b subunit and ATP synthase from chloroplasts, cyanobacteria and rhodobacteria have one copy of each b and b'. The b and b' are homologous; -, no subunit equivalence.

Figure 1. Schematic representation of F_OF_1 ATP synthase as a monomer.

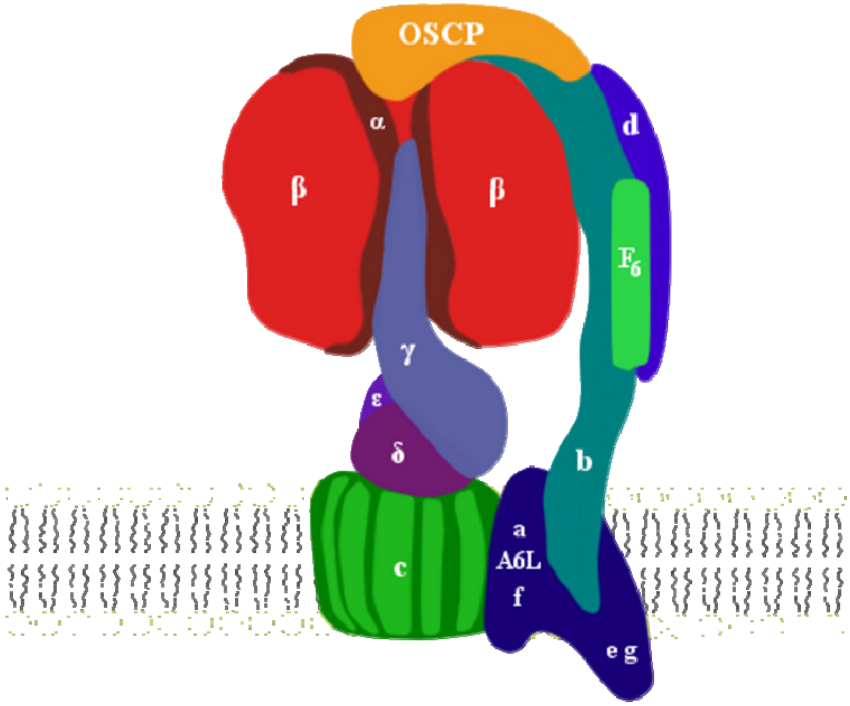

ATP synthase is commonly isolated as a functional monomer, but this is not the physiological state in yeast, mammalian and plant mitochondria [44,45]. Biochemical and electron microscopy studies demonstrated that within the IMM, the enzyme is organized in dimers associated with forming long rows of oligomers located at the cristae ridges to maintain a high local curvature [3] and normal cristae morphology [46,47]. Dimers interact within the IMM through the F_O subunits [48] with the peripheral stalks turned away from each other [38]. The proposed roles of the ATP synthase oligomers are higher efficiency and higher stability [3,49]. Consistently, in aged mitochondria of *Podospora anserina*, the disappearance of the typical IMM architecture and impairment of ATP synthesis were concomitant to ATP synthase dimer dissociation and formation of IMM vesicles [50]. Intriguingly, electron tomography evidenced the binding of a bell-shaped protein, possibly CyPD, between the F_O-F_O of dimers at the bases of the peripheral stalks in early-vesicular mitochondria followed by its dissociation from monomers in aged mitochondria. These observation prompted the authors to propose a role of CyPD in promoting dimer dissociation. We found that CyPD interacts with OSCP in the ATP synthase dimers promoting PTP formation [2,4], as will be discussed below. If CyPD binding between the two F_O will be confirmed by further investigation, the existence of distinct CyPD binding sites on ATP synthase dimers may be proposed.

The structural properties of dimers were initially characterized in yeast, where genetic approaches, cross-linking analyses and electron microscopy images established preferential interactions within the IMM, mainly through the Su6 [51], Su4 [52], e [53] and g subunits [54], which formed Su6/Su6, Su4/Su4 and e/g interactions, and also through the yeast-specific F_O subunits, h and i [55]. In keeping with its general occurrence, the involvement of subunits a [56], e [57] and g [44] in ATP synthase dimerization has been demonstrated also in mammals. In addition, a second interface (named the oligomerization interface) has been described in yeast; this interface was stabilized through e/e and g/g interactions allowing oligomer formation [45]. However, the existence of an oligomerization interface

has been criticized based on electron cryotomography data of mitochondria from different sources, including bovine heart, which evidenced variable distance between dimers, making direct protein contacts difficult [3]. Moreover, electron cryotomography showed that dimers of all species display fixed angles between two F_1-F_1 with an angle >70° [3], in contrast with previous single-particle electron microscopy images, which indicated angles ranging from 40° [58,59] to 70°–90° [48,60]. It has been proposed that the 40° dimers form upon the inhibitory binding of IF_1 [3], which was contained in considerable amounts in isolated dimers [58]. However, although IF_1 was not essential for ATP synthase dimerization both in yeast [61] and mammals [62], we found that in cardiomyoblasts undergoing cardiac differentiation, IF_1 binding promoted dimer/oligomer stabilization, possibly through a non-inhibitory interaction, which remains to be clarified. In fact, in differentiated cells, an increased IF_1 binding occurred in parallel with an increase of ATP synthesis, as already reported in human HeLa cells [63] overexpressing IF_1, as well as of ATP hydrolysis [64]. Intriguingly, a pH-independent interaction of IF_1 with OSCP has been described [65], whose functional implication remains to be established. A stabilizing effect on bovine ATP synthase dimers has been also reported for the matrix metalloprotein, called factor B, which interacts with the e and g subunits of F_O [66].

3. OSCP: Location and Structure

It has long been established that OSCP is essential for conferring sensitivity to the inhibition of ATP synthase by the antibiotic, oligomycin [67], although oligomycin does not bind OSCP. Sensitivity to oligomycin can be defined in two contexts. The first relates to the "coupling" of the enzyme assayed as the oligomycin-sensitive ATP hydrolytic (ATPase) activity. It is a measure of the structural integrity of the enzyme, since detachment of F_1 from F_O leads to a decrease in oligomycin-sensitive ATPase activity [68–72]. Under these conditions, ATP hydrolysis by F_1 still takes place, but ATP hydrolysis is no longer coupled to proton translocation, and the sensitivity to oligomycin is lost, demonstrating that oligomycin inhibits proton transport in F_O, thus affecting the V_{max} of ATP hydrolysis, only when F_O is correctly bound to F_1, *i.e.*, in the coupled enzyme [70]. In this context, depletion/reconstitution studies in isolated membranes demonstrated that OSCP is absolutely necessary in coupling proton translocation to ATP synthesis [71]. In keeping with this key function of the subunit, yeast OSCP knockouts failed to survive under normal growth conditions [73].

The second context relates to the ability of the assembled ATP synthase complex to bind oligomycin. In yeast, the oligomycin resistance phenotype is conferred by mutations in one of the two mitochondrially encoded subunits, a (Su6) and c (Su9), indicating that the oligomycin-binding site encompasses the *C*-terminal region of Su6 and the transmembrane domains of Su9 [74]. This is consistent with the role of these subunits in proton translocation through F_O, which requires the concerted action of both.

Boyle and Colleagues have examined the effect of a single residue change at a conserved glycine (Position 166) of yeast OSCP [75]. A G166N mutant allowed enzyme assembly into functional complexes and was able to grow on ethanol, albeit with a slower generation time. Mutant cells demonstrated a relative insensitivity to oligomycin during State 3 respiration, as well as a passive leak of protons across the IMM. Moreover, ATP synthase complexes containing the G166N mutation were found to be unstable, being more susceptible to dissociation than complexes containing native OSCP.

These properties suggested that altered protein-protein interactions between OSCP and the $\alpha_3\beta_3$ hexamer partially uncoupled the enzyme. Interestingly, binding of 17β-estradiol to OSCP promoted an intrinsically uncoupled state of ATP synthase, while the enzyme was actually catalyzing the ATP synthesis in rat liver mitochondria [76]. Fluorescence resonance energy transfer (FRET) measurements have documented the stress developing between F_1 and OSCP during ATP hydrolysis, which appears to match its role as part of the peripheral stalk [77].

Intriguingly, OSCP binds isolated F_1 in bovine, but not yeast, mitochondria [70,78] Moreover, *in organello* pulse-labeling and pulse-chase experiments run in yeast seem to indicate that OSCP binding is the last step in the assembly of F_OF_1 and that it occurs independently of the two pathways that converge to form the whole ATP synthase from the F_1/Su9-ring and Su6/Su8/peripheral stalk subcomplexes [79]. Consistent with these data, reducing OSCP levels in human cells did not alter the expression of other F_OF_1 subunits, as well as of the respiratory chain complexes [4,78]. Interestingly, in a model of Leigh syndrome obtained in a conditional knockout mouse heart for the mtDNA regulator, *Lrpprc* (leucine-rich pentatricopeptide repeat containing protein), the appearance has been recently observed of ATP synthase subcomplexes lacking OSCP and A6L. These subcomplexes contained a high amount of IF1, which blocked the ATP hydrolysis at physiological pH, counteracting the overall impairment of ATP production [16].

Rees and Colleagues [80] established the physical location of OSCP in the peripheral stalk by analyzing the crystal of a F_1-peripheral stalk subcomplex and demonstrated that the subunit sits on top of the F_1 domain (see Figure 1), in agreement with earlier experiments [81]. Its *N*-terminal domain (Residues 1–113) contains six α-helices and shows a similar fold to that of the *N*-terminal fragment of recombinant OSCP analyzed by NMR [82]. Helices 1 and 5 provide the binding site: (i) for Residues 6–17 of subunit α_E (which contacts β_E in $\alpha_3\beta_3$ subcomplex), largely via hydrophobic interactions and two possible charge-charge interactions through R15 and E91; and (ii) for E7 and R94 of subunits α and OSCP, respectively [80]. These interactions are similar to those determined with isolated OSCP and synthetic peptides from the *N*-terminals of mitochondrial and bacterial α subunits [81,83]. There is another region of interaction involving Residues 1–14 of the OSCP with the F_1 *N*-terminal β-barrel domains of the β_{DP}-subunit [80].

The structure of the *C*-terminal domain of OSCP, which is unstructured in the isolated protein [82], consists of a β-hairpin, which precisely locates along the α/β interface [38], followed by two α-helices, H7 and H8 [80]. H8 of the OSCP forms a three-helix bundle with the *N*-terminal α-helix of F_6 and a segment of subunit b. The *C*-terminal of subunit b also packs against helix H7 of the OSCP, resulting in an extensive interface between OSCP and subunits b and F_6.

4. Post Translational Modifications of OSCP Subunit

Information on post-translational modifications (PTM) of ATP synthase subunits has increased with the development of new techniques, such as PTM-specific mass spectrometry (MS)-based methods, selective dyes (ProQ Diamond) and specific antibodies. The association of several of these PTMs with specific biological processes, *i.e.*, PDGF-mediated phosphorylation of the δ subunit [84,85], or diseases (such as type 2 diabetes [86]) has been found. The challenge is now to find direct

functional implications for these PTMs. The OSCP subunit has been reported to be glycosylated [7], phosphorylated [6,87–90] and acetylated [8,91] (Table 2).

Table 2. Post-translational modifications of OSCP.

Modification	Method	Residue	Organism/Tissue	Reference
Acetylation	MS [1]	K60, K70, K159, K162, K172, K176, K192	Mouse/Liver	[91]
	K Ab		Human 143B osteosarcoma cells	[8]
Phosphorylation	ProQ		Pig/Heart	[6]
	PhosTag		Pig/Heart	[87]
	^{32}P		Pig/Heart	[90]
	MS	T145	Pig/Heart	[89]
	MS	S155	Human/Muscle	[88]
Glycosylation	Leptin resin		Bovine/Heart	[7]
Ubiquitination	Ub Ab		Human colon cancer cells	[92]

[1] Abbreviations: MS, mass spectrometry; K Ab, anti-lysine antibody; Ub Ab, anti-ubiquitin antibody.

Although the glycosylation of secreted, membrane and nucleocytosolic proteins has been well studied, information on the glycosylation of mitochondrial proteins is limited [93,94]. Recently, different authors have proposed that several proteins with mitochondrial function or with mitochondrial-annotation and, thus, putative mitochondrial function may be glycosylated [95–98].

Berninsone and Burnham-Marusich [7] identified glycosylated isoforms of OSCP and the d subunit in bovine heart mitochondria by using a leptin resin. The same authors also detected a glycosylated isoform of the ATP synthase α subunit in bovine heart tissue, in a primate cell line (COS-7) and in the *Caenorhabditis elegans* primary embryonic cell line [99]. These results indicate that glycosylated isoforms of proteins with established mitochondrial function exist and may be more common than previously appreciated. Computational prediction of OSCP (P13621 sequence) glycosylation sites revealed two *O*-glycosylation sites, one of which is near to Helix 6, contacting α_E [80] (NetOGlyc 4.0 algorithm [100]), thus suggesting an involvement in the modulation of enzyme activity. Interestingly, in rat cardiac myocytes, an increase of *O*-glycosylation of Complex I, III and IV is associated with impaired respiratory activity [96]. Taken together, these findings open questions about where in the cell and, consequently, by which glycosyltransferases these proteins, including OSCP, become glycosylated and the nature of glycosylation (the attachment site and structure of glycans).

Phosphorylation of OSCP was reported for the first time by Hopper *et al.* [6], who analyzed the phosphoproteome of the mitochondrial matrix in porcine heart, using the phosphorylation targeted dye, ProQ Diamond, in conjunction with 2D gel and mass spectrometry. A phosphorylated form of OSCP has been later found also in porcine heart by the Balaban group, who extensively studied mitochondrial phosphoproteome with PhosTag and ^{32}P labeling (for a review of ATP synthase phosphorylation, see [89]). In particular, the OSCP residues, Ser155 and Thr145, have been found phosphorylated in human skeletal muscle and pig heart, respectively [88,101]. Their location near the α_E subunit suggests that phosphorylation may participate in the regulation of motor function, but no evidence has been yet reported. Nevertheless, and in spite of these advances, kinases and phosphatases involved in ATP

synthase phosphorylation are still poorly defined, and further work will be needed to understand the consequences of phosphorylation on enzyme activity.

The first extensive proteomic study of mitochondrial protein acetylation was performed in mouse liver mitochondria [91] and revealed that more than 20% of mitochondrial proteins contain acetylated lysine residues, including OSCP and the other peripheral stalk subunits, the F_1 α, β, γ subunits and the F_O g and A6L subunits, for which the acetylated sites have been identified. More recently, acetylation of α and OSCP subunits was confirmed by Wei *et al.* [8], who discovered that Sirtuin3, which belongs to a large family of NAD^+-dependent protein deacetylases, interacts with OSCP and activates the enzyme through deacetylation of α and OSCP subunits. Such a finding is consistent with the ability of acetylation to neutralize the positive charge of lysine residues, as well as to increase the hydrophobicity and size of the lysine side chains, causing potential alterations of the protein propensity to interact with other proteins. Thus, the acetylation of OSCP can induce a conformational change of the protein itself or prevent complex formation with other proteins. The relevance of acetylation was confirmed by the observation that potentially every major metabolic enzyme is acetylated, both inside and outside the mitochondria [102,103].

Interestingly, selective immunoprecipitation of OSCP from mitochondrial lysates revealed that OSCP is ubiquitinated in colon cancer cells (human COLO 205 cell line) together with high levels of the expression of Hsp90 [92]. OSCP ubiquitination was not observed in an MS analysis of mouse heart, where, instead the α, β, γ and b subunits were found to be ubiquitinated [104], suggesting a specific role of OSCP ubiquitination in cancer cells.

In summary, several PTMs have been identified in the OSCP subunit, especially phosphorylation and acetylation, for which specific sites have been found (Table 2). However, for most of them, the functional consequences are still unknown, as well as the enzymes involved in these modifications.

5. OSCP Interactors: CyPD and PTP Formation

ATP synthase activity is regulated by the reversible association of a variety of regulatory peptides, including CyPD. Beside the already mentioned IF_1, an inhibitory interaction with protein kinase Cδ at subunit d of the lateral stalk has been described, whose disruption attenuated the injury resulting from prolonged oxygen deprivation in neonatal cardiac myocytes [105]. Conversely, the Ca^{2+}-dependent association of S100A1 with F_1 improved the enzyme performance in cardiomyocytes [106]. Binding of Bcl-X_L to the β subunit and binding of Factor B to the membrane-embedded part of F_O increased the aerobic ATP production by blocking a proton leak in healthy neurons [107] and in animal mitochondria [66,108], respectively. In addition, three new interactors have been described that selectively bind OSCP, *i.e.*, the already mentioned Sirtuin3, CyPD and, possibly, p53 [109].

Sirtuins control a variety of cellular function via their NAD^+-dependent deacetylase activity [110]. Sirtuin3 is the best characterized sirtuin in mitochondria and has emerged as a major regulator of mitochondrial metabolism and energy homeostasis through mitochondrial protein deacetylation [111]. As already mentioned, Wei and co-workers discovered that endogenous Sirt3 interacts with OSCP and mediates the deacetylation of the α and OSCP subunits. Interestingly, these authors found that ATPase acetylation and Sirtuin3 expression are altered in human cells harboring a pathogenic mtDNA mutation (the 4977 bp deletion), as well as under increased ROS production in human cells [8].

p53 is a transcription factor rapidly activated in response to multiple stresses regulating hundreds of genes implicated in cell cycle, senescence, apoptosis, metabolism and DNA repair [112]. For a human cell model expressing mitochondrially-targeted p53 (with a vector in which the sequence encoding a mitochondrial import leader was fused to the 5' end of wild-type p53), a transcription-independent activity of p53 able to increase oxygen consumption and to decrease ROS production in the absence of acute stress has been recently reported. By immunoprecipitation and mass spectrometry, the authors demonstrated that p53 interacts with OSCP, taking part in the assembly or stabilization of the mature F_OF_1 complex, thus suggesting that the mitochondrial fraction of p53, although very low, may be an important regulator of mitochondrial physiology, potentially exerting tumor suppression [109]. However, interaction domains between p53 and Sirt3 with OSCP have been not yet been determined.

CyPD belongs to a ubiquitous protein family with peptidyl-prolyl *cis-trans* isomerase (PPIase) activity, which is inhibited by cyclosporin (Cs) A [113]. CyPs share a common domain of approximately 109 amino acids, the CyP-like domain [17,114]. In spite of this, CyPs do not play a general role in protein folding, and the existence of tissue- and organelle-specific isoforms with the proper targeting and/or retention sequence(s) suggests that each CyP regulates a restricted number of unique partner proteins [114,115].

CyPD is the unique mitochondrial isoform of CyPs in mammals and is involved in the regulation of the PTP, but is not a structural pore component. PTP is a conserved high-conductance channel located in the inner mitochondrial membrane (IMM) that allows the diffusion of solutes up to about 1500 Da [116]. PTP openings of a short duration lead to transient IMM depolarization [117] and may be caused by physiological stimuli [118]; while long-lasting openings cause permanent depolarization, loss of ionic homeostasis, depletion of matrix pyridine nucleotides, resulting in respiratory inhibition, and the generation of reactive oxygen species (ROS). Moreover, the matrix swelling occurs as a consequence of its high oncotic pressure, and the outer mitochondrial membrane (OMM) may disrupt with the release of pro-apoptotic intermembrane proteins, including cytochrome *c*. Thus, long-lasting PTP opening may represent a point of no return in cell commitment to death, which can occur either through apoptosis (if enough ATP is present to sustain caspase activity) or through necrosis (when ATP is depleted) [5].

The role of CyPD as a PTP inducer was suggested by the demonstration that addition of CsA to isolated mitochondria desensitizes the PTP, in that pore opening requires about twice the Ca^{2+} load necessary to open the pore in the absence of CsA [119]. Genetic ablation of the *Ppif* gene (which encodes for CyPD in the mouse) has confirmed that CyPD is the mitochondrial receptor for CsA, and it is responsible for the modulation of the PTP, both *in vitro* and *in vivo* [120–123]. The crystal structure of human CypD in complex with CsA demonstrated that it is composed of eight β-strands, two α-helices and one 3_{10} helix [124].

A major step in the mechanistic understanding of the role of CyPD in PTP regulation has been the discovery that CyPD masks an inhibitory site for Pi, which is the actual PTP desensitizing agent [125]. Furthermore, PTP modulation by CyPD is affected by CyPD phosphorylation [5], acetylation [126] and nitrosylation [127]. Not surprisingly, several regulatory interactions of CyPD have been reported in the literature, including Hsp90 and its related molecule, TRAP-1 [128], Bcl-2 [129], ERK-2/GSK-3 [5] and possibly p53 [130], which also seems to bind OSCP [109].

The identification of CyPD interaction with the OSCP subunit of ATP synthase was an essential step for the identification of the PTP, whose molecular nature was still a matter of conjectures [2]. The previous model still postulated that PTP is formed by a supramolecular complex, including the voltage-dependent anion channel (VDAC) of the OMM, as well as the adenine nucleotide translocator (ANT) and the phosphate carrier (PiC) located in the IMM, but genetic testing has excluded this possibility for all of these proteins [2].

We observed that in mammals, CyPD binds the ATP synthase peripheral stalk in an apparent ratio of 1:1:1:1 with the OSCP, b and d subunits; that this interaction is favored by Pi, which exerts multiple effects on PTP [125], as well as on ATP synthase [131]; and that the interaction is competed by CsA concentrations known to displace CyPD from the IMM [132]. Importantly, CyPD preferentially binds to the ATP synthase dimers, causing a decrease of specific activity that can be reversed by CsA [133]. Consistent with a regulatory interaction, the stimulatory effect of CsA was lost in *Ppif*$^{-/-}$ mitochondria, indicating that it was mediated by CyPD, while the assembly of the ATP synthase was unaffected by CyPD ablation [133].

CyPD interaction with OSCP (which appears to be mostly electrostatic in nature) was confirmed by immunoprecipitation of OSCP from mitochondria [4]. When ATP synthase was immunoprecipitated from mitochondria with decreased OSCP levels, decreased levels of CyPD were detected, as well. A study of surface potentials and isopotential curves of CyPD and OSCP in the ATP synthase complex identified putative binding regions of CyPD on OSCP at the region overlapping with Helices 3 and 4, which represent the lowest (*i.e.*, most negative) average surface potential regions, as shown in Figure 2, where OSCP in the context of ATP synthase is depicted. These helices are also the binding site of benzodiazepine (Bz)-423, a well-characterized inhibitor of ATP synthase (Figure 2) [78]. Treatment of mitochondria with Bz-423 induced CyPD displacement from ATP synthase, suggesting competition for a common binding site. Such localization is therefore consistent with the CyPD inhibitory activity of ATP synthase and may allow CyPD binding to all classes of dimers, including those displaying small angles between two F_1, which have the peripheral stalks in contact, mutually hiding their subunits, except OSCP. These latter dimers probably form upon IF_1 binding [3,58], *i.e.*, when ATP synthase hydrolyses ATP generating high Pi, which, in turn, is necessary for CyPD binding [133]. Further work is needed to define the amino acids involved in these interactions.

Consistent with the involvement of ATP synthase in PTP formation, mitochondria treated with Bz-423 or expressing decreased levels of OSCP also decreased the threshold Ca^{2+} required for PTP opening, revealing a striking analogy between the effects of Bz-423 and OSCP on PTP and ATP synthase. Direct evidence that PTP forms from ATP synthase was obtained by electrophysiology, which demonstrated that the addition of Bz-423 in the presence of Ca^{2+} to ATP synthase dimers isolated and incorporated in azolectin bilayers triggered Ca^{2+}-dependent currents with features indistinguishable from those of the PTP [134], which were inhibited by Mg^{2+}-ADP and by AMP-PNP (γ-imino ATP), a nonhydrolyzable ATP analog. Taken together, these findings prompted us to hypothesize that Ca^{2+}, which is able to sustain only uncoupled ATP hydrolysis [29], replaces Mg^{2+} and induces conformational changes in F_O, which could then mediate PTP formation from ATP synthase dimers. OSCP may thus act as a negative modulator of PTP affecting Ca^{2+} accessibility, except when it binds CyPD or Bz-423, which favor PTP formation.

Beyond CyPD and Ca^{2+}, many other effectors regulate the open-closed transitions of PTP, including Mg^{2+}, Mn^{2+}, nucleotides and low pH (which favor its closure); and low membrane potential, high Pi, and ROS (which favor its opening) [118,135]. ROS may induce the PTP, but also form as a consequence of PTP opening, in a feed-forward loop that may stabilize the pore in the open conformation. The F_OF_1 ATP synthase potentially accommodates all these PTP pathophysiological effectors, since divalent cations, nucleotides and Pi bind to the catalytic sites of F_1, and the membrane potential and pH regulate the catalytic activity, as well as IF_1 binding; however, the underlying conformational changes responsible for PTP formation are still far from being characterized.

Interestingly, OSCP contains one conserved histidine residue (His 112 in the bovine enzyme) exposed to the matrix and located in one of the lowest surface potential regions (Figure 2), which could be involved in the regulation of PTP by pH and ROS. In fact, previous studies highlighted an essential role of matrix-exposed histidine residue(s) in PTP regulation; histidine protonation at low pH indeed induced CyPD release and PTP closure [132,136]. Moreover, *in vitro* experiments demonstrated that oxidation of critical histidine residue(s) located on the PTP matrix side by singlet oxygen photogenerated *in situ* favored the PTP closed conformation by causing a secondary drop of reactivity to the cross-linking of pore-activating cysteine residues [137]. OSCP also contains a unique cysteine (Cys 118 in bovine mitochondria) conserved in mammals, whose function in ATP synthase catalysis is unclear [69]. We suspect that this residue may be involved in PTP activation by forming a dithiol cross-linking with a cysteine of another matrix protein, possibly only when His 112 is not oxidized. On the other hand, ATP synthase from various organisms is susceptible to different ROS species produced in *in vitro* experiments [138–140], as well as to oxidative/nitrative stress associated with central nervous system (CNS) disorders [141,142], caloric restriction [143] and aging [144,145]. We showed that isolated F_1 from bovine heart ATP synthase is selectively inactivated by hydrogen peroxide through redox-active iron-protein adducts, probably generating highly reactive oxygen species [139]. More recently, an exclusive target of singlet oxygen and hydrogen peroxide has been identified in a highly conserved methionine-cysteine cluster of the chloroplast γ subunit that is essential for the enzyme coupling and whose oxidation appeared to be directly involved in the loss of enzyme activity [146]. Due to its conservation, it is tempting to hypothesize that also this cluster may be a candidate for ROS-mediated PTP modulation. Other selective ATP synthase targets of ROS may be three of the five Trp residues of the d subunit identified in human heart mitochondria [147] and a single Trp of the α subunit identified in *Podospora anserina* and possibly involved in protein quality control [148]. Their oxidation may occur as a consequence of PTP formation. Moreover, in *Podospora anserina*, an age-related post-translational modification of OSCP has been identified by 2D-PAGE and matrix-assisted laser desorption/ionization-Time-of-Flight mass spectrometry (MALDI-TOF MS) whose nature is still to be clarified [144].

Figure 2. Surface potential regions on OSCP. The two lowest potential regions on OSCP are highlighted by a yellow circle. The average surface atom potential is displayed on the left; the cartoon structure is shown on the right with positively (blue) and negatively (red) charged side chains. The color code for the potential is: saturated red, −8.0 kJ/(mol·q); saturated blue, 8.0 kJ/(mol·q). The F_1 structure is shown as transparent. The yellow circle in the upper panel is located at OSCP residues E48, D71, E76 and F78. The latter region, discussed in the text, encompasses Helices 3 and 4. For the sake of completeness, the yellow circle in the lower panel is located at the other lowest potential region located at OSCP residues H112, E115, V116, E128 and E133. The surface potential is computed as previously described [4,149].

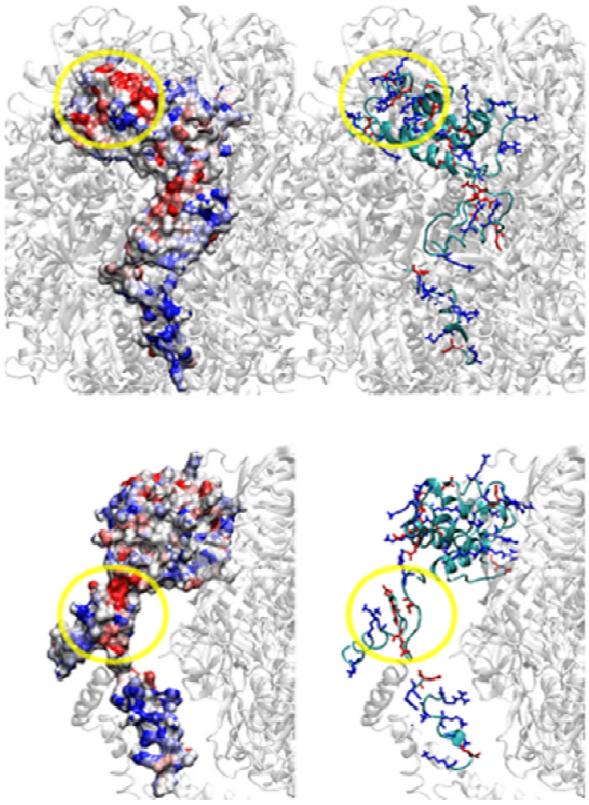

6. Concluding Remarks

Through its contacts with the F_1 $\alpha_3\beta_3$ hexamer and the peripheral stalk, OSCP not only ensures the structural and functional coupling between F_O and F_1, which is necessary for ATP synthesis, but also modulates the enzyme complex and is the target of inhibitors and interactors, including CyPD. CyPD affects ATP synthase activity and, most importantly, decreases the threshold matrix Ca^{2+} required for PTP opening. This finding, together with the electrophysiological demonstration that ATP synthase dimers give rise to Ca^{2+}-dependent currents with features indistinguishable from those of the PTP, indicate that ATP synthase is directly involved in PTP formation and that OSCP plays a fundamental role in this process, acting as a sensor for signal(s) that switch the enzyme of life in a channel able to induce cell death. CyPD and OSCP are the targets of signaling pathways (such as phosphorylation and acetylation) and of common interactors (such as Hsp90). Many open questions remain, in particular: (i) How does CyPD interaction with OSCP change the apparent affinity of the ATP synthase for Ca^{2+},

triggering a conformational change that leads to PTP formation? (ii) Where is (are) the Ca^{2+} binding site(s)? (iii) Is the redox sensitivity of the transition of the ATP synthase to PTP formation mediated by a dithiol-disulfide interconversion, and where are the relevant cysteines located? (iv) Is the pH-dependent inhibition of the PTP due to IF_1 binding, which is pH-dependent? These and many other questions can now be addressed with the powerful methods of genetics, and we have little doubt that the future has a lot in store toward our molecular understanding of the permeability transition.

Acknowledgments

This work was supported by grants from Telethon, the Italian Association for Cancer Research (AIRC), the Italian Ministry for University and Research (MIUR), and the University of Padova, Italy.

Conflicts of Interest

Conflict of interest statement: Bz-423 is licensed to a company in which Gary D. Glick has ownership interest and receives compensation.

References

1. Scorrano, L. Keeping mitochondria in shape: A matter of life and death. *Eur. J. Clin. Investig.* **2013**, *43*, 886–893.
2. Bernardi, P. The mitochondrial permeability transition pore: A mystery solved? *Front. Physiol.* **2013**, *4*, 95.
3. Davies, K.M.; Strauss, M.; Daum, B.; Kief, J.H.; Osiewacz, H.D.; Rycovska, A.; Zickermann, V.; Kühlbrandt, W. Macromolecular organization of ATP synthase and complex I in whole mitochondria. *Proc. Natl. Acad. Sci. USA* **2011**, *108*, 14121–14126.
4. Giorgio, V.; von Stockum, S.; Antoniel, M.; Fabbro, A.; Fogolari, F.; Forte, M.; Glick, G.D.; Petronilli, V.; Zoratti, M.; Szabò, I.; *et al*. Dimers of mitochondrial ATP synthase form the permeability transition pore. *Proc. Natl. Acad. Sci. USA* **2013**, *110*, 5887–5892.
5. Rasola, A.; Sciacovelli, M.; Chiara, F.; Pantic, B.; Brusilow, W.S.; Bernardi, P. Activation of mitochondrial ERK protects cancer cells from death through inhibition of the permeability transition. *Proc. Natl. Acad. Sci. USA* **2010**, *107*, 726–731.
6. Hopper, R.K.; Carroll, S.; Aponte, A.M.; Johnson, D.T.; French, S.; Shen, R.F.; Witzmann, F.A.; Harris, R.A.; Balaban, R.S. Mitochondrial matrix phosphoproteome: Effect of extra mitochondrial calcium. *Biochemistry* **2006**, *45*, 2524–2536.
7. Burnham-Marusich, A.; Berninsone, P. Multiple proteins with essential mitochondrial functions have glycosylated isoforms. *Mitochondrion* **2012**, *12*, 423–427.
8. Wu, Y.T.; Lee, H.C.; Liao, C.C.; Wei, Y.H. Regulation of mitochondrial F(o)F(1)ATPase activity by Sirt3-catalyzed deacetylation and its deficiency in human cells harboring 4977 bp deletion of mitochondrial DNA. *Biochim. Biophys. Acta* **2013**, *1832*, 216–227.
9. Elstner, M.; Andreoli, C.; Ahting, U.; Tetko, I.; Klopstock, T.; Meitinger, T.; Prokisch, H. MitoP2: An integrative tool for the analysis of the mitochondrial proteome. *Mol. Biotechnol.* **2008**, *40*, 306–315.

10. Lotz, C.; Lin, A.J.; Black, C.M.; Zhang, J.; Lau, E.; Deng, N.; Wang, Y.; Zong, N.C.; Choi, J.H.; Xu, T.; *et al.* Characterization, Design, and Function of the Mitochondrial Proteome: From Organs to Organisms. *J. Proteome Res.* **2013**, *13*, 433–446.
11. Baker, M.J.; Frazier, A.E.; Gulbis, J.M.; Ryan, M.T. Mitochondrial protein-import machinery: Correlating structure with function. *Trends Cell Biol.* **2007**, *17*, 456–464.
12. Wallace, D.C.; Brown, M.D.; Lott, M.T. Mitochondrial DNA variation in human evolution and disease. *Gene* **1999**, *238*, 211–230.
13. Jonckheere, A.I.; Smeitink, J.A.M.; Rodenburg, R.J.T. Mitochondrial ATP synthase: Architecture, function and pathology. *J. Inherit. Metab. Dis.* **2012**, *35*, 211–225.
14. Mattiazzi, M.; Vijayvergiya, C.; Gajewski, C.D.; DeVivo, D.C.; Lenaz, G.; Wiedmann, M.; Manfredi, G. The mtDNA T8993G (NARP) mutation results in an impairment of oxidative phosphorylation that can be improved by antioxidants. *Hum. Mol. Genet.* **2004**, *13*, 869–879.
15. Mrácek, T.; Pecina, P.; Vojtísková, A.; Kalous, M.; Sebesta, O.; Houstek, J. Two components in pathogenic mechanism of mitochondrial ATPase deficiency: Energy deprivation and ROS production. *Exp. Gerontol.* **2006**, *41*, 683–687.
16. Mourier, A.; Ruzzenente, B.; Brandt, T.; Ku, W. Loss of LRPPRC causes ATP synthase deficiency. *Hum. Mol. Genet.* **2014**, *23*, 1–13.
17. Giorgio, V.; Soriano, M.E.; Basso, E.; Bisetto, E.; Lippe, G.; Forte, M.A.; Bernardi, P. Cyclophilin D in mitochondrial pathophysiology. *Biochim. Biophys. Acta* **2010**, *1797*, 1113–1118.
18. Mitchell, P. Keilin's respiratory chain concept and its chemiosmotic consequences. *Science* **1979**, *206*, 1148–1159.
19. Boyer, P.D. The ATP synthase A splendid molecular machine. *Annu. Rev. Biochem.* **1997**, *66*, 717–749.
20. Abrahams, J.P.; Leslie, A.G.; Lutter, R.; Walker, J.E. Structure at 2.8 Å resolution of F1-ATPase from bovine heart mitochondria. *Nature* **1994**, *370*, 621–628.
21. Vantourout, P.; Radojkovic, C.; Lichtenstein, L.; Pons, V.; Champagne, E.; Martinez, L.O. Ecto-F_1-ATPase: A moonlighting protein complex and an unexpected apoA-I receptor. *World J. Gastroenterol.* **2010**, *16*, 5925–5935.
22. Rai, A.K.; Spolaore, B.; Harris, D.A.; Dabbeni-Sala, F.; Lippe, G. Ectopic F_OF_1 ATP synthase contains both nuclear and mitochondrially-encoded subunits. *J. Bioenerg. Biomembr.* **2013**, *45*, 569–579.
23. Futai, M.; Nakanishi-Matsui, M.; Okamoto, H.; Sekiya, M.; Nakamoto, R.K. Rotational catalysis in proton pumping ATPases: From *E. coli* F-ATPase to mammalian V-ATPase. *Biochim. Biophys. Acta* **2012**; *1817*, 1711–1721.
24. Stock, D.; Gibbons, C.; Arechaga, I.; Leslie, A.G.; Walker, J.E. The rotary mechanism of ATP synthase. *Curr. Opin. Struct. Biol.* **2000**, *10*, 672–679.
25. Weber, J.; Senior, A.E. ATP synthesis driven by proton transport in F_1F_O-ATP synthase. *FEBS Lett.* **2003**, *545*, 61–70.
26. Martin, J.L.; Ishmukhametov, R.; Hornung, T.; Ahmad, Z.; Frasch, W.D. Anatomy of F1-ATPase powered rotation. *Proc. Natl. Acad. Sci. USA* **2014**, *111*, 3715–3720.
27. Sielaff, H.; Börsch, M. Twisting and subunit rotation in single $F(_O)(F_1)$-ATP synthase. *Philos. Trans. R. Soc. Lond. Ser. B, Biol. Sci.* **2013**, *368*, 20120024.

28. Nathanson, L.; Gromet-Elhanan, Z. Mutations in the beta-subunit Thr(159) and Glu(184) of the Rhodospirillum rubrum $F_{(O)}F_{(1)}$ ATP synthase reveal differences in ligands for the coupled Mg(2+)- and decoupled Ca(2+)-dependent F(0)F(1) activities. *J. Biol. Chem.* **2000**, *275*, 901–905.
29. Papageorgiou, S.; Melandri, A.B.; Solaini, G. Relevance of divalent cations to ATP-driven proton pumping in beef heart mitochondrial F_OF_1-ATPase. *J. Bioenerg. Biomembr.* **1998**, *30*, 533–541.
30. Junge, W.; Sielaff, H.; Engelbrecht, S. Torque generation and elastic power transmission in the rotary $F_{(O)}F_{(1)}$-ATPase. *Nature* **2009**, *459*, 364–370.
31. Bason, J.V.; Runswick, M.J.; Fearnley, I.M.; Walker, J.E. Binding of the inhibitor protein $IF_{(1)}$ to bovine F(1)-ATPase. *J. Mol. Biol.* **2011**, *406*, 443–453.
32. Campanella, M.; Parker, N.; Tan, C.; Hall, A.; Duchen, M. $IF_{(1)}$: Setting the pace of the $F_{(1)}F_{(O)}$-ATP synthase. *Trends Biochem. Sci.* **2009**, *34*, 343–350.
33. Formentini, L.; Pereira, M.P.; Sánchez-Cenizo, L.; Santacatterina, F.; Lucas, J.J.; Navarro, C.; Martínez-Serrano, A.; Cuezva, J.M. *In vivo* inhibition of the mitochondrial H^+-ATP synthase in neurons promotes metabolic preconditioning. *EMBO J.* **2014**, *33*, 762–778.
34. Di Pancrazio, F.; Mavelli, I.; Isola, M.; Losano, G.; Pagliaro, P.; Harris, D.A.; Lippe, G. *In vitro* and *in vivo* studies of $F_{(O)}F_{(1)}$ATP synthase regulation by inhibitor protein $IF_{(1)}$ in goat heart. *Biochim. Biophys. Acta* **2004**, *1659*, 52–62.
35. Nakamura, J.; Fujikawa, M.; Yoshida, M. IF1, a natural inhibitor of mitochondrial ATP synthase, is not essential for the normal growth and breeding of mice. *Biosci. Rep.* **2013**, *33*, e00067.
36. Collinson, I.R.; Fearnley, I.M.; Skehel, J.M.; Runswick, M.J.; Walker, J.E. ATP synthase from bovine heart mitochondria: Identification by proteolysis of sites in F_O exposed by removal of F_1 and the oligomycin-sensitivity conferral protein. *Biochem. J.***1994**, *303*, 639–645.
37. Watt, I.N.; Montgomery, M.G.; Runswick, M.J.; Leslie, A.G.W.; Walker, J.E. Bioenergetic cost of making an adenosine triphosphate molecule in animal mitochondria. *Proc. Natl. Acad. Sci. USA* **2010**, *107*, 16823–16827.
38. Baker, L.A.; Watt, I.N.; Runswick, M.J.; Walker, J.E.; Rubinstein, J.L. Arrangement of subunits in intact mammalian mitochondrial ATP synthase determined by cryo-EM. *Proc. Natl. Acad. Sci. USA* **2012**, *109*, 11675–11680.
39. Devenish, R.J.; Prescott, M.; Boyle, G.M.; Nagley, P. The oligomycin axis of mitochondrial ATP synthase: OSCP and the proton channel. *J. Bioenerg. Biomembr.* **2000**, *32*, 507–515.
40. Chen, R.; Runswick, M.J.; Carroll, J.; Fearnley, I.M.; Walker, J.E. Association of two proteolipids of unknown function with ATP synthase from bovine heart mitochondria. *FEBS Lett.* **2007**, *581*, 3145–3148.
41. Meyer, B.; Wittig, I.; Trifilieff, E.; Karas, M.; Schägger, H. Identification of two proteins associated with mammalian ATP synthase. *Mol. Cell. Proteomics* **2007**, *6*, 1690–1699.
42. Ohsakaya, S.; Fujikawa, M.; Hisabori, T.; Yoshida, M. Knockdown of DAPIT (diabetes-associated protein in insulin-sensitive tissue) results in loss of ATP synthase in mitochondria. *J. Biol. Chem.* **2011**, *286*, 20292–20296.
43. Carroll, J.; Fearnley, I.M.; Wang, Q.; Walker, J.E. Measurement of the molecular masses of hydrophilic and hydrophobic subunits of ATP synthase and complex I in a single experiment. *Anal. Biochem.* **2009**, *395*, 249–255.

44. Habersetzer, J.; Larrieu, I.; Priault, M.; Salin, B.; Rossignol, R.; Brèthes, D.; Paumard, P. Human F_1F_O ATP synthase, mitochondrial ultrastructure and OXPHOS impairment: A (super-) complex Matter? *PLoS One* **2013**, *8*, e75429.
45. Habersetzer, J.; Ziani, W.; Larrieu, I.; Stines-Chaumeil, C.; Giraud, M.-F.; Brèthes, D.; Dautant, A.; Paumard, P. ATP synthase oligomerization: From the enzyme models to the mitochondrial morphology. *Int. J. Biochem. Cell Biol.* **2013**, *45*, 99–105.
46. Paumard, P.; Vaillier, J.; Coulary, B.; Schaeffer, J.; Soubannier, V.; Mueller, D.M.; Brèthes, D.; di Rago, J.-P.; Velours, J. The ATP synthase is involved in generating mitochondrial cristae morphology. *EMBO J.* **2002**, *21*, 221–230.
47. Davies, K.M.; Anselmi, C.; Wittig, I.; Faraldo-Gomez, J.D.; Kuhlbrandt, W. Structure of the yeast F_1F_O-ATP synthase dimer and its role in shaping the mitochondrial cristae. *Proc. Natl. Acad. Sci. USA* **2012**, *109*, 13602–13607.
48. Thomas, D.; Bron, P.; Weimann, T.; Dautant, A.; Giraud, M.-F.; Paumard, P.; Salin, B.; Cavalier, A.; Velours, J.; Brèthes, D. Supramolecular organization of the yeast F_1F_O-ATP synthase. *Biol. Cell* **2008**, *100*, 591–601.
49. Bisetto, E.; di Pancrazio, F.; Simula, M.P.; Mavelli, I.; Lippe, G. Mammalian ATPsynthase monomer *versus* dimer profiled by blue native PAGE and activity stain. *Electrophoresis* **2007**, *28*, 3178–3185.
50. Daum, B.; Walter, A.; Horst, A.; Osiewacz, H.D.; Kühlbrandt, W. Age-dependent dissociation of ATP synthase dimers and loss of inner-membrane cristae in mitochondria. *Proc. Natl. Acad. Sci. USA* **2013**, *110*, 15301–15306.
51. Wittig, I.; Velours, J.; Stuart, R.; Schägger, H. Characterization of domain interfaces in monomeric and dimeric ATP synthase. *Mol. Cell. Proteomics* **2008**, *7*, 995–1004.
52. Spannagel, C.; Vaillier, J.; Arselin, G.; Graves, P.V; Grandier-Vazeille, X.; Velours, J. Evidence of a subunit 4 (subunit b) dimer in favor of the proximity of ATP synthase complexes in yeast inner mitochondrial membrane. *Biochim. Biophys. Acta* **1998**, *1414*, 260–264.
53. Everard-gigot, V.; Dunn, C.D.; Dolan, B.M.; Brunner, S.; Jensen, R.E.; Stuart, R.A. Functional Analysis of Subunit e of the F_1F_O-ATP Synthase of the Yeast *Saccharomyces cerevisiae*: Importance of the *N*-Terminal Membrane Anchor Region. *Eucaryot Cell* **2005**, *4*, 346–55.
54. Bustos, D.M.; Velours, J. The modification of the conserved GXXXG motif of the membrane-spanning segment of subunit g destabilizes the supramolecular species of yeast ATP synthase. *J. Biol. Chem.* **2005**, *280*, 29004–29010.
55. Fronzes, R.; Weimann, T.; Vaillier, J.; Velours, J.; Brèthes, D. The peripheral stalk participates in the yeast ATP synthase dimerization independently of e and g subunits. *Biochemistry* **2006**, *45*, 6715–6723.
56. Wittig, I.; Meyer, B.; Heide, H.; Steger, M.; Bleier, L.; Wumaier, Z.; Karas, M.; Schägger, H. Assembly and oligomerization of human ATP synthase lacking mitochondrial subunits a and A6L. *Biochim. Biophys. Acta* **2010**, *1797*, 1004–1011.
57. Bisetto, E.; Picotti, P.; Giorgio, V.; Alverdi, V.; Mavelli, I.; Lippe, G. Functional and stoichiometric analysis of subunit e in bovine heart mitochondrial $F(_O)F(_1)$ATP synthase. *J. Bioenerg. Biomembr.* **2008**, *40*, 257–267.

58. Couoh-Cardel, S.J.; Uribe-Carvajal, S.; Wilkens, S.; García-Trejo, J.J. Structure of dimeric F_1F_O-ATP synthase. *J. Biol. Chem.* **2010**, *285*, 36447–36455.
59. Minauro-Sanmiguel, F.; Wilkens, S.; García, J.J. Structure of dimeric mitochondrial ATP synthase: Novel F_O bridging features and the structural basis of mitochondrial cristae biogenesis. *Proc. Natl. Acad. Sci. USA* **2005**, *102*, 12356–12358.
60. Dudkina, N.V.; Sunderhaus, S.; Braun, H.-P.; Boekema, E.J. Characterization of dimeric ATP synthase and cristae membrane ultrastructure from *Saccharomyces* and *Polytomella* mitochondria. *FEBS Lett.* **2006**, *580*, 3427–3432.
61. Dienhart, M.; Pfeiffer, K.; Schagger, H.; Stuart, R.A. Formation of the yeast F_1F_O-ATP synthase dimeric complex does not require the ATPase inhibitor protein, Inh1. *J. Biol. Chem.* **2002**, *277*, 39289–39295.
62. Tomasetig, L.; di Pancrazio, F.; Harris, D.A.; Mavelli, I.; Lippe, G. Dimerization of F_OF_1ATP synthase from bovine heart is independent from the binding of the inhibitor protein IF_1. *Biochim. Biophys. Acta* **2002**, *1556*, 133–141.
63. Campanella, M.; Seraphim, A.; Abeti, R.; Casswell, E.; Echave, P.; Duchen, M.R. IF1, the endogenous regulator of the $F(_1)F(_O)$-ATPsynthase, defines mitochondrial volume fraction in HeLa cells by regulating autophagy. *Biochim. Biophys. Acta* **2009**, *1787*, 393–401.
64. Bisetto, E.; Comelli, M.; Salzano, A.M.; Picotti, P.; Scaloni, A.; Lippe, G.; Mavelli, I. Proteomic analysis of F_1F_O-ATP synthase super-assembly in mitochondria of cardiomyoblasts undergoing differentiation to the cardiac lineage. *Biochim. Biophys. Acta* **2013**, *1827*, 807–816.
65. Zanotti, F.; Raho, G.; Gaballo, A.; Papa, S. Inhibitory and anchoring domains in the ATPase inhibitor protein IF_1 of bovine heart mitochondrial ATP synthase. *J. Bioenerg. Biomembr.* **2004**, *36*, 447–457.
66. Lee, J.K.; Belogrudov, G.I.; Stroud, R.M. Crystal structure of bovine mitochondrial factor B at 0.96-A resolution. *Proc. Natl. Acad. Sci. USA* **2008**, *105*, 13379–13384.
67. Slater, E.C. An evaluation of the Mitchell hypothesis of chemiosmotic coupling in oxidative and photosynthetic phosphorylation. *Eur. J. Biochem. FEBS* **1967**, *1*, 317–326.
68. Tzagoloff, A. Assembly of the Mitochondrial Membrane System. *J. Biol. Chem.* **1970**, *245*, 1545–1551.
69. Dupuis, A.; Issartel, J.P.; Lunardi, J.; Satre, M.; Vignais, P.V. Interactions between the oligomycin sensitivity conferring protein (OSCP) and beef heart mitochondrial F_1-ATPase. 1. Study of the binding parameters with a chemically radiolabeled OSCP. *Biochemistry* **1985**, *24*, 728–733.
70. Mukhopadhyay, A.; Zhou, X.Q.; Uh, M.; Mueller, D.M. Heterologous expression, purification, and biochemistry of the oligomycin sensitivity conferring protein (OSCP) from yeast. *J. Biol. Chem.* **1992**, *267*, 25690–25696.
71. Joshi, S.; Cao, G.J.; Nath, C.; Shah, J. Oligomycin sensitivity conferring protein (OSCP) of bovine heart mitochondrial ATP synthase: High-affinity OSCP-F_O interactions require a local α-helix at the *C*-terminal end of the subunit. *Biochemistry* **1997**, *36*, 10936–10943.
72. Golden, T.R.; Pedersen, P.L. The oligomycin sensitivity conferring protein of rat liver mitochondrial ATP synthase: Arginine 94 is important for the binding of OSCP to F_1. *Biochemistry* **1998**, *37*, 13871–13881.

73. Prescott, M.; Bush, N.C.; Nagley, P.; Devenish, R.J. Properties of yeast cells depleted of the OSCP subunit of mitochondrial ATP synthase by regulated expression of the ATP5 gene. *Biochem. Mol. Biol. Int.* **1994**, *34*, 789–799.
74. Devenish, R.; Prescott, M.; Roucou, X.; Nagley, P. Insights into ATP synthase assembly and function through the molecular genetic manipulation of subunits of the yeast mitochondrial enzyme complex. *Biochim. Biophys. Acta* **2000**, *1458*, 428–442.
75. Boyle, G.M.; Roucou, X.; Nagley, P.; Devenish, R.J.; Prescott, M. Modulation at a distance of proton conductance through the *Saccharomyces cerevisiae* mitochondrial F_1F_O-ATP synthase by variants of the oligomycin sensitivity-conferring protein containing substitutions near the *C*-terminus. *J. Bioenerg. Biomembr.* **2000**, *32*, 595–607.
76. Moreno, A.J.M.; Moreira, P.I.; Custódio, J.B.A.; Santos, M.S. Mechanism of inhibition of mitochondrial ATP synthase by 17β-estradiol. *J. Bioenerg. Biomembr.* **2013**, *45*, 261–270.
77. Gavin, P.D.; Devenish, R.J.; Prescott, M. FRET reveals changes in the F_1–stator stalk interaction during activity of F_1F_0-ATP synthase. *Biochim. Biophys. Acta* **2003**, *1607*, 167–179.
78. Johnson, K.M.; Chen, X.; Boitano, A.; Swenson, L.; Opipari, A.W.; Glick, G.D. Identification and validation of the mitochondrial F_1F_O-ATPase as the molecular target of the immunomodulatory benzodiazepine Bz-423. *Chem. Biol.* **2005**, *12*, 485–496.
79. Rak, M.; Gokova, S.; Tzagoloff, A. Modular assembly of yeast mitochondrial ATP synthase. *EMBO J.* **2011**, *30*, 920–930.
80. Rees, D.M.; Leslie, A.G.W.; Walker, J.E. The structure of the membrane extrinsic region of bovine ATP synthase. *Proc. Natl. Acad. Sci. USA* **2009**, *106*, 21597–21601.
81. Carbajo, R.J.; Kellas, F.A; Yang, J.C.; Runswick, M.J.; Montgomery, M.G.; Walker, J.E.; Neuhaus, D. How the *N*-terminal domain of the OSCP subunit of bovine F_1F_O-ATP synthase interacts with the *N*-terminal region of an α subunit. *J. Mol. Biol.* **2007**, *368*, 310–318.
82. Stelzer, A.C.; Frazee, R.W.; van Huis, C.; Cleary, J.; Opipari, A.W.; Glick, G.D.; Al-Hashimi, H.M. NMR studies of an immunomodulatory benzodiazepine binding to its molecular target on the mitochondrial $F(_1)F(_O)$-ATPase. *Biopolymers* **2010**, *93*, 85–92.
83. Wilkens, S.; Borchardt, D.; Weber, J.; Senior, A.E. Structural characterization of the interaction of the delta and alpha subunits of the Escherichia coli F_1F_O-ATP synthase by NMR spectroscopy. *Biochemistry* **2005**, *44*, 11786–11794.
84. Zhang, F.X.; Pan, W.; Hutchins, J. Phosphorylation of F_1F_O ATPase delta-subunit is regulated by platelet-derived growth factor in mouse cortical neurons *in vitro*. *J. Neurochem.* **1995**, *65*, 2812–2815.
85. Ko, Y.H.; Pan, W.; Inoue, C.; Pedersen, P.L. Signal transduction to mitochondrial ATP synthase: Evidence that PDGF-dependent phosphorylation of the delta-subunit occurs in several cell lines, involves tyrosine, and is modulated by lysophosphatidic acid. *Mitochondrion* **2002**, *1*, 339–348.
86. Højlund, K.; Wrzesinski, K.; Larsen, P.M.; Fey, S.J.; Roepstorff, P.; Handberg, A.; Dela, F.; Vinten, J.; McCormack, J.G.; Reynet, C.; *et al.* Proteome analysis reveals phosphorylation of ATP synthase β-subunit in human skeletal muscle and proteins with potential roles in type 2 diabetes. *J. Biol. Chem.* **2003**, *278*, 10436–10442.

87. Aponte, A.M.; Phillips, D.; Harris, R.A; Blinova, K.; French, S.; Johnson, D.T.; Balaban, R.S. 32P labeling of protein phosphorylation and metabolite association in the mitochondria matrix. *Methods Enzymol.* **2009**; *457*, 63–80.
88. Zhao, X.; León, I.R.; Bak, S.; Mogensen, M.; Wrzesinski, K.; Højlund, K.; Jensen, O.N. Phosphoproteome analysis of functional mitochondria isolated from resting human muscle reveals extensive phosphorylation of inner membrane protein complexes and enzymes. *Mol. Cell. Proteomics* **2011**, *10*, 1–14.
89. Covian, R.; Balaban, R.S. Cardiac mitochondrial matrix and respiratory complex protein phosphorylation. *Am. J. Physiol. Heart Circ. Physiol.* **2012**, *303*, 940–966.
90. Phillips, D.; Aponte, A.M.; Covian, R.; Balaban, R.S. Intrinsic protein kinase activity in mitochondrial oxidative phosphorylation complexes. *Biochemistry* **2011**, *50*, 2515–2529.
91. Kim, S.C.; Sprung, R.; Chen, Y.; Xu, Y.; Ball, H.; Pei, J.; Cheng, T.; Kho, Y.; Xiao, H.; Xiao, L.; *et al*. Substrate and functional diversity of lysine acetylation revealed by a proteomics survey. *Mol. Cell* **2006**, *23*, 607–618.
92. Margineantu, D.H.; Emerson, C.B.; Diaz, D.; Hockenbery, D.M. Hsp90 inhibition decreases mitochondrial protein turnover. *PLoS One* **2007**, *2*, e1066.
93. Chandra, N.C. Identification of a Glycoprotein from rat liver mitochondrial inner membrane and demonstration of its origin in the endoplasmic reticulum. *J. Biol. Chem.* **1998**, *273*, 19715–19721.
94. Levrat, C.; Louisot, P.; Morelis, R. Distribution of glycosyltransferase activities in different compartments of mitochondria. *Biochem. Int.* **1989**, *18*, 813–823.
95. Clark, P.M.; Dweck, J.F.; Mason, D.E.; Hart, C.R.; Buck, S.B.; Peters, E.C.; Agnew, B.J.; Hsieh-Wilson, L.C. Direct in-gel fluorescence detection and cellular imaging of *O*-GlcNAc-modified proteins. *J. Am. Chem. Soc.* **2008**, *130*, 11576–11577.
96. Hu, Y.; Suarez, J.; Fricovsky, E.; Wang, H.; Scott, B.T.; Trauger, S.A.; Han, W.; Hu, Y.; Oyeleye, M.O.; Dillmann, W.H. Increased enzymatic *O*-GlcNAcylation of mitochondrial proteins impairs mitochondrial function in cardiac myocytes exposed to high glucose. *J. Biol. Chem.* **2009**, *284*, 547–555.
97. Kung, L.A.; Tao, S.C.; Qian, J.; Smith, M.G.; Snyder, M.; Zhu, H. Global analysis of the glycoproteome in *Saccharomyces cerevisiae* reveals new roles for protein glycosylation in eukaryotes. *Mol. Syst. Biol.* **2009**, *5*, 308.
98. Teo, C.F.; Wollaston-Hayden, E.E.; Wells, L. Hexosamine flux, the *O*-GlcNAc modification, and the development of insulin resistance in adipocytes. *Mol. Cell. Endocrinol.* **2010**, *318*, 44–53.
99. Burnham-Marusich, A.R.; Snodgrass, C.J.; Johnson, A.M.; Kiyoshi, C.M.; Buzby, S.E.; Gruner, M.R.; Berninsone, P.M. Metabolic labeling of *Caenorhabditis elegans* primary embryonic cells with azido-sugars as a tool for glycoprotein discovery. *PLoS One* **2012**, *7*, e49020.
100. Steentoft, C.; Vakhrushev, S.Y.; Joshi, H.J.; Kong, Y.; Vester-Christensen, M.B.; Schjoldager, K.T.B.G.; Lavrsen, K.; Dabelsteen, S.; Pedersen, N.B.; Marcos-Silva, L.; *et al.* Precision mapping of the human *O*-GalNAc glycoproteome through SimpleCell technology. *EMBO J.* **2013**, *32*, 1478–1488.
101. Boja, E.S.; Phillips, D.; French, S.A.; Harris, R.A.; Robert, S. Quantitative mitochondrial phosphoproteomics using iTRAQ on an LTQ-Orbitrap with high energy collision dissociation. *J. Proteome Res.* **2009**, *8*, 4665–4675.

102. Wang, Q.; Zhang, Y.; Yang, C.; Xiong, H.; Lin, Y.; Yao, J.; Li, H.; Xie, L.; Zhao, W.; Yao, Y.; *et al.* Acetylation of metabolic enzymes coordinates carbon source utilization and metabolic flux. *Science* **2010**, *327*, 1004–1007.
103. Zhao, S.; Xu, W.; Jiang, W.; Yu, W.; Lin, Y.; Zhang, T.; Yao, J.; Zhou, L.; Zeng, Y.; Li, H.; *et al.* Regulation of cellular metabolism by protein lysine acetylation. *Science* **2010**, *327*, 1000–1004.
104. Jeon, H.B.; Choi, E.S.; Yoon, J.H.; Hwang, J.H.; Chang, J.W.; Lee, E.K.; Choi, H.W.; Park, Z.Y.; Yoo, Y.J. A proteomics approach to identify the ubiquitinated proteins in mouse heart. *Biochem. Biophys. Res. Commun.* **2007**, *357*, 731–736.
105. Nguyen, T.T.; Ogbi, M.; Yu, Q.; Fishman, J.B.; Thomas, W.; Harvey, B.J.; Fulton, D.; Johnson, J.A. Modulation of the protein kinase Cdelta interaction with the "d" subunit of F_1F_0-ATP synthase in neonatal cardiac myocytes: Development of cell-permeable, mitochondrially targeted inhibitor and facilitator peptides. *J. Biol. Chem.* **2010**, *285*, 22164–22173.
106. Boerries, M.; Most, P.; Gledhill, J.R.; Walker, J.E.; Katus, H.A.; Koch, W.J.; Aebi, U.; Schoenenberger, C.-A. Ca^{2+}-dependent interaction of S100A1 with F_1-ATPase leads to an increased ATP content in cardiomyocytes. *Mol. Cell. Biol.* **2007**, *27*, 4365–4373.
107. Alavian, K.N.; Li, H.; Collis, L.; Bonanni, L.; Zeng, L.; Sacchetti, S.; Lazrove, E.; Nabili, P.; Flaherty, B.; Graham, M.A.; *et al.* Bcl-xL regulates metabolic efficiency of neurons through interaction with the mitochondrial F_1F_O ATP synthase. *Nat. Cell Biol.* **2011**, *13*, 1224–1233.
108. Belogrudov, G.I. Factor B is essential for ATP synthesis by mitochondria. *Arch. Biochem. Biophys.* **2002**, *406*, 271–274.
109. Bergeaud, M.; Mathieu, L.; Guillaume, A.; Moll, U.M.; Mignotte, B.; Le Floch, N.; Vayssière, J.L.; Rincheval, V. Mitochondrial p53 mediates a transcription-independent regulation of cell respiration and interacts with the mitochondrial F_1F_O-ATP synthase. *Cell Cycle* **2013**, *12*, 2781–2793.
110. Finkel, T.; Deng, C.X.; Mostoslavsky, R. Recent progress in the biology and physiology of sirtuins. *Nature* **2009**, *460*, 587–591.
111. Lombard, D.B.; Alt, F.W.; Cheng, H.-L.; Bunkenborg, J.; Streeper, R.S.; Mostoslavsky, R.; Kim, J.; Yancopoulos, G.; Valenzuela, D.; Murphy, A.; *et al.* Mammalian Sir2 homolog SIRT3 regulates global mitochondrial lysine acetylation. *Mol. Cell. Biol.* **2007**, *27*, 8807–8814.
112. Reinhardt, H.C.; Schumacher, B. The p53 network: Cellular and systemic DNA damage responses in aging and cancer. *Trends Genet.* **2012**, *28*, 128–136.
113. Borel, J.F.; Feurer, C.; Magnée, C.; Stähelin, H. Effects of the new anti-lymphocytic peptide cyclosporin A in animals. *Immunology* **1977**, *32*, 1017–1025.
114. Wang, P.; Heitman, J. The cyclophilins. *Genome Biol.* **2005**, *6*, 226.
115. Dolinski, K.; Muir, S.; Cardenas, M.; Heitman, J. All cyclophilins and FK506 binding proteins are, individually and collectively, dispensable for viability in Saccharomyces cerevisiae. *Proc. Natl. Acad. Sci. USA* **1997**, *94*, 13093–13098.
116. Bernardi, P. Mitochondrial transport of cations: Channels, exchangers, and permeability transition. *Physiol. Rev.* **1999**, *79*, 1127–1155.

117. Scorrano, L.; Ashiya, M.; Buttle, K.; Weiler, S.; Oakes, S.A.; Mannella, C.A.; Korsmeyer, S.J. A distinct pathway remodels mitochondrial cristae and mobilizes cytochrome c during apoptosis. *Dev. Cell* **2002**, *2*, 55–67.
118. Barsukova, A.; Komarov, A.; Hajnóczky, G.; Bernardi, P.; Bourdette, D.; Forte, M. Activation of the mitochondrial permeability transition pore modulates Ca^{2+} responses to physiological stimuli in adult neurons. *Eur. J. Neurosci.* **2011**, *33*, 831–842.
119. Fournier, N.; Ducet, G.; Crevat, A. Action of cyclosporine on mitochondrial calcium fluxes. *J. Bioenerg. Biomembr.* **1987**, *19*, 297–303.
120. Basso, E.; Fante, L.; Fowlkes, J.; Petronilli, V.; Forte, M.A.; Bernardi, P. Properties of the permeability transition pore in mitochondria devoid of Cyclophilin D. *J. Biol. Chem.* **2005**, *280*, 18558–18561.
121. Baines, C.P.; Kaiser, R.A.; Purcell, N.H.; Blair, N.S.; Osinska, H.; Hambleton, M.A.; Brunskill, E.W.; Sayen, M.R.; Gottlieb, R.A.; Dorn, G.W.; *et al.* Loss of cyclophilin D reveals a critical role for mitochondrial permeability transition in cell death. *Nature* **2005**, *434*, 658–662.
122. Nakagawa, T.; Shimizu, S.; Watanabe, T.; Yamaguchi, O.; Otsu, K.; Yamagata, H.; Inohara, H.; Kubo, T.; Tsujimoto, Y. Cyclophilin D-dependent mitochondrial permeability transition regulates some necrotic but not apoptotic cell death. *Nature* **2005**, *434*, 652–658.
123. Schinzel, A.C.; Takeuchi, O.; Huang, Z.; Fisher, J.K.; Zhou, Z.; Rubens, J.; Hetz, C.; Danial, N.N.; Moskowitz, M.A.; Korsmeyer, S.J. Cyclophilin D is a component of mitochondrial permeability transition and mediates neuronal cell death after focal cerebral ischemia. *Proc. Natl. Acad. Sci. USA* **2005**, *102*, 12005–12010.
124. Kajitani, K.; Fujihashi, M.; Kobayashi, Y.; Shimizu, S.; Tsujimoto, Y.; Miki, K. Crystal structure of human cyclophilin D in complex with its inhibitor, cyclosporin A at 0.96-A resolution. *Proteins* **2008**, *70*, 1635–1639.
125. Basso, E.; Petronilli, V.; Forte, M.A.; Bernardi, P. Phosphate is essential for inhibition of the mitochondrial permeability transition pore by cyclosporin A and by cyclophilin D ablation. *J. Biol. Chem.* **2008**, *283*, 26307–26311.
126. Shulga, N.; Wilson-Smith, R.; Pastorino, J.G. Sirtuin-3 deacetylation of cyclophilin D induces dissociation of hexokinase II from the mitochondria. *J. Cell Sci.* **2010**, *123*, 894–902.
127. Kohr, M.J.; Aponte, A.M.; Sun, J.; Wang, G.; Murphy, E.; Gucek, M.; Steenbergen, C. Characterization of potential *S*-nitrosylation sites in the myocardium. *Am. J. Physiol. Heart Circ. Physiol.* **2011**, *300*, 1327–1335.
128. Kang, B.H.; Plescia, J.; Dohi, T.; Rosa, J.; Doxsey, S.J.; Altieri, D.C. Regulation of tumor cell mitochondrial homeostasis by an organelle-specific Hsp90 chaperone network. *Cell* **2007**, *131*, 257–270.
129. Eliseev, R.A; Malecki, J.; Lester, T.; Zhang, Y.; Humphrey, J.; Gunter, T.E. Cyclophilin D interacts with Bcl2 and exerts an anti-apoptotic effect. *J. Biol. Chem.* **2009**, *284*, 9692–9699.
130. Vaseva, A.V; Marchenko, N.D.; Ji, K.; Tsirka, S.E.; Holzmann, S.; Moll, U.M. P53 Opens the Mitochondrial Permeability Transition Pore to Trigger Necrosis. *Cell* **2012**, *149*, 1536–1548.
131. Zharova, T.V; Vinogradov, A.D. Energy-linked binding of Pi is required for continuous steady-state proton-translocating ATP hydrolysis catalyzed by F_OF_1 ATP synthase. *Biochemistry* **2006**, *45*, 14552–14558.

132. Nicolli, A.; Basso, E.; Petronilli, V.; Wenger, R.M.; Bernardi, P. Interactions of cyclophilin with the mitochondrial inner membrane and regulation of the permeability transition pore, and cyclosporin A-sensitive channel. *J. Biol. Chem.* **1996**, *271*, 2185–2192.
133. Giorgio, V.; Bisetto, E.; Soriano, M.E.; Dabbeni-Sala, F.; Basso, E.; Petronilli, V.; Forte, M.A.; Bernardi, P.; Lippe, G. Cyclophilin D modulates mitochondrial F0F1-ATP synthase by interacting with the lateral stalk of the complex. *J. Biol. Chem.* **2009**, *284*, 33982–33988.
134. Szabó, I.; Zoratti, M. The giant channel of the inner mitochondrial membrane is inhibited by cyclosporin A. *J. Biol. Chem.* **1991**, *266*, 3376–3379.
135. Bernardi, P.; Krauskopf, A.; Basso, E.; Petronilli, V.; Blachly-Dyson, E.; Blalchy-Dyson, E.; di Lisa, F.; Forte, M.A. The mitochondrial permeability transition from *in vitro* artifact to disease target. *FEBS J.* **2006**, *273*, 2077–2099.
136. Nicolli, A.; Petronilli, V.; Bernardi, P. Modulation of the mitochondrial cyclosporin A-sensitive permeability transition pore by matrix pH. Evidence that the pore open-closed probability is regulated by reversible histidine protonation. *Biochemistry* **1993**, *32*, 4461–4465.
137. Petronilli, V.; Sileikyte, J.; Zulian, A.; Dabbeni-Sala, F.; Jori, G.; Gobbo, S.; Tognon, G.; Nikolov, P.; Bernardi, P.; Ricchelli, F. Switch from inhibition to activation of the mitochondrial permeability transition during hematoporphyrin-mediated photooxidative stress. Unmasking pore-regulating external thiols. *Biochim. Biophys. Acta* **2009**, *1787*, 897–904.
138. Zhang, Y.; Marcillat, O.; Giulivi, C.; Ernster, L.; Davies, K.J. The oxidative inactivation of mitochondrial electron transport chain components and ATPase. *J. Biol. Chem.* **1990**, *265*, 16330–16336.
139. Lippe, G.; Comelli, M.; Mazzilis, D.; Sala, F.D.; Mavelli, I. The inactivation of mitochondrial F_1 ATPase by H_2O_2 is mediated by iron ions not tightly bound in the protein. *Biochem. Biophys. Res. Commun.* **1991**, *181*, 764–770.
140. Comelli, M.; Lippe, G.; Mavelli, I. Differentiation potentiates oxidant injury to mitochondria by hydrogen peroxide in Friend's erythroleukemia cells. *FEBS Lett.* **1994**, *352*, 71–75.
141. Poon, H.F.; Calabrese, V.; Calvani, M.; Butterfield, A. Proteomics analyses of specific protein oxidation and protein expression in aged rat brain and its modulation by L-acetylcarnitine: insights into the mechanisms of action of this proposed therapeutic agent for CNS disorders associated with oxidative stres. *Antioxid. Redox Signal.* **2006**, *8*, 381–394.
142. Sultana, R.; Poon, H.F.; Cai, J.; Pierce, W.M.; Merchant, M.; Klein, J.B.; Markesbery, W.R.; Butterfield, D.A. Identification of nitrated proteins in Alzheimer's disease brain using a redox proteomics approach. *Neurobiol. Dis.* **2006**, *22*, 76–87.
143. Poon, H.F.; Shepherd, H.M.; Reed, T.T.; Calabrese, V.; Stella, A.-M.G.; Pennisi, G.; Cai, J.; Pierce, W.M.; Klein, J.B.; Butterfield, D.A. Proteomics analysis provides insight into caloric restriction mediated oxidation and expression of brain proteins associated with age-related impaired cellular processes: Mitochondrial dysfunction, glutamate dysregulation and impaired protein synthesis. *Neurobiol. Aging* **2006**, *27*, 1020–1034.
144. Groebe, K.; Krause, F.; Kunstmann, B.; Unterluggauer, H.; Reifschneider, N.H.; Scheckhuber, C.Q.; Sastri, C.; Stegmann, W.; Wozny, W.; Schwall, G.P.; *et al.* Differential proteomic profiling of mitochondria from *Podospora anserina*, rat and human reveals distinct patterns of age-related oxidative changes. *Exp. Gerontol.* **2007**, *42*, 887–898.

145. Haynes, V.; Traaseth, N. Nitration of specific tyrosines in F_0F_1 ATP synthase and activity loss in aging. *Am. J. Physiol. Endocrinol. Metab.* **2010**, *95616*, 978–987.
146. Buchert, F.; Schober, Y.; Römpp, A.; Richter, M.L.; Forreiter, C. Reactive oxygen species affect ATP hydrolysis by targeting a highly conserved amino acid cluster in the thylakoid ATP synthase γ subunit. *Biochim. Biophys. Acta* **2012**, *1817*, 2038–2048.
147. Taylor, S.W.; Fahy, E.; Murray, J.; Capaldi, R.A; Ghosh, S.S. Oxidative post-translational modification of tryptophan residues in cardiac mitochondrial proteins. *J. Biol. Chem.* **2003**, *278*, 19587–19590.
148. Rexroth, S.; Poetsch, A.; Rögner, M.; Hamann, A.; Werner, A.; Osiewacz, H.D.; Schäfer, E.R.; Seelert, H.; Dencher, N.A. Reactive oxygen species target specific tryptophan site in the mitochondrial ATP synthase. *Biochim. Biophys. Acta* **2012**, *1817*, 381–387.
149. Fogolari, F.; Corazza, A.; Yarra, V.; Jalaru, A.; Viglino, P.; Esposito, G. Bluues: A program for the analysis of the electrostatic properties of proteins based on generalized Born radii. *BMC Bioinform.* **2012**, *13*, S18.

Dimers of mitochondrial ATP synthase form the permeability transition pore

Valentina Giorgio[a], Sophia von Stockum[a], Manuela Antoniel[b], Astrid Fabbro[b], Federico Fogolari[c], Michael Forte[d], Gary D. Glick[e], Valeria Petronilli[a], Mario Zoratti[a], Ildikó Szabó[f], Giovanna Lippe[b,1], and Paolo Bernardi[a,1]

[a]Consiglio Nazionale delle Ricerche Institute of Neuroscience and Department of Biomedical Sciences and [f]Department of Biology, University of Padova, 35121 Padua, Italy; Departments of [b]Food Science and [c]Medical and Biological Sciences, University of Udine, 33100 Udine, Italy; [d]Vollum Institute, Oregon Health and Sciences University, Portland, OR 97239; and [e]Department of Chemistry, Graduate Program in Immunology, University of Michigan, Ann Arbor, MI 48109

Edited* by Tullio Pozzan, Foundation for Advanced Biomedical Research, Padua, Italy, and approved March 4, 2013 (received for review October 12, 2012)

Here we define the molecular nature of the mitochondrial permeability transition pore (PTP), a key effector of cell death. The PTP is regulated by matrix cyclophilin D (CyPD), which also binds the lateral stalk of the F_OF_1 ATP synthase. We show that CyPD binds the oligomycin sensitivity-conferring protein subunit of the enzyme at the same site as the ATP synthase inhibitor benzodiazepine 423 (Bz-423), that Bz-423 sensitizes the PTP to Ca^{2+} like CyPD itself, and that decreasing oligomycin sensitivity-conferring protein expression by RNAi increases the sensitivity of the PTP to Ca^{2+}. Purified dimers of the ATP synthase, which did not contain voltage-dependent anion channel or adenine nucleotide translocator, were reconstituted into lipid bilayers. In the presence of Ca^{2+}, addition of Bz-423 triggered opening of a channel with currents that were typical of the mitochondrial megachannel, which is the PTP electrophysiological equivalent. Channel openings were inhibited by the ATP synthase inhibitor AMP-PNP (γ-imino ATP, a nonhydrolyzable ATP analog) and Mg^{2+}/ADP. These results indicate that the PTP forms from dimers of the ATP synthase.

The permeability transition (PT) defines an increased permeability of the inner mitochondrial membrane to ions and solutes triggered by matrix Ca^{2+} in the presence of specific inducers, the most classical being Pi and thiol oxidants (1). The sensitivity to Ca^{2+} is decreased by several compounds, including Mg^{2+}, adenine nucleotides, and cyclosporin A (CsA) (2). In vitro at least, the PT is accompanied by swelling of mitochondria, which has long been known to prevent ATP synthesis (3). The idea that swelling could be mediated by a Ca^{2+}-regulated pore was advanced in the 1970s (4, 5), and its basic regulatory features were defined in a series of seminal studies in 1979 (6–8). The PT is mediated by opening of a high-conductance channel, the PT pore (PTP), which was identified by patch-clamping of the inner membrane and called mitochondrial megachannel (MMC) (9–12). Opening of the PTP is causally involved in cell death associated with many diseases, including heart ischemia (13), and its role is particularly well-documented in muscular dystrophy caused by defects of collagen VI (14). The molecular nature of the channel(s) involved remains a mystery. The long-standing idea that the PTP forms at contact sites of the inner and outer membranes through voltage-dependent anion channel (VDAC) and the adenine nucleotide translocator (ANT) (15) proved incorrect, because VDAC- and ANT-null mitochondria still display a CsA-sensitive PT (16–18).

A well-characterized protein regulator of the PTP is cyclophilin D (CyPD), which in the mouse is encoded by the *Ppif* gene. CyPD sensitizes the PTP to Ca^{2+}, as deduced from experiments in mitochondria from *Ppif*$^{-/-}$ mice where the PT required higher loads of matrix Ca^{2+} (19–22), a behavior that is perfectly matched by the MMC (23). CyPD binds the F_OF_1 ATP synthase (complex V), the rotary enzyme that synthesizes the vast majority of ATP in respiring cells (24). This complex is formed by the catalytic F_1, the membrane-bound proton-translocating F_O, and a lateral stalk linking F_1 and F_O. CyPD binds the lateral stalk, which acts as a stator to counter the tendency of the $\alpha_3\beta_3$-subcomplex of the F_1-catalytic domain to rotate with the rotor containing the F_1 subunits-γ, -δ, and -ε and a ring of F_O subunits c (25). CyPD binding requires Pi and results in partial inhibition of ATP synthase activity, whereas CsA displaces CyPD, resulting in enzyme reactivation (24). Despite the striking analogy with PTP regulation, whether these interactions are relevant for the PT remains unknown. Here, we show that dimers of the F_OF_1 ATP synthase incorporated into lipid bilayers form Ca^{2+}-activated channels with the key features of the MMC-PTP (10–12).

Results

CyPD Binds Oligomycin Sensitivity-Conferring Protein Subunit of ATP Synthase. We identified potential binding site(s) of CyPD to the F_OF_1 ATP synthase in the b, d, and oligomycin sensitivity-conferring protein (OSCP) subunits of the lateral stalk (24). To more precisely define the specific partner(s) of CyPD within this complex, we devised conditions optimizing its binding to the ATP synthase, while separating the subunits of the peripheral stalk. The first condition was met by using 10 mM Pi and low ionic strength (24); the second condition was met by adding a low concentration of SDS to the Triton X-100–based extraction buffer and using a polyclonal antibody against a peptide mapping near the C terminus of OSCP, which disrupts the interaction of the OSCP C-terminal domain with the N-terminal portion of subunit b (25). This strategy allowed the immunoprecipitation of individual OSCP, b, and d subunits, because no other stalk protein was detected in the specific immunoblots (Fig. 1*A*). CyPD was found exclusively in the immunoprecipitation with OSCP antibody, suggesting that OSCP is the direct interactor of CyPD in the ATPase complex (Fig. 1*A*). We next used OSCP-specific siRNAs in HQB17 cells (26), where we studied the expression of selected ATP synthase subunits in total extracts of mitochondria. We found the expected decrease of OSCP, but not of F_1 α- and β- subunits or CyPD (Fig. 1*B*, *Left*). When the ATP synthase was immunoprecipitated from mitochondria with decreased levels of OSCP, decreased levels of CyPD were detected as well, which precisely matched the decreased association of OSCP to the enzyme complex (Fig. 1*B*, *Right*). It should be noted that cells with stably reduced OSCP levels do not display decreased levels of α-, β-, and d subunits or alterations of mitochondrial membrane potential or mitochondrial ultrastructure, indicating that assembly and function of ATP synthase are not compromised (27).

Author contributions: V.G., S.v.S., F.F., M.Z., I.S., G.L., and P.B. designed research; V.G., S.v.S., M.A., A.F., F.F., and I.S. performed research; M.F. and G.D.G. contributed new reagents/analytic tools; V.G., F.F., M.F., G.D.G., V.P., M.Z., I.S., G.L., and P.B. analyzed data; and G.L. and P.B. wrote the paper.

Conflict of interest statement: Bz-423 is licensed to a company in which G.D.G. has ownership interest and receives compensation.

*This Direct Submission article had a prearranged editor.

[1]To whom correspondence may be addressed. E-mail: giovanna.lippe@uniud.it or bernardi@bio.unipd.it.

This article contains supporting information online at www.pnas.org/lookup/suppl/doi:10.1073/pnas.1217823110/-/DCSupplemental.

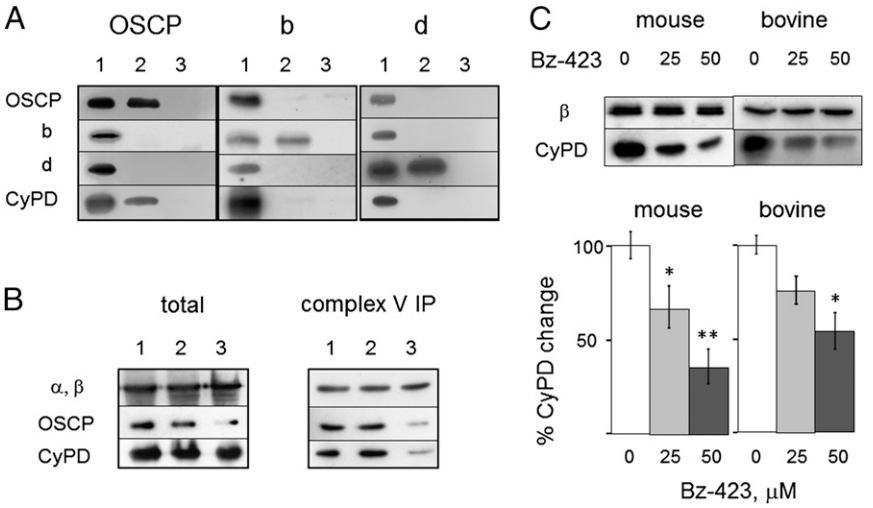

Fig. 1. CyPD interacts with OSCP and is displaced by Bz-423. (*A*) Extracts and immunoprecipitates of BHM with anti-OSCP or b or d subunit antibodies were immunoblotted as indicated. Lane 1, mitochondria; lane 2, immunoprecipitates with OSCP (*Left*), b (*Center*), and d (*Right*) antibodies; lanes 3, IgG antibody. (*B*) Total cell extracts (*Left*) and complex V immunoprecipitates (*Right*) of mitochondria from cells either untreated (lane 1) or treated with scrambled siRNA (lane 2) or OSCP siRNA (lane 3) probed for F_1 α,β-subunits, OSCP, and CyPD. (*C*) Heart mitochondria were treated with the indicated concentrations of Bz-423 (μM), immunoprecipitated with anticomplex V antibodies, and immunoblotted with antibodies against β-subunit or CyPD. Ratio between CyPD and β-band intensities is reported ($n = 3 \pm$ SE). $^*P \leq 0.02$; $^{**}P = 0.0015$, Student *t* test.

CyPD–OSCP interactions were mostly electrostatic in nature, because they could be disrupted by increased ionic strength (Fig. S1*A*). A study of surface potentials and isopotential curves of CyPD and OSCP in the ATP synthase complex (Fig. S1 *B* and *C*) identified putative binding regions of CyPD on OSCP at the residues indicated in Fig. S1*C*. This region overlaps with helices 3 and 4, the binding site of benzodiazepine 423 (Bz-423), a well-characterized inhibitor of the F_OF_1 ATP synthase that readily permeates mitochondria (27, 28). We, therefore, tested the effect of Bz-423 on the association of CyPD to mouse and bovine complex V at 10 mM Pi, and we found a concentration-dependent displacement that is consistent with competition for a common binding site (Fig. 1*C*). This set of experiments documents that OSCP is the partner of CyPD on the lateral stalk, that no CyPD binding occurs in the absence of OSCP, and that the binding site covers the same region where Bz-423 binds the OSCP subunit.

Bz-423 Induces the PTP. To test whether the interaction of Bz-423 with OSCP is also relevant for PTP modulation, we studied the Ca^{2+} retention capacity (CRC) of mitochondria allowing the definition of the threshold matrix Ca^{2+} load required to trigger pore opening. Bz-423 decreased the CRC of mitochondria at 1 mM Pi but not 5 mM Pi (Fig. 2*A*). In the presence of CsA (Fig. 2*B*), which displaces CyPD from OSCP (24), or in CyPD-null mitochondria (Fig. 2*C*), the PTP-sensitizing effect of Bz-423 was observed at 5 mM Pi as well. This behavior matched the inhibitory profile of Bz-423 on ATP hydrolysis, which required higher concentrations of Bz-423 only in CyPD-competent mitochondria at high Pi concentrations (Fig. S2). Inhibition of ATP synthase with resveratrol (29) and oligomycin was instead independent of CyPD (Fig. S3). These results highlight a striking analogy between the effects of Bz-423 on PTP and ATP synthase.

ATP Synthase Activity and OSCP Affect the PTP. Adenine nucleotides are inhibitors of the PT (6), but their mechanism of action is unknown. We explored the hypothesis that nucleotides affect the Ca^{2+} sensitivity of the PTP through the catalytic activity of the F_OF_1 ATP synthase. We incubated mitochondria either (*i*) with ADP and respiratory substrates in the presence of an ATP-hydrolyzing system based on hexokinase plus glucose (so that mitochondria were energized by the respiratory chain, the ADP concentration was constant, and rotation of the ATP synthase was clockwise when viewed from the membrane side) (30) or (*ii*) with ATP in the presence of an ATP-regenerating system based on phosphocreatine and creatine kinase in the absence of substrates (so that mitochondria were energized by ATP hydrolysis at constant levels of ATP, and rotation of the ATP synthase was in the opposite direction) (30). In either case, mitochondria developed a membrane potential as shown by accumulation of Rhodamine 123 (Fig. 3*A*), which responded appropriately to the addition of oligomycin [i.e., with hyperpolarization in ATP-synthesizing mitochondria (Fig. 3*A*, trace a) and depolarization in ATP-hydrolyzing mitochondria (Fig. 3*A*, trace b)] and the uncoupler carbonylcyanide-*p*-trifluoromethoxyphenyl hydrazone. PTP opening in ATP-hydrolyzing mitochondria (constant ATP levels) required two times the Ca^{2+} load of ATP-synthesizing mitochondria (constant ADP levels) (Fig. 3*B*). The mean ratio between ATP-hydrolyzing and -synthesizing mitochondria was 2.06 ± 0.27 in four independent experiments per condition, an effect that matches the effect of CsA in mouse liver mitochondria (20). This difference was not due to the nucleotides per se,

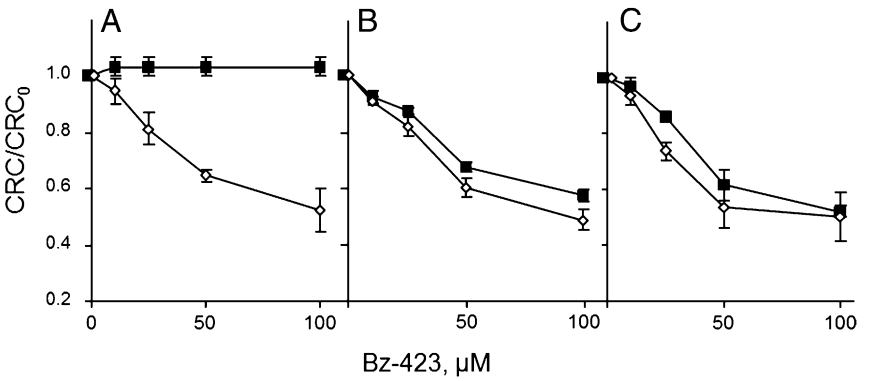

Fig. 2. Bz-423 decreases the mitochondrial Ca^{2+} retention capacity. Isolated WT (*A* and *B*) or *Ppif*$^{-/-}$ mouse liver mitochondria (*C*) were incubated in the presence of 1 (open symbols) or 5 mM (closed symbols) Pi·Tris and Bz-423 as indicated. In *B* only, 1.6 μM CsA was added. Extramitochondrial Ca^{2+} was monitored, and CRC was determined by stepwise addition of 10 μM Ca^{2+} pulses. The measured CRC (i.e., the amount of Ca^{2+} accumulated before onset of Ca^{2+}-induced Ca^{2+} release) was normalized to that obtained in absence of Bz-423 (CRC_0), and data are average of triplicate experiments ± SE. Absolute CRC values (nmol Ca^{2+}/mg protein) at 1 mM Pi were 120 ± 0, 160 ± 20, and 166.7 ± 30.6 for *A*, *B*, and *C*, respectively; absolute CRC values (nmol Ca^{2+}/mg protein) at 5 mM Pi were 86.7 ± 11.5, 126.7 ± 30.6, and 160 ± 20 for *A*, *B*, and *C*, respectively ($n = 3 \pm$ SD).

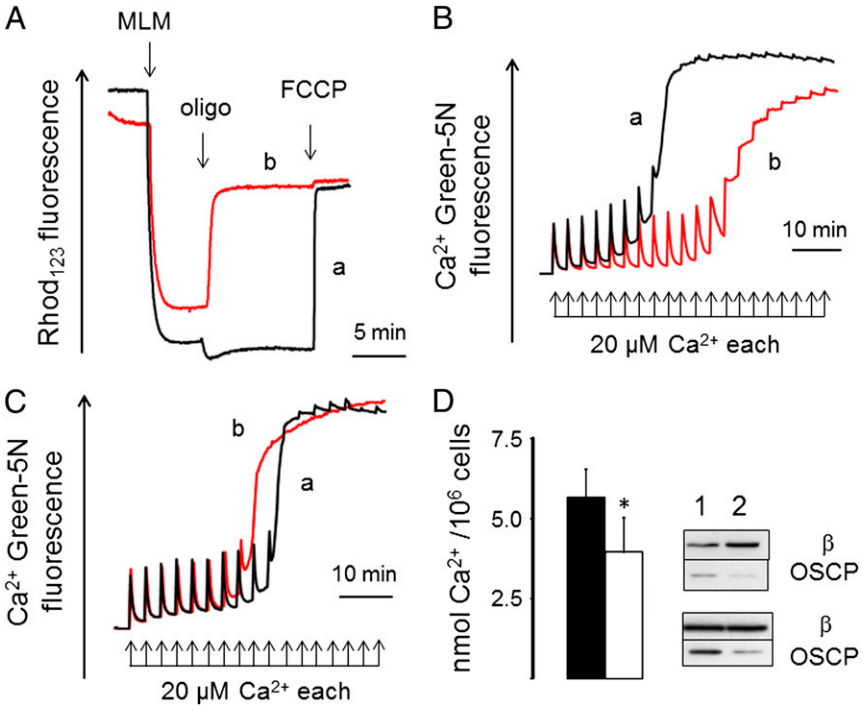

Fig. 3. ATP synthase catalysis and OSCP knockdown affect the Ca^{2+} sensitivity of the PT. (*A*) Membrane potential was measured in mitochondria incubated with respiratory substrate and ADP plus an ATP-consuming system (trace a) or no substrate, ATP, and an ATP-regenerating system (trace b) as detailed in *Materials and Methods*. Where indicated, 2 mg mouse liver mitochondria (MLM), 1 μg/mL oligomycin (oligo), and 1 μM carbonylcyanide-*p*-trifluoromethoxyphenyl hydrazone (FCCP). (*B*) Conditions for traces a and b were exactly as in *A*, but Ca^{2+} was measured. (*C*) The incubation medium contained respiratory substrate and 1 μg/mL oligomycin, and it was supplemented with 0.4 mM ADP (trace a) or 0.4 mM ATP (trace b); one experiment representative of three is shown. (*D*) Scrambled siRNA- or OSCP siRNA-treated cells (closed and open bars, respectively) were permeabilized with digitonin, and their CRC was measured in the presence of an ATP-regenerating system. Data are average ± SD of nine independent determinations per condition. $*P = 0.0025$ (Student *t* test). The blots display the levels of OSCP and F_1 β-subunits in the two batches of cells used (lanes 1, scrambled siRNA; lanes 2, OSCP siRNA).

because in the presence of oligomycin ADP was actually slightly more effective than ATP (Fig. 3*C*, traces a and b, respectively). We could exclude any contribution from endoplasmic reticulum contaminants, because no Ca^{2+} uptake was seen in the presence of ATP plus oligomycin (Fig. S4). These results indicate that the catalytic activity of ATP synthase (synthesis vs. hydrolysis) affects the Ca^{2+} sensitivity of the PTP.

We also tested the effect of OSCP knockdown on the sensitivity of the PTP to Ca^{2+} in permeabilized HQB17 cells using ATP hydrolysis to generate the proton gradient. Lowered OSCP expression decreased the threshold Ca^{2+} required for opening (Fig. 3*D*). It should be noted that OSCP-depleted mitochondria did take up a sizeable amount of Ca^{2+} before onset of the PT (Fig. 3*D*), consistent with a conserved catalytic activity of ATP synthase and the buildup of the proton gradient (27). Thus, lack of the stalk subunit OSCP increases the Ca^{2+} sensitivity of the PTP, suggesting that the F_OF_1 ATP synthase is involved in its formation. This hypothesis was tested in ATP synthase preparations.

Purified ATP Synthase Dimers Have PTP Channel Activity. We separated mitochondrial proteins by blue native electrophoresis (BNE) (31) and identified the ATP synthase by in-gel activity (Fig. 4*A*). SDS/PAGE of dimers and monomers eluted from BNE gels (Fig. 4*B*) displayed the same subunit pattern previously shown in high-resolution gels (32). Western blotting detected the occasional presence of some respiratory complexes I and III in the dimers (the I + III supercomplex runs very close to complex V dimers in BNE) but not VDAC, CyPD, or ANT (Fig. 4*C*), which in BNE with digitonin migrates with the electrophoretic front as an individual protein (31).

The gel-purified ATP synthase dimers or monomers were incorporated in planar lipid bilayers. Addition of Bz-423 to the dimer in the presence of Ca^{2+} elicited channel activity, whereas no such activity was observed when the drug was added to the monomer (Fig. 5*A*). Addition of phenylarsine oxide (PhAsO), one of the most powerful sensitizers of the PTP to Ca^{2+} (1), was not sufficient to induce channel opening, but the subsequent addition of Bz-423 induced activity with similar characteristics to Bz-423 alone (Fig. 5*B* and Fig. S5). Moreover, γ-imino ATP (AMP-PNP), a nonhydrolyzable ATP analog (33), inhibited current conduction even in the presence of PhAsO (Fig. 5*B*). The characteristics of the pore closely matched the features of MMC-PTP (10–12): the maximal chord conductance was 1.0–1.3 nS in 150 mM KCl, and various subconductance states were commonly entered (Fig. 5 *C* and *D*). Transitions of about 1.0 and 0.5 nS, typical of MMC-PTP activity, are shown in Fig. S6*A*. Again in keeping with the properties of MMC, the activity could be largely inhibited by Mg^{2+} and nearly completely inhibited by Mg^{2+} plus ADP (Fig. 5*C*); however, it could not be inhibited by CsA, like the MMC of *Ppif*$^{-/-}$ mitochondria (23), coherently with the lack of CyPD in the preparation (Fig. 4*C*). Other inducers beside Pi and Ca^{2+} were not strictly necessary to induce PTP currents, as shown in Fig. S6*B*, where Ca^{2+} was added at 3 mM and the ATP synthase dimer was extracted in the presence of 10 mM Pi, which sensitizes the PTP even in the absence of CyPD (1).

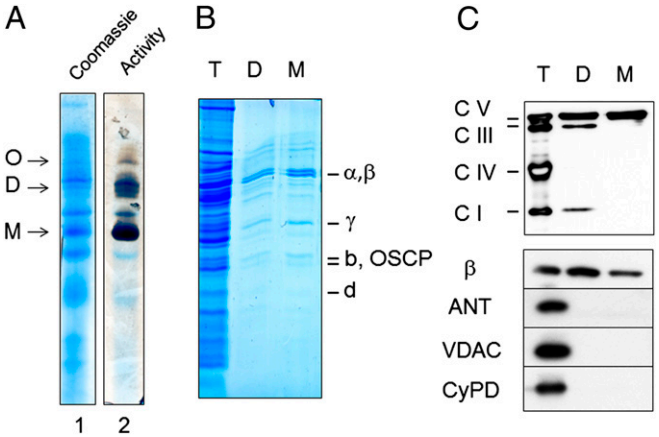

Fig. 4. Purification of F_OF_1 ATP synthase. (*A*) BHM were subjected to BNE to separate oligomers (O), dimers (D), and monomers (M) of ATP synthase, which were identified by Coomassie blue (lane 1) and in-gel activity staining (lane 2). Dimers and monomers were excised, eluted, subjected to SDS/PAGE, and stained with colloidal Coomassie (*B*), or they were transferred to nitrocellulose and tested for respiratory complexes and ATP synthase, subunit-β of F_1, ANT, VDAC, and CyPD (*C*). T, D, and M refer to total extract, dimer, and monomer, respectively. One experiment representative of three is shown.

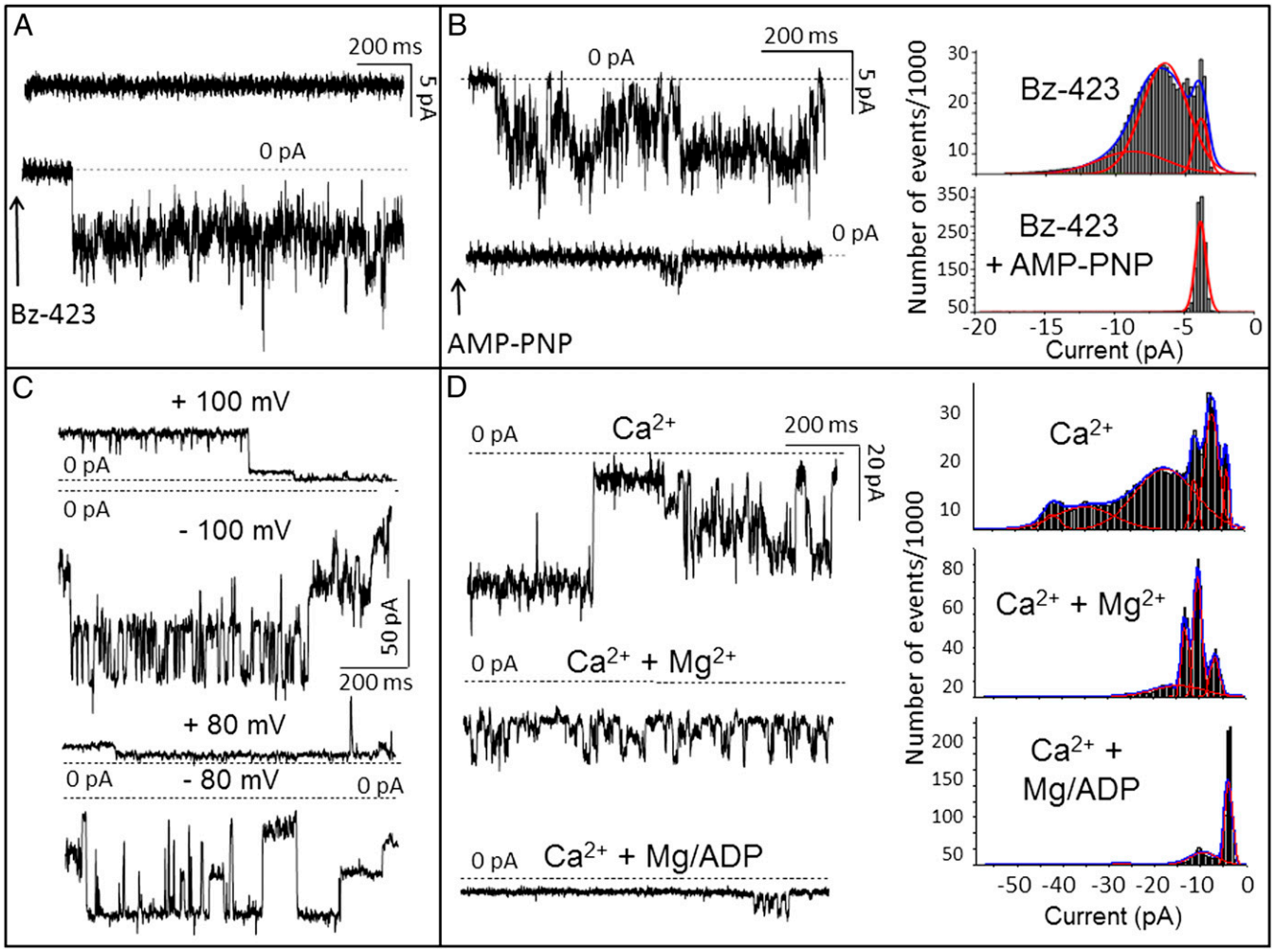

Fig. 5. Dimers of F_OF_1 ATP synthase generate currents matching MMC-PTP. (*A*) A bilayer experiment in 50 mM KCl, 1 mM Pi, and 0.3 mM Ca^{2+} (Ca^{2+} only *in trans*; $V_{cis} = -60$ mV). After addition of dimeric ATP synthase, no activity could be observed (*Upper*) until immediately after the addition of 0.1 mM Bz-423 to the *trans* side (*Lower*; arrow). When monomers were used, the recording was identical to *Upper*, which was not modified by the addition of Bz-423. (*B*) A similar experiment in the presence of 0.1 mM PhAsO *in trans*. Activity (*Upper*) was elicited by the addition of Bz-423 as in *A* and inhibited by 0.1 mM AMP-PNP in *trans* (*Lower*; arrow). Corresponding current amplitude histograms from gap-free 60-s traces are shown in *Right*. (*C*) Current traces (150 mM KCl; V_{cis} as indicated) with dimeric ATP synthase and 0.3 mM Ca^{2+}, 0.1 mM Bz-423, and 50 μM PhAsO added to the *trans* side. Note numerous substates. (*D*, *Left*) Activity ($V_{cis} = -80$ mV) recorded as in *C* (first trace) and after sequential additions of Mg^{2+} (0.6 mM) and ADP (0.6 mM) to the *trans* side; (*D*, *Right*) corresponding amplitude histograms from gap-free 100-s traces. Representative experiments are shown of a total of 28 experiments performed under various conditions using six different ATP synthase dimer preparations.

Channel openings were still observed in the presence of bongkrekic acid and could not be elicited by atractyloside, selective inhibitors of ANT. Rather, in some cases, atractyloside induced a small conductance (Fig. S7). Of note, channels were not observed with gel-purified complex I, indicating that this occasional contaminant also cannot be responsible for the current that we observe in the purified dimers of F_OF_1 ATP synthase (Fig. S7). The ATP synthase preparations still possessed enzymatic activity after extraction from the gels for incorporation in the bilayers, which was shown by a second BNE and activity staining (Fig. S8).

Discussion

We have shown that CyPD interacts with the ATP synthase at OSCP subunit. This observation, which builds on our previous work on regulation of the ATP synthase by CyPD (24), led to identification of the elusive PTP as a dimer of the F_OF_1 ATP synthase. The electrophysiological features displayed by our ATP synthase preparation are very different from the currents of the ANT, which has been proposed to take part in PTP formation (15) and is still included in models of the PTP in association with the Pi carrier (34). The ANT exhibits a conductance ranging between 50 and 700 pS in 100 mM KCl (35), which is lower than the currents displayed by the MMC (9–12); it shows low probability of current fluctuation at voltages lower than 150 mV at variance from the reconstituted ATP synthase dimers (Fig. 5), and it can be inhibited only by ADP and bongkrekic acid together, whereas ADP alone had a marginal effect (35–37). Patch-clamp experiments with the reconstituted, functionally active mitochondrial Pi carrier revealed an anion channel function with a mean conductance as low as 40 ± 10 pS, which was decreased to 25 ± 5 pS by Ca^{2+} and Mg^{2+}, inhibited by Pi, and unaffected by ADP (38). These features make the Pi carrier a very unlikely candidate as a PTP component, and they rule out that the currents observed here may be related to this protein.

Bz-423 was discovered and characterized as an apoptosis-inducing agent acting through mitochondria (39); identification of OSCP as its target was achieved through the screening of a human cDNA T7 phage display library (27) and the interaction with ATP synthase resulting in inhibition of enzyme activity confirmed by NMR (28). The striking selectivity of action of Bz-423

on OSCP and its ability to trigger channel activity of ATP synthase dimers, together with the lack of activity of monomer preparations, argues against the possibility that the currents that we observe are caused by unidentified contaminating proteins. This conclusion is strengthened by the inhibitory effect of AMP-PNP and Mg^{2+}/ADP on channel activity.

The PTP-inducing effect of Bz-423 and CyPD (which both act through OSCP on top of the lateral stalk in the matrix) is necessarily indirect, because it impinges on the permeability properties of the inner membrane. Because a current is only seen with the dimers, it is logical to conclude that the PTP forms at the membrane interface between two adjacent F_O sectors, which would be in keeping with the well-characterized effects of fatty acids and lysophospholipids on the PTP (1). The essential role of matrix Ca^{2+} in PTP formation is intriguing. Ca^{2+} is able to sustain ATP hydrolysis by complex V with a similar K_m as Mg^{2+} and to compete with Mg^{2+} for the catalytic sites (40). Interestingly and in contrast with other divalent metal–ATP complexes, the ATPase activity is not coupled to proton translocation when Ca^{2+} is bound, suggesting that Ca^{2+} induces conformational changes in F_O, which could then mediate PTP formation and explain the inability of Ca^{2+} to sustain ATP synthesis (41). As shown here, accessibility of the PTP Ca^{2+} binding sites is influenced by enzyme catalysis and OSCP. One possible explanation is that the OSCP subunit affects the affinity of the metal binding sites of ATP synthase, and thus the ease with which matrix Ca^{2+} can replace Mg^{2+}, causing PTP opening. OSCP as such would be a negative modulator, and its effect would be counteracted by binding of the positive effector CyPD (which indeed increases the Ca^{2+} affinity of the PTP). Removal of OSCP, or CyPD binding to OSCP, would induce similar conformational effects, consistent with the data presented here as well as with previous findings on CyPD interactions with the lateral stalk (24).

Although defining the detailed mechanism of PTP formation requires additional work, the demonstration that the PTP forms from dimers of the F_OF_1 ATP synthase solves a long-lasting issue in cell biology and readily accommodates key pathophysiological effectors of the PT. Indeed, Ca^{2+}, Mg^{2+}, adenine nucleotides, and Pi bind the catalytic core at F_1, and the membrane potential and matrix pH, which are key PTP modulators (1), are also key regulators of the ATP synthase. Channel formation by purified ATP synthase dimers confirms our long-standing stance that the PT is an inner membrane event that does not require outer membrane components (1), which is also in keeping with recent results that we obtained in mitoplasts (42). The present findings suggest a dual function for complex V, i.e., ATP synthesis and PTP formation. The enzyme of life seems, therefore, to be also the molecular switch that may signal the presence of fully depolarized, dysfunctional mitochondria to stimulate cell death (1) and/or mitophagy (43). The detailed mechanisms through which this transition is achieved can now be addressed with the powerful tools of genetics, and we have little doubt that clarification of the molecular determinants of PTP formation will provide the solution to outstanding problems on the role of PTP in pathophysiology.

Materials and Methods

Immunoprecipitation and Western Blotting. Immunoprecipitation (IP) of ATP synthase was performed from 0.5 mg bovine, mouse heart, or human osteosarcoma HQB17 cells mitochondria prepared by standard methods (44, 45) using anticomplex V monoclonal antibody covalently linked to protein G-Agarose beads (MS501 immunocapture kit; Abcam) as reported (24). For isolated subunits, 30 μL *Staphylococcus aureus* protein A-Sepharose 4B (Sigma) were coupled with 10 μg OSCP subunit antibody, 2 μg b subunit, or nonimmune antibody in IP buffer (15 mM Tris, 10 mM Pi·Tris, 2 mM EDTA·Tris, 1.8 mM EGTA·Tris, 0.5% vol/vol Triton X-100, 0.005% wt/vol BSA, 0.25% SDS, pH 7.4) and incubated for 2 h at 4 °C. Then, 0.5 mg bovine heart mitochondria (BHM) solubilized and precleared in IP buffer were added with protein A-coupled antibody and incubated overnight at 4 °C. For d subunit, BHM was suspended in IP buffer, incubated for 1 h at 4 °C with 4 μg anti-d or rabbit anti-mouse antibodies, and then incubated for 3 h at 4 °C with 30 μL protein A. IP supernatants were separated by SDS/PAGE followed by Western blot analysis. Antibodies were polyclonal rabbit anti-α and -β F_1 subunit, anti-b subunit (a gift from John Walker, Medical Research Council—Mitochondrial Biology Unit, Cambridge), anti-ANT Q18 (Santa Cruz Biotechnology), monoclonal anti-β, anti-d subunit, anti-OXPHOS (Mitoscience), anti-CyPD (Calbiochem), anti-OSCP (Abcam), and anti-VDAC1 (a gift from F. Thinnes, Max-Planck-Institut für Experimentelle Medizin, Abteilung Immunchemie, Göttingen, Germany). Immunoreactive bands were detected by enhanced chemiluminescence (Pierce). CyPD is expressed as CyPD/β-ratio of bands analyzed with Quantity One software (Biorad). Statistics were calculated by GrafPad software.

Transfection with siRNAs. HQB17 cells (26) were transfected with an siRNA duplex OSCP oligo ribonucleotides pool (Invitrogen) as follows: ATP5OHSS100870 (-GGA ACC CAA AGU GGC UGC UUC UGU U-, -AAC AGA AGC AGC CAC UUU GGG UUC C-), ATP5OHSS100872 (-CAG GGC UAU GCG GGA GAU UGU CUA A-, -UUA GAC AAU CUC CCG CAU AGC CCU G-), or scrambled sequence at 0.2 μM. Before treatment, cybrids were cultured without antibiotics for 24 h and then transfected with siRNA and Lipofectamine 2000 in Opti-MEM (Invitrogen). After 6 h, the medium was replaced with culture medium without siRNA for 66 h before preparation of mitochondria.

Mitochondrial CRC and Membrane Potential. Extramitochondrial Ca^{2+} was measured by Calcium Green-5N (Molecular Probes) fluorescence (46) using a Fluoroskan Ascent FL (Thermo Electron) plate reader at a mitochondrial concentration of 1 mg × mL^{-1}. Membrane potential was measured at 25 °C using a Perkin-Elmer LS50B spectrofluorometer based on the fluorescence quenching of 0.15 μM Rhodamine 123 (46). For measurements of CRC and membrane potential during ATP synthesis at constant [ADP] (Fig. 3 *A*, trace a and *B*, trace a), the incubation medium contained 0.1 M glucose, 80 mM KCl, 10 mM Mops·Tris, 5 mM succinate·Tris, 4 mM $MgCl_2$, 1 mM Pi·Tris, 0.5 mM $NADP^+$, 0. 4 mM ADP, 50 μM P1,P5-di(adenosine-5′) pentaphosphate, 10 μM EGTA, 2 μM rotenone, 4 U/mL glucose-6-phosphate dehydrogenase, and 3 U/mL hexokinase. We ascertained that mitochondrial respiration was maximally stimulated and that the added enzymes were in excess by measuring O_2 consumption with a Clark oxygen electrode. For measurements of CRC and membrane potential during ATP hydrolysis at constant [ATP] (Fig. 3 *A*, trace b and *B*, trace b), the incubation medium contained 0.1 M sucrose, 80 mM KCl, 10 mM Mops·Tris, 4 mM $MgCl_2$, 2 mM phosphocreatine, 1 mM Pi·Tris, 0.4 mM ATP, 10 μM EGTA, 2 μM rotenone, and 1.5 U/mL creatine kinase. We ascertained that the ATP-regenerating activity was in excess by measuring the mitochondrial membrane potential, which was sustained at the maximal value beyond the duration of the CRC experiments. For all other CRC measurements (Figs. 2 and 3*C* and Fig. S4), the incubation medium contained 0.1 M sucrose, 80 mM KCl, 10 mM Mops·Tris, 5 mM succinate·Tris, 4 mM $MgCl_2$, 1 mM Pi·Tris, 10 μM EGTA·Tris, 2 μM rotenone, 0.5 μM Ca^{2+} Green-5N, and 1 mg/mL mitochondria. Additional modifications or additions are specified. Measurements of ATP hydrolysis were performed according to published methods (47, 48).

BNE Gel and Sample Preparation for Electrophysiology. Pellets of mitochondria were suspended at 10 mg/mL in 1 M aminocaproic acid and 50 mM Bis·Tris, pH 7.0 (24), solubilized with 2% (wt/vol) digitonin, and immediately centrifuged at 100,000 × *g* for 25 min at 4 °C. The supernatants were supplemented with Coomassie Blue G-250 (Serva) and rapidly applied to 1D 4–11% polyacrylamide gradient BNE (Invitrogen). After electrophoresis, gels were stained with Coomassie Blue, used for in-gel activity staining, or prepared for an overnight native complex protein elution from BNE gel as follows. Bands corresponding to monomers and dimers of complex V or monomer of complex I were excised and diluted with 25 mM tricine, 7.5 mM Bis·Tris, and 1% (wt/vol) n-heptyl β-D-thioglucopyranoside, pH 7.0 (49) supplemented with 8 mM ATP·Tris and 10 mM $MgSO_4$. After overnight incubation at 4 °C, samples were centrifuged at 20,000 × *g* for 10 min at 4 °C, and supernatants were (*i*) used directly for reconstitution in electrophysiological studies, (*ii*) subjected to 2D-SDS PAGE separation followed by Western blotting, or (*iii*) loaded in 2D-BNE followed by Coomassie Blue or in-gel activity staining (ATPase activity was amplified as in ref. 50).

Electrophysiology. Planar lipid bilayer experiments were performed as described (51). Briefly, bilayers of about 150–200 pF capacity were prepared using purified soybean azolectin. The standard experimental medium was 150 mM KCl and 10 mM Hepes, pH 7.4. Control experiments with empty membrane or detergents used for the purification showed no activity. All voltages reported refer to the *cis* chamber, zero being assigned by convention to the *trans* (grounded) side. Currents are considered as positive when carried by cations flowing from the *cis* to the *trans* compartment. Data were acquired at 100 μs/point, filtered at 500 Hz, and analyzed offline using the pClamp program set (Axon Instruments). Histograms were fitted using the Origin7.5 program set.

Electrostatic Calculations. The molecular structures of the membrane extrinsic region of the bovine ATP synthase (Protein Data Bank ID code 2WSS, chains) (25) and human CyPD complexed with CsA (Protein Data Bank ID code 2Z6W) (52) were used for the calculation of surface potential with the Generalized Born model (53) and isopotential surfaces within the Poisson–Boltzmann theoretical framework (54). The calculations performed on the apo-form of CyPD and OSCP in the ATP–synthase complex did not reveal apparent complementarity in the surface potential and isopotential curves because of the complexity and extension of OSCP in the context of ATP synthase. For CyPD, the dominant surface contribution is positive and located at a region flanking the binding site for CsA. The face of CyPD opposite to the CsA binding site shows less extended but negative potential. The overall charge at pH 7.0 of CyPD, based on the sequence (GenBank accession no. NP_005720.1, mature peptide), is strongly positive (six proton charges), and therefore, we expected that the target region on OSCP should be at negative potential. By using the software BLUUES (53), we identified the lowest potential regions on OSCP (calculations performed in the ATP–synthase complex). In particular, we considered the atoms listed in Fig. S1*C* with lowest average surface potential.

ACKNOWLEDGMENTS. We thank Anna Raffaello for advice on siRNA transfection. Professor Sir John Walker at the Medical Research Council—Mitochondrial Biology Unit in Cambridge is the source of the antisubunit b antibody and Prof. Friedrich P. Thinnes, Max-Planck-Institut für Experimentelle Medizin, Abteilung Immunchemie, Göttingen, Germany, of the VDAC1 antibodies. This work was supported by grants from Telethon, Associazione Italiana per la Ricerca sul Cancro (Italy), Ministero dell'Istruzione, dell'Università e della Ricerca, Italy, and the University of Padova, Italy and National Institutes of Health Grant 1R01GM069883.

1. Bernardi P, et al. (2006) The mitochondrial permeability transition from *in vitro* artifact to disease target. *FEBS J* 273(10):2077–2099.
2. Crompton M, Ellinger H, Costi A (1988) Inhibition by cyclosporin A of a Ca^{2+}-dependent pore in heart mitochondria activated by inorganic phosphate and oxidative stress. *Biochem J* 255(1):357–360.
3. Raaflaub J (1953) Die schwellung isolierter leberzell mitochondrien und ihre physikalisch beeinflußarkeit. *Helv Physiol Pharmacol Acta* 11:142–156.
4. Pfeiffer DR, Kuo TH, Tchen TT (1976) Some effects of Ca^{2+}, Mg^{2+}, and Mn^{2+} on the ultrastructure, light-scattering properties, and malic enzyme activity of adrenal cortex mitochondria. *Arch Biochem Biophys* 176(2):556–563.
5. Hunter DR, Haworth RA, Southard JH (1976) Relationship between configuration, function, and permeability in calcium-treated mitochondria. *J Biol Chem* 251(16): 5069–5077.
6. Hunter DR, Haworth RA (1979) The Ca^{2+}-induced membrane transition in mitochondria. I. The protective mechanisms. *Arch Biochem Biophys* 195(2):453–459.
7. Haworth RA, Hunter DR (1979) The Ca^{2+}-induced membrane transition in mitochondria. II. Nature of the Ca^{2+} trigger site. *Arch Biochem Biophys* 195(2):460–467.
8. Hunter DR, Haworth RA (1979) The Ca^{2+}-induced membrane transition in mitochondria. III. Transitional Ca^{2+} release. *Arch Biochem Biophys* 195(2):468–477.
9. Kinnally KW, Campo ML, Tedeschi H (1989) Mitochondrial channel activity studied by patch-clamping mitoplasts. *J Bioenerg Biomembr* 21(4):497–506.
10. Petronilli V, Szabò I, Zoratti M (1989) The inner mitochondrial membrane contains ion-conducting channels similar to those found in bacteria. *FEBS Lett* 259(1):137–143.
11. Szabó I, Zoratti M (1991) The giant channel of the inner mitochondrial membrane is inhibited by cyclosporin A. *J Biol Chem* 266(6):3376–3379.
12. Szabó I, Bernardi P, Zoratti M (1992) Modulation of the mitochondrial megachannel by divalent cations and protons. *J Biol Chem* 267(5):2940–2946.
13. Griffiths EJ, Halestrap AP (1993) Protection by Cyclosporin A of ischemia/reperfusion-induced damage in isolated rat hearts. *J Mol Cell Cardiol* 25(12):1461–1469.
14. Palma E, et al. (2009) Genetic ablation of cyclophilin D rescues mitochondrial defects and prevents muscle apoptosis in collagen VI myopathic mice. *Hum Mol Genet* 18(11): 2024–2031.
15. Beutner G, Rück A, Riede B, Welte W, Brdiczka D (1996) Complexes between kinases, mitochondrial porin and adenylate translocator in rat brain resemble the permeability transition pore. *FEBS Lett* 396(2-3):189–195.
16. Kokoszka JE, et al. (2004) The ADP/ATP translocator is not essential for the mitochondrial permeability transition pore. *Nature* 427(6973):461–465.
17. Krauskopf A, Eriksson O, Craigen WJ, Forte MA, Bernardi P (2006) Properties of the permeability transition in *VDAC1*$^{-/-}$ mitochondria. *Biochim Biophys Acta* 1757(5-6): 590–595.
18. Baines CP, Kaiser RA, Sheiko T, Craigen WJ, Molkentin JD (2007) Voltage-dependent anion channels are dispensable for mitochondrial-dependent cell death. *Nat Cell Biol* 9(5):550–555.
19. Baines CP, et al. (2005) Loss of cyclophilin D reveals a critical role for mitochondrial permeability transition in cell death. *Nature* 434(7033):658–662.
20. Basso E, et al. (2005) Properties of the permeability transition pore in mitochondria devoid of Cyclophilin D. *J Biol Chem* 280(19):18558–18561.
21. Nakagawa T, et al. (2005) Cyclophilin D-dependent mitochondrial permeability transition regulates some necrotic but not apoptotic cell death. *Nature* 434(7033):652–658.
22. Schinzel AC, et al. (2005) Cyclophilin D is a component of mitochondrial permeability transition and mediates neuronal cell death after focal cerebral ischemia. *Proc Natl Acad Sci USA* 102(34):12005–12010.
23. De Marchi U, Basso E, Szabò I, Zoratti M (2006) Electrophysiological characterization of the Cyclophilin D-deleted mitochondrial permeability transition pore. *Mol Membr Biol* 23(6):521–530.
24. Giorgio V, et al. (2009) Cyclophilin D modulates mitochondrial F_0F_1-ATP synthase by interacting with the lateral stalk of the complex. *J Biol Chem* 284(49):33982–33988.
25. Rees DM, Leslie AG, Walker JE (2009) The structure of the membrane extrinsic region of bovine ATP synthase. *Proc Natl Acad Sci USA* 106(51):21597–21601.
26. Giorgio V, et al. (2012) The effects of idebenone on mitochondrial bioenergetics. *Biochim Biophys Acta* 1817(2):363–369.
27. Johnson KM, et al. (2005) Identification and validation of the mitochondrial F1F0-ATPase as the molecular target of the immunomodulatory benzodiazepine Bz-423. *Chem Biol* 12(4):485–496.
28. Stelzer AC, et al. (2010) NMR studies of an immunomodulatory benzodiazepine binding to its molecular target on the mitochondrial F1F0-ATPase. *Biopolymers* 93(1): 85–92.
29. Gledhill JR, Montgomery MG, Leslie AG, Walker JE (2007) Mechanism of inhibition of bovine F1-ATPase by resveratrol and related polyphenols. *Proc Natl Acad Sci USA* 104(34):13632–13637.
30. Adachi K, et al. (2007) Coupling of rotation and catalysis in F1-ATPase revealed by single-molecule imaging and manipulation. *Cell* 130(2):309–321.
31. Wittig I, Schägger H (2008) Structural organization of mitochondrial ATP synthase. *Biochim Biophys Acta* 1777(7-8):592–598.
32. Tomasetig L, Di Pancrazio F, Harris DA, Mavelli I, Lippe G (2002) Dimerization of F0F1ATP synthase from bovine heart is independent from the binding of the inhibitor protein IF1. *Biochim Biophys Acta* 1556(2-3):133–141.
33. Garrett NE, Penefsky HS (1975) Physical and enzymatic properties of nucleotide-depleted beef heart mitochondrial adenosine triphosphatase. *J Supramol Struct* 3(5-6):469–478.
34. Halestrap AP (2009) What is the mitochondrial permeability transition pore? *J Mol Cell Cardiol* 46(6):821–831.
35. Brustovetsky N, Klingenberg M (1996) Mitochondrial ADP/ATP carrier can be reversibly converted into a large channel by Ca^{2+}. *Biochemistry* 35(26):8483–8488.
36. Brenner C, et al. (2000) Bcl-2 and Bax regulate the channel activity of the mitochondrial adenine nucleotide translocator. *Oncogene* 19(3):329–336.
37. Brustovetsky N, Tropschug M, Heimpel S, Heidkämper D, Klingenberg M (2002) A large Ca^{2+}-dependent channel formed by recombinant ADP/ATP carrier from Neurospora crassa resembles the mitochondrial permeability transition pore. *Biochemistry* 41(39):11804–11811.
38. Herick K, Krämer R, Lühring H (1997) Patch clamp investigation into the phosphate carrier from Saccharomyces cerevisiae mitochondria. *Biochim Biophys Acta* 1321(3): 207–220.
39. Blatt NB, et al. (2002) Benzodiazepine-induced superoxide signals B cell apoptosis: Mechanistic insight and potential therapeutic utility. *J Clin Invest* 110(8):1123–1132.
40. Papageorgiou S, Melandri AB, Solaini G (1998) Relevance of divalent cations to ATP-driven proton pumping in beef heart mitochondrial F0F1-ATPase. *J Bioenerg Biomembr* 30(6):533–541.
41. Nathanson L, Gromet-Elhanan Z (2000) Mutations in the beta-subunit Thr^{159} and Glu^{184} of the *Rhodospirillum rubrum* F_0F_1 ATP synthase reveal differences in ligands for the coupled Mg^{2+}- and decoupled Ca^{2+}-dependent F_0F_1 activities. *J Biol Chem* 275(2):901–905.
42. Sileikyte J, et al. (2011) Regulation of the inner membrane mitochondrial permeability transition by the outer membrane translocator protein (peripheral benzodiazepine receptor). *J Biol Chem* 286(2):1046–1053.
43. Youle RJ, Narendra DP (2011) Mechanisms of mitophagy. *Nat Rev Mol Cell Biol* 12(1): 9–14.
44. Nicolli A, Basso E, Petronilli V, Wenger RM, Bernardi P (1996) Interactions of cyclophilin with the mitochondrial inner membrane and regulation of the permeability transition pore, and cyclosporin A-sensitive channel. *J Biol Chem* 271(4):2185–2192.
45. Frezza C, Cipolat S, Scorrano L (2007) Organelle isolation: Functional mitochondria from mouse liver, muscle and cultured fibroblasts. *Nat Protoc* 2(2):287–295.
46. Fontaine E, Eriksson O, Ichas F, Bernardi P (1998) Regulation of the permeability transition pore in skeletal muscle mitochondria. Modulation by electron flow through the respiratory chain complex I. *J Biol Chem* 273(20):12662–12668.
47. Di Pancrazio F, et al. (2004) In vitro and in vivo studies of F0F1ATP synthase regulation by inhibitor protein IF1 in goat heart. *Biochim Biophys Acta* 1659(1):52–62.
48. Ritov VB, et al. (1992) Alamethicin-induced pore formation in biological membranes. *Gen Physiol Biophys* 11(1):49–58.
49. Rehling P, et al. (2003) Protein insertion into the mitochondrial inner membrane by a twin-pore translocase. *Science* 299(5613):1747–1751.
50. Suhai T, Heidrich NG, Dencher NA, Seelert H (2009) Highly sensitive detection of ATPase activity in native gels. *Electrophoresis* 30(20):3622–3625.
51. Szabò I, Soddemann M, Leanza L, Zoratti M, Gulbins E (2011) Single-point mutations of a lysine residue change function of Bax and Bcl-xL expressed in Bax- and Bak-less mouse embryonic fibroblasts: Novel insights into the molecular mechanisms of Bax-induced apoptosis. *Cell Death Differ* 18(3):427–438.
52. Kajitani K, et al. (2008) Crystal structure of human cyclophilin D in complex with its inhibitor, cyclosporin A at 0.96-A resolution. *Proteins* 70(4):1635–1639.
53. Fogolari F, et al. (2012) Bluues: A program for the analysis of the electrostatic properties of proteins based on generalized Born radii. *BMC Bioinformatics* 13(Suppl 4):S18.
54. Madura JD, et al. (1995) Electrostatics and diffusion of molecules in solution: Simulations with the University of Houston Brownian Dynamics program. *Comput Phys Commun* 91(1–3):57–95.